Characterization of rapid adenosine neuromodulation in mouse brain slices

Yuanyu Chang

Changchun, Jilin, China

Bachelor of Science in Chemistry, Sichuan University, 2017

A Dissertation Presented to the Graduate Faculty of the University of Virginia in Candidacy for the Degree of Doctor of Philosophy

Department of Chemistry

University of Virginia

May 2022

Abstract

Adenosine is an important neuromodulator in the brain, it modulates neurotransmitter release and provides neuroprotection during physiological and pathological conditions. The mechanisms of rapid adenosine release in the brain have been investigated for several years using fast-scan cyclic voltammetry (FSCV). However, the mechanisms of rapid adenosine neuromodulation and formation are still not fully understood. This thesis explored the rapid adenosine modulation and formation by using global knockout mice, and the range of rapid adenosine effects in the brain was also characterized with dual-channel FSCV.

In Chapter 2, spontaneous adenosine and mechanically-stimulated adenosine were separately measured in the caudate-putamen region in a mouse brain. Here, I investigated the regulation of rapid adenosine by adenosine receptors, using global A_1 or A_{2A} knockout mice. The results indicate that A_1 receptors presynaptically modulate the frequency of spontaneous adenosine but do not modulate the concentration. However, A_{2A} receptors modulate the concentration of spontaneous adenosine but do not significantly influence the frequency of spontaneous adenosine. For the mechanically-stimulated adenosine, adenosine receptors do not significantly influence the concentration of adenosine *in vivo*, but A_1 receptors significantly modulate the concentration of stimulated adenosine in the brain slice model. Understanding the role of adenosine receptors on rapid adenosine release will help for future treatments for different diseases that are related to adenosine neuromodulation. Chapter 3 investigated the mechanisms of rapid adenosine formation in the hippocampus CA1 region using Pannexin 1 knockout mice. There was no significant difference in spontaneous adenosine release between wild-type mice and Pannexin 1 knockout mice. Therefore, Pannexin 1 channels might not be the formation pathways of spontaneous adenosine release. However, the concentration of mechanically-stimulated adenosine decreased around 50% in Panx1KO mice indicating that Pannexin 1 channels partially influence the formation of mechanically-stimulated adenosine due

to their mechanosensitive property. In addition, a high dose of a non-selective drug, Carbenoxolone (CBX) did not further influence the rapid adenosine release, indicating that other pannexin channels and connexins are not contributed to the rapid adenosine formation. These results prove that spontaneous adenosine and mechanically-stimulated adenosine has different mechanisms of modulation and formation. Future studies could focus on the impact of exocytosis for rapid adenosine formation.

Chapter 4 describes the range of rapid adenosine effects by using dual channel FSCV. Rapid adenosine was simultaneously detected in two different sites in hippocampus CA1 in the mouse brain slice. By varying the distance of two working electrodes, the spatial range of rapid adenosine was characterized. Mechanically-stimulated adenosine can be detected up to 150 µm away from where it was stimulated, although the signal is smaller and delayed. Spontaneous adenosine was randomly and localized released and could not diffuse to a 50 µm distance. This study shows that spontaneous adenosine events are very localized and thus provide only local neuromodulation. Injury, such as mechanical stimulation, allows adenosine to diffuse farther, but neuroprotective effects are still regional.

Chapter 5 presents a graphene oxide (GO) modified carbon fiber microelectrode (CFME) for dopamine detection in FSCV. GO coating improved the electrode sensitivity by providing more oxygen-functional groups for dopamine adsorption. Different methods, such as drop casting, dip coating, and electrodeposition, were also compared in this chapter. Drop casting was likely to cause a huge GO aggregation which slows down the electron transfer rate of dopamine detection. Dip coating did not sufficiently coat the electrode surface, GO particles tended to form sediments under the solution instead. Electrodeposition showed the best coating on CFME, and the sensitivity of the modified electrode enhanced nearly two folds for dopamine detection. In addition, the modified electrodes were successfully applied to mouse brain slices to

monitor the electrically-stimulated dopamine release. Thus, GO is good for improving sensitivity and is stable for complex tissue measurement.

Overall, my thesis demonstrates the new findings of the mechanisms of rapid adenosine modulation and formation by using different types of knockout mouse models, I also characterized the range of rapid adenosine with dual channel FSCV in mouse brain slices. The new information provides more understanding of rapid adenosine release in the brain which will be useful for future treatments of adenosine-related diseases. Furthermore, I also optimized new GO-modified CFMEs to improve the sensitivity of dopamine detection in brain slices. Better method developments, better sensors, and better analytical tools will reveal more understanding of rapid neuromodulation in the future.

Table of Contents

Acknowledgments

I would like to acknowledge my advisor, Professor B. Jill Venton. Before I joined the lab, I never believed that I could do well in electrochemistry and neurochemistry. I did not even have any background in this research field. Professor Venton was really patient and taught me how to understand FSCV from the very beginning. Without her patience and trust, I will not have a chance to become a Ph.D. candidate to obtain my degree. And thanks to my committee members, Prof. Ian Harrison, Prof. Sen Zhang, Prof. David Cafiso, and Prof. Brant Isakson for the help and support on my Ph.D. study. I also want to thank my group members for always being supportive on my research and everyday life. Dr. Pumidech Puthongkham and Dr. Qun Cao, taught me all the electrochemistry knowledge and trained me how to do and think in a scientific way. Dr. Scott Lee trained me how to do the brain slice experiment, which is the main method for my whole thesis. Dr. Scott Lee also performed spontaneous adenosine measurement and analyzed the data in Chapter 3. I would also like to thank Dr. Ying Wang for doing the *in vivo* experiment in Chapter 2. Dr. Mimi Shin and Dr. Malli Ganesana provided me tons of advice during my Ph.D. career. Kelly Dunham and Dr. Dana DiSenza were also really helpful on my writing and presentation skills, thanks for the supporting on my poor English writing and speaking. I also want to thank all my friends either in the US or in China for the support. Finally, I would like to specially thank Zijun Shao, who is not only the colleague in the lab but also my girlfriend. We have conquered so many challenges since undergraduate study; without the long time of staying together, it would be more difficult for my on the whole journey.

I also want to thank my whole family on supporting me to obtain my degree. It is difficult to study overseas alone, but my parents always encourage me to become stronger to face everything. My aunts also gave me lots of advice to make me feel more optimistic when I stuck in my research project. I also want to thank my cousin, Dr. Wenjian Wang. She is a really hardworking scientist in chemistry, and I am always motivated by her intelligence and diligence. We also always shared interesting things to each other. Overall, without my family support, I could not reach to this step. I hope everyone in my family will feel proud of me.

Chapter 1

Introduction

1.1 Overview of adenosine

Adenosine is a major byproduct of adenosine triphosphate (ATP) degeneration, and it plays an important role in neuromodulation in the central nervous system (CNS) and other parts of the body.[1–3] For example, adenosine acts as a neuromodulator to modulate neurotransmitter release in the CNS. Adenosine also modulates multiple biological functions such as blood flow, sleep-wake cycles, pain, and memory. Dysfunction of adenosine metabolism may cause Alzheimer's disease and Parkinson's disease.[4–11] Additionally, adenosine signaling is neuroprotective during brain injury, stroke, ischemia, and epileptic seizures.[12] Therefore, investigating the mechanisms of adenosine neuromodulation will help us understand its role in different diseases.

Adenosine was first discovered by Drury and Szent-Gyorgyi in cardiac and vascular tissues in 1929, and Berne identified the physiological role of adenosine as a mediator of coronary vasodilation in 1963.[13,14] Since then, adenosine has been broadly investigated as part of purinergic signaling with different types of techniques. For example, microdialysis has been used for neurotransmitter detection, including adenosine; however, the slow time resolution (minutes to hours) limits the ability to monitor rapid signaling.[15,16] Electrophysiology and electrochemistry techniques, such as amperometry and fast-scan cyclic voltammetry (FSCV), possess enhanced temporal resolution in subsecond scales. Specifically, FSCV rapid detection found rapid adenosine release in the brain, which only lasts few seconds.[17,18] Additionally, Dale's group designed a three-enzyme microelectrode biosensor to detect adenosine in the central nervous system with good selectivity and high temporal resolution (10–90% rise time, 2±0.23 s).[19] Further, new genetically-encoded sensors (GRAB sensors) combined with fluorescence measurements provide good selectivity and spatial resolution for adenosine measurement.[20] All of these methods provide different advantages and have been applied to

investigate the mechanisms of adenosine. However, the role of rapid adenosine in the brain is still not fully understood.

In this thesis, I explore the mechanisms of rapid adenosine using a mouse brain slice model. Different types of globally knock-out mice are compared to investigate the role of adenosine receptors on rapid adenosine release. I also investigated if the Pannexin 1 channel is one of the pathways of extracellular rapid adenosine release. Finally, the spatial range of rapid adenosine diffusion is characterized via dual-channel FSCV. Overall, this thesis develops techniques for rapid adenosine detection and unveils a better understanding of rapid adenosine neuromodulation in the brain.

1.1.1 Adenosine formation and pathways

Adenosine is a purine nucleoside consisting of adenine and ribose. Adenosine formation occurs via both intracellular and extracellular pathways via different mechanisms. Figure 1.1 shows the mechanisms of adenosine formation and adenosine metabolic pathways in the cell. ATP metabolism in the cell is the main source for adenosine intracellular formation.[21] ATP first degenerates to adenosine monophosphate (AMP) by ATP/ADPase, and AMP diphosphate to adenosine via 5' nucleotidase.[22] Because the intracellular ATP concentration is about 50 times more than AMP, a slight change in ATP concentration will cause significant adenosine formation.[23] Intracellular adenosine can either be phosphorylated back to AMP by adenosine kinase, or be degenerated to inosine by adenosine deaminase and decompose into uric acid for further metabolism.[22,24] Adenosine is also released into the extracellular space via equilibrative or concentrative transporters (ENTs, CNTs).[21] Another method for adenosine intracellular formation comes from S-Adenosyl-L-homocysteine (SAH) hydrolysis.[25] Adenosylhomocysteinase (SAHH) coverts SAH to homocysteine and adenosine in the cells, but this process has a low impact on adenosine formation in the brain.

In the extracellular space, adenosine is released multiple ways. ATP can be packaged into vesicles by the vesicular nucleotide transporter (VNUT) and released by exocytosis into the extracellular space.[26] Then, ATP is rapidly hydrolyzed to adenosine by ectoenzymes such as CD39 and CD73 within 200 milliseconds.[27,28] Although, exocytosis of ATP is the main source of extracellular ATP, ATP is also released extracellularly via other membrane channels such as pannexin and connexin channels.[29,30] In addition, adenosine is also released via ENTs into the extracellular space when the intracellular adenosine concentration is high.

Extracellular adenosine interacts with different adenosine receptors either presynaptically or postsynaptically for further neuromodulation.[31,32] It also diffuses to a broader range of tissue if the concentration is high. Details are shown in Figure 1.2 and section 1.1.2. Cells reuptake adenosine via ENTs. There are two main enzymes that metabolize adenosine, adenosine deaminase (ADA) and adenosine kinase (ADK). ADA catalyzes adenosine deamination into inosine and then inosine is decomposed into uric acid via other enzymes. ADK catalyzes adenosine phosphorylation to AMP. The K_m of ADK (about 1 μM) is much lower than the K_m of ADA (25-150 μM); therefore, ADK is the primary enzyme for adenosine metabolism.[32]

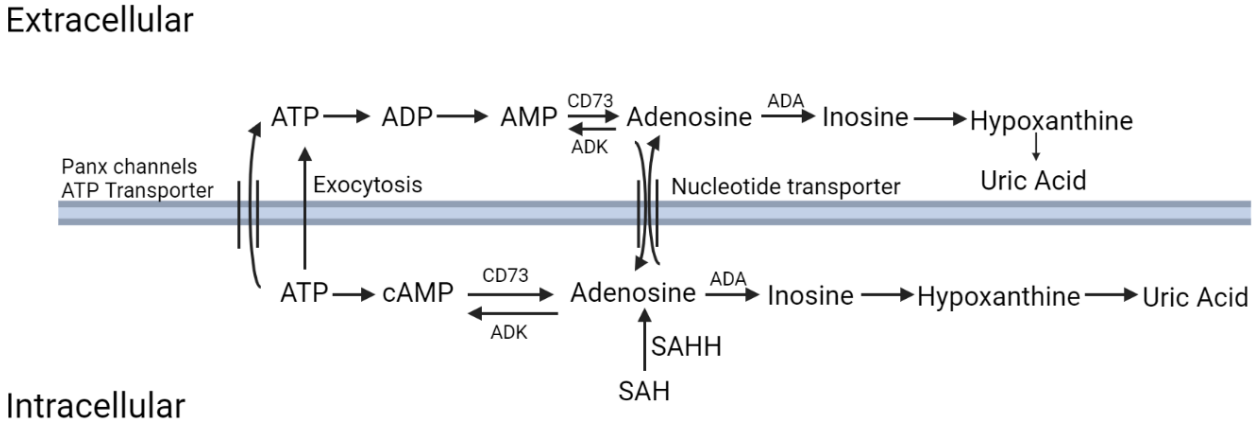

Figure 1.1 The mechanism of adenosine formation and metabolic pathways in cells. Adenosine is generated in both intra- and extracellular spaces from ATP hydrolysis. ATP is released via exocytosis into the extracellular space and quickly broken down into adenosine by enzymes. Adenosine is also released into the extracellular space via ENTs. SAH is another source of adenosine formation, but it is not abundant in the brain. Adenosine can be phosphorylated back to AMP by ADK, or metabolized to inosine via ADA and decomposed to uric acid.

1.1.2 Adenosine receptors

Adenosine is an important neuromodulator in the brain, and it modulates neurotransmitter release by interacting with adenosine receptors. Adenosine receptors are G protein-coupled, and there are four subtypes of adenosine receptors: A_1, A_{2A}, $A_{2B,}$ and A_3.[33] A_1 receptors are the most abundant adenosine receptor type in the brain, and they act as inhibitory receptors by inhibiting adenylyl cyclase to decrease AMP concentrations. A_{2A} receptors are also broadly distributed in the brain, but they act as excitatory receptors by stimulating adenylyl cyclase to increase AMP concentrations. However, A_{2B} and A_3 receptors are less abundant, and A_{2B} receptors are excitatory receptors, but A_3 are inhibitory receptors.[32,34] In addition, the affinity (K_d) of A_1 and A_{2A} receptors is relatively high, around 70 nM and 150 nM, respectively. A_{2B} and A_3 have much lower affinity for adenosine, 5100 nM and 6500 nM, respectively;[35] therefore, A_{2B} and A_3 receptors are less effective, and adenosine signaling is mainly modulated through A_1 and A_{2A} receptors. Figure 1.2 shows how adenosine receptors modulate adenosine in the synapse. Adenosine receptors can pre-synaptically or post-synaptically affect adenosine synthesis via inhibition or excitation.[36]

1.1.2.1 A_1 receptors

Adenosine A_1 receptors are broadly distributed in the CNS and are located pre-synaptically, post-synaptically, and non-synaptically in the membranes.[37] A_1 receptors modulate the release of multiple neurotransmitters such as acetylcholine, dopamine, serotonin, glutamate, and GABA.[2,38–40] Activation of presynaptic A_1 receptors cause inhibition of neurotransmitter release. For example, the release of glutamate in the CA1 region is highly sensitive to inhibition via A_1 receptors.[41] In addition, A_1 receptors inhibit calcium channels and stimulate potassium channels.[42,43] Post-synaptically, A_1 receptors can interact with NMDA receptors for neuromodulation;[44] however, how A_1 receptors modulate rapid adenosine release in real-time is still unclear.

1.1.2.2 A_{2A} receptors

A_{2A} receptors are highly distributed in certain regions in the CNS such as the striatum, nucleus accumbens, and olfactory tubercle.[45] In the striatum, some A_{2A} receptors are co-expressed with D_2 receptors and coexist as A_{2A}-D_2 heterodimers, which indicate that A_{2A} receptors modulate dopamine signaling in the brain.[46] A_{2A} receptors also influence the release of neurotransmitters such as GABA, glutamate, and acetylcholine.[47–51] A_{2A} receptors are the main target for caffeine to decrease cAMP stimulation to lower adenosine levels.[52] There are also drugs designed to specifically target A_{2A} receptors either as antagonists or agonists to treat brain disorders, such as Parkinson's diseases.[11]

1.1.2.3 A_{2B} and A_3 receptors

A_{2B} receptors are excitatory receptors that regulate vascular permeability and may also play a role in neuroprotection in the brain. Since A_{2B} and A_3 are poorly distributed in the brain, there is a lack of pharmacological tools available to investigate their receptors. Therefore, the role of A_{2B} and A_3 receptors in the brain is still unclear.[32]

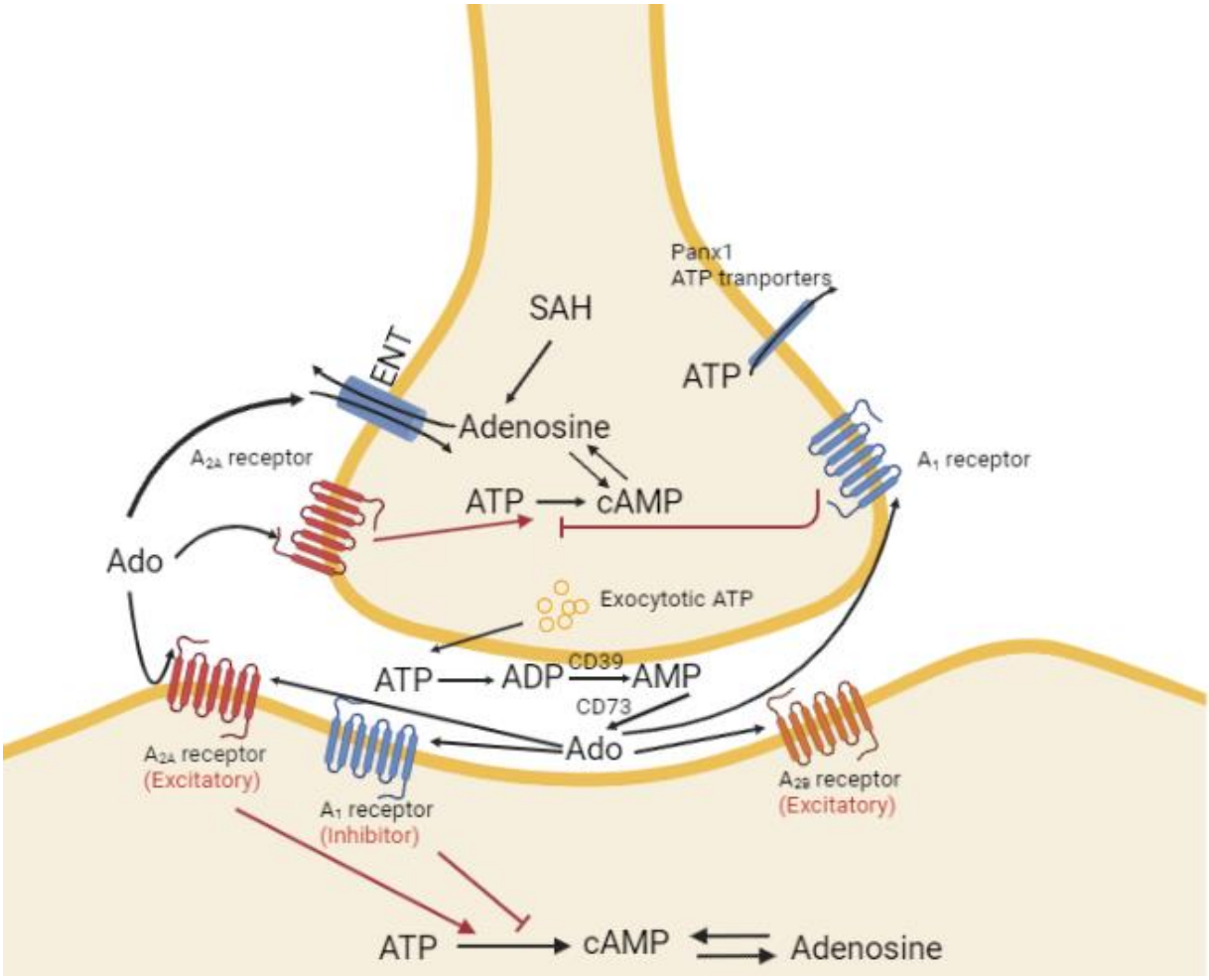

Figure 1.2 Adenosine formation and release in the synapse with mechanisms of adenosine receptor modulation on adenosine concentration. Adenosine receptors are G protein coupled receptors (GPCRs). A_1 and A_3 are inhibitory receptors that block adenylyl cyclase, but A_{2A} and A_{2B} are excitatory receptors that stimulate adenylyl cyclase to enhance cAMP. Adenosine receptors are distributed both pre-synaptically and post-synaptically on the membrane for adenosine modulation.

1.1.3 Adenosine Transporters

Adenosine transporters play pivotal roles for the adenosine pathways between the intra- and extracellular spaces. There are two types of adenosine transporters, equilibrative nucleotide transporters (ENTs) and concentrative nucleotide transporters.[21,53] ENTs are the primary transporters for extracellular adenosine regulation via concentration gradient changes.[54]

1.1.4 Pannexin channels

Recently, Pannexin channels were discovered as gap junction proteins that consist of large transmembrane channels that connect the intracellular and extracellular space.[55] There are three subtypes of Pannexin channels called Panx1, Panx2, and Panx3. Panx1 and Panx2 are distributed in multiple brain regions, but Panx3 can only be found in osteoblasts and synovial fibroblasts.[56,57] Panx1 is an important channel for ATP release, and it is mechanically sensitive.[58] However, ATP release from Panx1 degenerates to adenosine extracellularly, so Pannexin channels could be another source of extracellular adenosine in the brain.

1.1.5 Adenosine neuromodulation and diseases

As a neuromodulator, adenosine plays different roles in the body and affects blood flow, heart rate, pain, and sleep. For example, adenosine modulates blood flow by vasodilation, which controls oxygen delivery and blood pressure.[7,59] It also acts as a neuroprotector that inhibits other neurotransmitter release in the brain during injury, such as stroke.[60] Adenosine neuromodulation influences many functions in the body, and adenosine concentration changes influence chemical energy available and neuronal activity.[1] For instance, adenosine concentration significantly increases during hypoxia or ischemia, which indicates the neuroprotective role of adenosine during injury.[60,61] In addition, several drugs that target adenosine receptors have been recently developed to treat neuronal diseases, such as epilepsy, traumatic brain injury, Parkinson's disease, and Alzheimer's disease.[11] These treatments indicate that adenosine plays an important role in different brain diseases as a neuroprotective agent.

1.1.5.1 Epilepsy

Neurological disorders in the brain including adenosine dysfunction could lead to serious neurological diseases such as epilepsy.[62] Upregulation of ADK in astrocytes reduces adenosine

concentration, which causes seizures and suggests that adenosine acts a potential anticonvulsant in the brain.[63] Overexpressing ADK in transgenic mice brain tissue also produces epileptogenesis, but ADK-deficient stem cells suppress epileptogenesis.[64] Therefore, extracellular adenosine in the brain prevents epilepsy, and drugs that target adenosine receptors, such as A_1 receptor agonists, or suppress ADK, like ADK inhibitors, might help as epilepsy treatments.[65]

1.1.5.2 Traumatic brain injury

Traumatic brain injury (TBI) is a violent blow or jolt to the head or body that causes damage to brain cells.[66] This injury in brain tissue leads to multiple diseases including epilepsy, blood vessel damage, memory loss, sleep disorders, and movement problems.[67–69] During TBI, adenosine plays a role in neuroprotection. A previous study found that adenosine concentrations are significantly increased after TBI, and this concentration is related to the severity of the injury.[70] Higher adenosine release causes inhibition of glutamate neurotransmission and inhibits inflammation.[38] Mechanically-stimulated adenosine may also cause mild tissue damage since inserting the electrode into the brain tissue generates a large amount of adenosine release. However, these release mechanisms of mechanically-stimulated adenosine are still not clear because of the lack of knowledge on its formation. Therefore, characterization of the ranges of mechanically-stimulated adenosine modulation and the amount of adenosine release could provide a clearer understanding between mechanically-stimulated adenosine and injury.

1.1.5.3 Parkinson's disease

Parkinson's disease (PD) is a neurological disease caused by disorder in the central nervous system that mainly affects the motor system. There are many potential causes of PD, but many symptoms are due to dopamine loss, and both environmental influences and genetic mutations may also trigger it.[71] Although we do not fully understand the causes of PD, there are

current drug treatments that target different types of receptors in the brain to help alleviate patient's symptoms. Recently, A_{2A} receptors have become a target of interest as a treatment for PD.[72] In recent studies, dopamine deficiency was reduced by blocking A_{2A} and D_2 receptor interactions.[46,73] Consequently, A_{2A} receptor antagonists are being considered as potential candidates for PD treatment, and the A_{2A} antagonist KW-6002 has been used in clinical trials.[74]

1.1.5.4 Alzheimer's disease

Alzheimer's disease is another common neurological disease caused by disorder in the nervous system that affects memory, cognition, and behavior. Alzheimer's disease patients are usually over the age of 65 and suffer from cognitive deficits and memory loss.[75] Amyloid beta (Aβ) is a small protein fragment of amyloid precursor protein (APP) that can aggregate and cause inflammatory responses that disrupt cellular communication.[76] The accumulation of Aβ in the extracellular space is the major diagnostic clue for Alzheimer's disease. Currently, adenosine receptors are actively being investigated as drug targets for Alzheimer's disease, including caffeine, an A_{2A} receptor antagonist, which prevents Aβ aggregation in mice. [77,78] Thus, several drug development methods that target adenosine receptors are under investigation for the treatment of Alzheimer's disease.

1.1.5.5 Ischemia

Brain ischemia is normally caused by insufficient blood flow to the brain. Adenosine levels significantly increase in the extracellular space during ischemia, which indicate that adenosine acts as a neuroprotector in the brain.[61] Rapid adenosine release leads to the activation of A_1 receptors, which inhibits excitatory synaptic neurotransmission to protect the brain during ischemia and reduces other presynaptic neurotransmitter release as a result.[4,79] Previous studies also found that ADK in astrocytic cells was downregulated after middle cerebral artery occlusion in the mouse brain.[80] This also demonstrates that adenosine concentration increases due to ischemia.

In summary, adenosine regulates multiple biological functions and modulates complicated neurotransmission in the brain. However, adenosine neuromodulation is still not well characterized in real-time. In this thesis, I will investigate the mechanisms of adenosine neuromodulation, the pathways of adenosine formation, and the range of adenosine effects in real time.

1.2 Rapid adenosine

In 1993, Dunwiddie's group discovered that adenosine responses are on the time scale of milliseconds to seconds using electrophysiology.[17] Our lab started to investigate the mechanisms of rapid adenosine release in the brain in 2008, and we found that adenosine is released after electrical stimulation in the rodent brain. In addition, adenosine is also released by mechanical stimulation both *in vivo* and in brain slices.[18,81–85] Recently, Zylka's group found that adenosine was rapidly and spontaneously released in the rat brain, which spurred our group to extensively characterize spontaneous adenosine release.[17,27,86] In this section, I will introduce the three types of rapid adenosine release: electrically-stimulated adenosine, mechanically-stimulated adenosine, and spontaneous adenosine.

1.2.1 Electrically-stimulated adenosine

Our lab first characterized electrically-stimulated adenosine in the caudate-putamen region. The rapid adenosine signal detected was around 1 μM and cleared in about 15 s.[87] The transient signal was confirmed to be adenosine by pharmacological experiments using an adenosine kinase inhibitor, adenosine transport inhibitor, and a histamine synthetic precursor. Electrically-stimulated adenosine is regulated by A_1 receptors. The A_1 receptor agonist (N^6-cyclopentyladenosine) decreased stimulated adenosine and dopamine release, and the A_1 receptor antagonist (DPCPX) increased stimulated adenosine release.[88] The concentrations of electrically-stimulated adenosine are variable in different brain regions; for example, the dorsal

caudate-putamen has the highest concentration (~340 nM), but in the cortex, the stimulated adenosine concentration is only around 40-80 nM. Electrically-stimulated adenosine was partially formed from ATP degeneration, and it is activity-dependent in the brain.[83]

1.2.2 Mechanically-stimulated adenosine

Mechanically-stimulated adenosine is another type of rapid adenosine release, which is generated by lowering the working electrode or a glass pipette nearby the working electrode into the brain tissue. Shear stress, or minor tissue damage, due to the electrode's movement will cause adenosine release.[84] Compared to electrical stimulation, mechanical stimulation is more reproducible in repeated experiments. Mechanically-stimulated adenosine has a much larger concentrations than spontaneous adenosine and lasts around 30 s, which is longer. Mechanically-stimulated adenosine is also activity-dependent and is mainly formed from ATP degeneration. Furthermore, mechanically-stimulated adenosine modulates the concentration of stimulated dopamine via A_1 receptors in the caudate in brain slices.[39] However, mechanically-stimulated adenosine concentration is not influenced by ATP degeneration enzymes, such as CD39 or CD73, in knockout mice.[89] Although lowering the electrode may cause some tissue damage, the stimulation can be repeated multiple times in a single area, which indicates the tissue is not dying. The mechanisms of mechanically-stimulated adenosine formation is still not known, and how the adenosine receptors modulate adenosine release has not been investigated. In addition, ATP is also rapidly released through Pannexin 1 channels into the extracellular space, which indicates Pannexin 1 could be a release channel for rapid adenosine formation. Pannexin 1 channels are also mechanosensitive and open when the plasma membrane stretches.[58] These stimulated adenosine pathways are still not clear, and we have not investigated whether Pannexin 1 channels play a part in the pathway for mechanical stimulation. Further, the range of mechanically-stimulated adenosine affects in the brain have also not been characterized. Therefore, in this thesis, I will investigate the range and

mechanism of adenosine formation using knockout mice models and dual-channel FSCV in Chapters 2, 3, and 4.

1.2.3 Spontaneous adenosine

Transient adenosine is not only released by external stimulations in the brain, but adenosine is also released spontaneously. The concentration of spontaneous adenosine is smaller than the stimulated adenosine, normally 0.1 μM in brain slices.[90] In addition, spontaneous adenosine only lasts few seconds and is randomly released in the brain. Using pharmacology and global knockout mice, our lab determined spontaneous adenosine is modulated pre-synaptically by A_1 receptors and is dependent of CD39 and CD73.[89,91] Because CD39 and CD73 are the enzymes that convert ATP to adenosine in the extracellular space, vesicular ATP release is the main source of spontaneous adenosine.[10] Also, SCH442416, a A_{2A} receptor antagonists, eliminated spontaneous adenosine release during ischemia/reperfusion *in vivo*.[92] We also investigated how other receptors modulate spontaneous adenosine *in vivo*. For example, a glutamate NMDA antagonist enhanced the frequency and concentration of spontaneous adenosine, and the $GABA_B$ antagonist CGP 52432 (30 mg/kg i.p.) significantly decreased the number of adenosine release events.[93] These results indicate spontaneous adenosine release is modulated by NMDA and GABA receptors. Spontaneous adenosine also shows some sex differences in the rat brain *in vivo*.[89,94] However, how adenosine receptors modulate rapid adenosine itself is still not clear, and rapid ATP release channels, such as Pannexin 1, have not been investigated to understand rapid adenosine formation.

In summary, we have characterized some of the mechanisms and functions of rapid adenosine in rodent brain models, but it is still unclear how adenosine receptors and Pannexin 1 channel affect rapid adenosine. Therefore, we will investigate how A_1 and A_{2A} receptors modulate spontaneous adenosine and mechanically-stimulated adenosine using A_1KO and A_{2A}KO mice in Chapter 3. A Pannexin 1 KO mouse model is also used to investigate if Pannexin

1 channels are a part of the mechanism to release ATP that breaks down to form extracellular adenosine. In addition, the range of rapid adenosine release is first characterized in brain slices by dual-channel FSCV and the results are discussed in Chapter 4.

1.3 Tools for neurotransmitter detection

Neurotransmitters, like dopamine, serotonin, glutamate, and adenosine are important chemical messengers that regulate multiple biological functions. Dysfunction of neurotransmitter release causes many serious problems such as depression, Parkinson's disease, and Alzheimer's disease. Analytical tools have been developed for decades for neurotransmitter detection. For example, microdialysis combined with HPLC analysis is the traditional method for adenosine detection and provides measurement of multiple molecules, typically in the time frame of 10 minutes.[16,95–97] Electrochemical techniques, including amperometry and fast-scan cyclic voltammetry (FSCV), are well-known for their real-time detection of neurotransmitters such as dopamine, serotonin, and adenosine.[98–101] Recently, a new, analytical tool, genetically encoded sensors combined with high-resolution imaging have also been explored. The sensors provide high spatial resolution and selectivity for neurotransmitter detection.[20,102–104] In this section, I will introduce these different tools for neurotransmitter measurement, especially their applications for adenosine and dopamine detection.

1.3.1 Microdialysis for neurotransmitter detection

The traditional method of neurotransmitter detection is microdialysis. Microdialysis uses a 200-500 μm diameter probe to collect samples and combines the samples with HPLC to separate and analyze the dialysate.[105] Microdialysis is coupled with separations and provides basal level concentrations of neurotransmitters in the brain, but it has limited temporal and spatial resolution.[96] Normally, microdialysis detection occurs at minute to hour long time scales,

which limits the rapid measurement of neurotransmitters in real-time. The large probe size also causes cell damage to tissue in the brain.[15,106]

1.3.2 Amperometry

In order to enhance temporal resolution for real-time detection, electrochemical methods, like amperometry, were developed to monitor neurotransmitter release. In amperometry, electroactive analytes are oxidized by applying a specific potential, and electron transfer on the electrode (sensor) will cause a current change which is regarded as the signal for detection. However, amperometry has specific issues with selectivity, since some neurotransmitters like dopamine, serotonin, epinephrine, and ascorbic acid have similar oxidation potentials.[107] Therefore, enzyme-based biosensors, conducting polymer-based biosensors, and aptamer-based electrodes have been developed for specific neurotransmitter detection.[108–111] For example, Dale's group developed an adenosine biosensor that entrapped xanthine oxidase, purine nucleoside phosphorylase, and adenosine deaminase on a platinum microelectrode using a derivatized pyrrole polymer.[19] These enzymes selectively breakdown adenosine into uric acid and hydrogen peroxide. Then the hydrogen peroxide was detected on the sensor using amperometry, and the concentration of hydrogen peroxide is proportional to the adenosine concentration. The enzymes or DNA coating improve selectivity for the target analytes, and they also detect some nonelectroactive neurotransmitters, like glutamate, via electrochemical methods.[112] However, the temporal resolution of biosensors is limited by the reaction between enzymes (or DNA structure) and analytes, and the thick coating layer on the sensor also limits the electron transfer rate. Moreover, the fabrication of micro-sized biosensors is more difficult than normal microelectrodes. However, amperometry has also been used to measure cell content. Recently, Ewing's group used open carbon nanopipettes with vesicle impact electrochemical cytometry (VIEC) to count the number of neurotransmitters released via

a vesicle, which creates a new, exciting direction for exocytosis measurement using amperometry.[113–115]

1.3.3 Fast-scan cyclic voltammetry (FSCV)

Fast-scan cyclic voltammetry (FSCV), combined with carbon-fiber microelectrodes (CFMEs), is another popular electrochemical technique for electroactive neurotransmitter detection *in vitro* and *in vivo*.[98] The 7 μm diameter of a CFME limits tissue damage, and the carbon-based material limits the toxicity of electrode implantation. The traditional triangular FSCV waveform, termed the dopamine waveform, is normally used for dopamine measurement.[98] Figure 1.3 A shows an example of the dopamine waveform applied to the CFME and scans from -0.4 V to 1.3 V and back to -0.4 V (vs. an Ag/AgCl reference electrode) with a scan rate of 400 V/s at 10 Hz. The fast scan rate not only gives millisecond temporal resolution, but also generates a huge background charging current. Therefore, background subtraction is needed to obtain the small faradic current change caused by dopamine detection, which is shown in a background subtracted cyclic voltammogram (CV) in Figure 1.3 B and C. The relatively unique CV offers better selectivity compared to amperometry. However, some neurotransmitters, such as dopamine, epinephrine, and norepinephrine, have similar chemical structures and are still difficult to distinguish by CV alone. Figure 1.3 D and E presents an example 3D false color plot for a 5 s injection of 1 μM dopamine followed by a PBS buffer washing. The x-axis is the time scale, the y-axis means shows the triangular voltage applied, and the false color represents the amount of current detected. The green color shows positive, oxidative current, while the blue color shows the negative, reductive current.

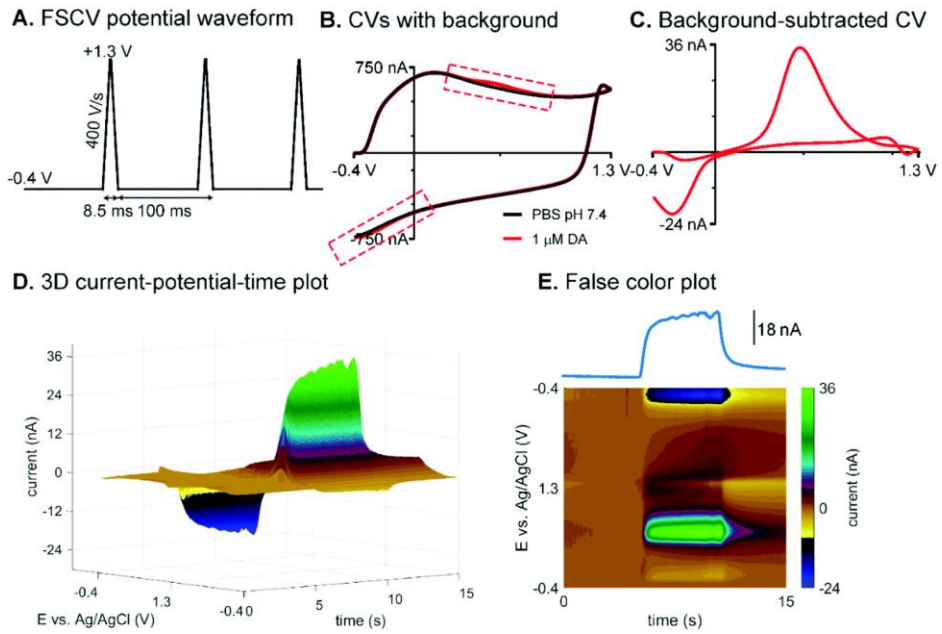

Figure 1.3 Example of dopamine detection via FSCV. A. FSCV dopamine waveform. The triangular waveform is applied on a CFME from -0.4 V to 1.3 V and back to -0.4 V at 400 V/s with a 10 Hz frequency. B. Example background cyclic voltammogram (CV). The black line is the background charging current for a CFME in PBS buffer (pH=7.4), the red line is the buffer with 1 µM dopamine. C. Background-subtracted CV of 1 µM dopamine. D. FSCV 3D current-potential-time plot of 1 µM dopamine. E. Conventional false color plot with anodic peak current–time trace of 5 s bolus injection of 1 µM dopamine. Figure re-print with permission from Puthongkham P, Venton BJ. Recent advances in fast-scan cyclic voltammetry. Analyst. 2020, 145, 1087-1102

Purinergic neuromodulators like adenosine require a higher oxidation potential than dopamine, therefore, the waveform's switching potential extends to 1.45 V for adenosine detection as shown in Figure 1.4 A. Figure 1.4 B presents the color plot of the 5 s bolus injection of adenosine and the peak current-time trace is shown above. Adenosine has three oxidation steps, but normally only the first two steps are detected on CFMEs. In FSCV, the primary peak appears around 1.3 V on the cathodic scan, and the secondary peak occurs at 1.1-1.2 V on the anodic scan. Figure 1.4 C shows the background subtracted CV for adenosine with this waveform. Additionally, the secondary peak at 1.1 V makes adenosine CV different from hydrogen peroxide. The two-peak shape in the adenosine CV is the fingerprint for its measurement *in vivo* or *ex vivo.*

Other waveforms have also been explored to improve sensitivity or selectivity in FSCV measurements. For example, the Jackson waveform was designed for serotonin detection in order to selectively detect serotonin over other interferents like dopamine. Further, the fast scan rate of the Jackson waveform also decreased serotonin polymerization, which fouls the electrode surface and ruins accurate long term measurements.[116] A sawhorse waveform was also explored to enhance the discrimination of adenosine, ATP, and hydrogen peroxide.[117]

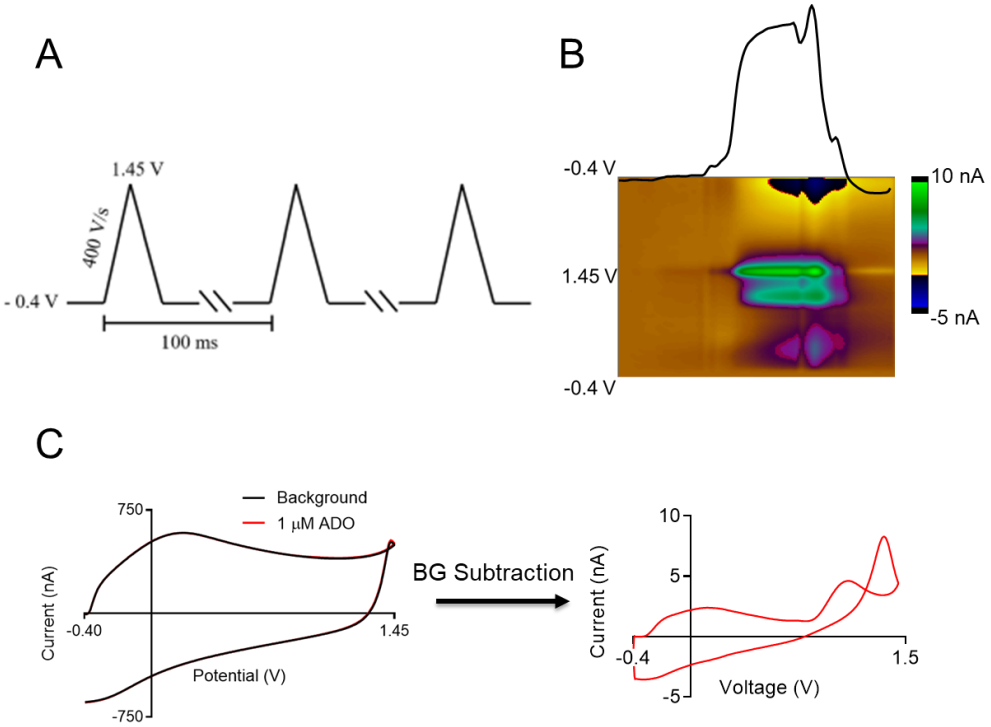

Figure 1.4 A. FSCV Adenosine waveform. B. The color plot with primary oxidation peak current-time trace of 5 s bolus injection of 1 μM adenosine. C. Background charging current and the background subtracted CV of 1 μM adenosine in FSCV.

1.3.3.1 Rapid adenosine with FSCV

Rapid adenosine release in the brain requires fast detection, and is normally monitored by FSCV because of its high temporal resolution. Figure 1.5 and 1.6 show representative data for rapid adenosine detection with FSCV in the rodent brain.

Figure 1.5 shows example color plots of spontaneous adenosine release *in vivo*. Similar to previous flow cell data, the primary and secondary oxidation peaks in the color plot are the fingerprints for adenosine detection. The primary peak current vs time traces is located above the color plot. The average concentration of spontaneous adenosine is in hundreds of nanomolar range, ~600 nM. In addition, spontaneous adenosine is randomly released and only lasts a few seconds. The frequency and the concentration of spontaneous adenosine events are different in different brain region.[90]

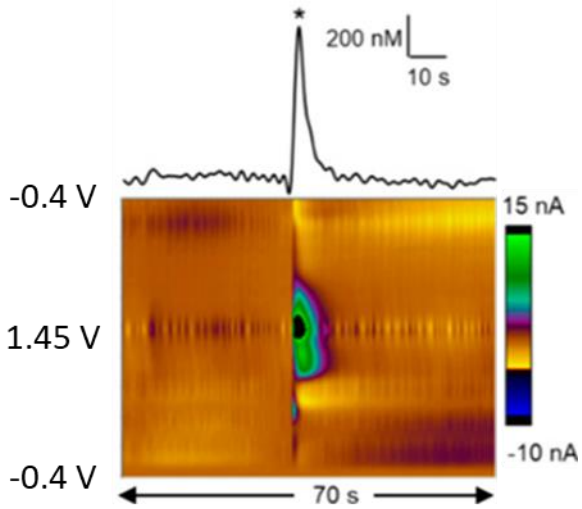

Figure 1.5 Example color plot of spontaneous adenosine release *in vivo* using FSCV. Concentration traces (top) and 3D color plot (bottom) for spontaneous adenosine detection in the hippocampus CA1 region. Adenosine transients are marked with stars in the concentration traces. The primary peak adenosine concentration is ~ 600 nM. Figure reprint with permission from Wang Y, Copeland J, Shin M, Chang Y, and Venton BJ. CD73 or CD39 Deletion Reveals Different Mechanisms of Formation for Spontaneous and Mechanically Stimulated Adenosine and Sex Specific Compensations in ATP Degradation. ACS Chem. Neurosci. 2020, 11, 6, 919–928.

Figure 1.6 is an example of mechanically-stimulated adenosine detection with FSCV. The color plots present two oxidation peaks for adenosine, and the CVs on the top present the 'fingerprint' for adenosine. The positive current in the color plot around 0.5 V could be from ionic changes due to the stimulation.[118] Mechanically-stimulated adenosine has a larger signal and lasts for 30-60 s, which is higher and longer than spontaneous adenosine. In addition, the concentration of mechanically-stimulated adenosine is smaller, and the duration is shorter in the brain slice model compared to *in vivo* measurements. The average concentration of

mechanically-stimulated adenosine could reach several micromolar *in vivo*, but the concentration of mechanically-stimulated adenosine in brain slices is only 0.5-1.0 µM.

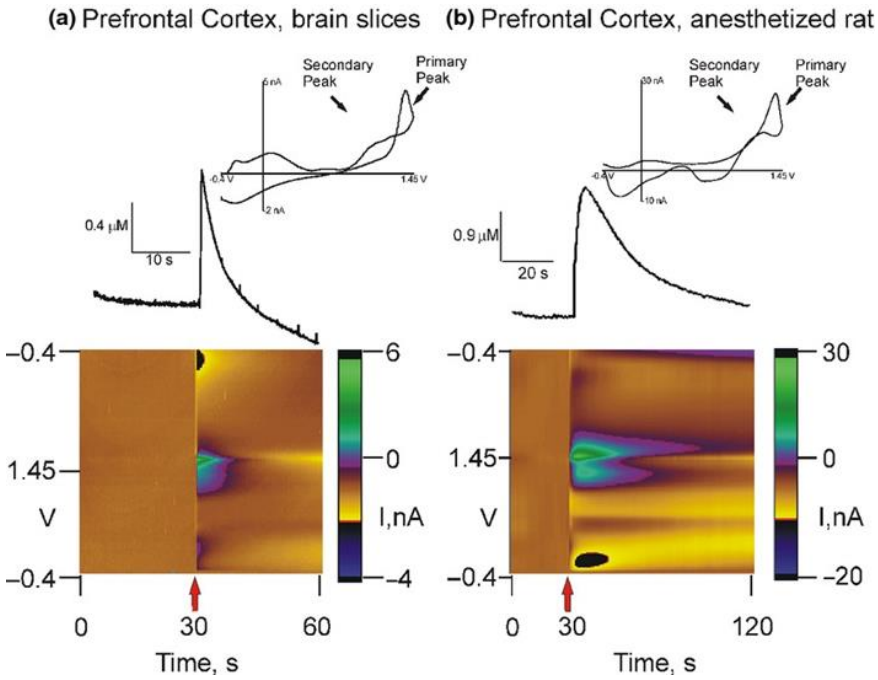

Figure 1.6 Mechanically-stimulated adenosine in rodent brain via FSCV. A. Mechanically-stimulated adenosine detection in the prefrontal cortex (PFC) in a brain slice. Inset CVs on the top show both the primary peak at 1.4 V and secondary peak at 1.2 V that indicate the signal is adenosine. The concentration vs time trace shows the primary peak change with time. The green/purple in the center of the 3D color plot represent the two peaks for adenosine oxidation shown in the CV. B. Mechanically-stimulated adenosine release in PFC *in vivo*. Figure reprint with permission from Ross AE, Nguyen MD, Privman E, Venton BJ. Mechanical stimulation evokes rapid increases in extracellular adenosine concentration in the prefrontal cortex. J Neurochem. 2014;130(1):50-60. Copyright 2014 John Wiley and Sons.

1.3.4 Multi-electrode measurements

Electrochemical methods combined with microelectrodes provide good sensitivity and high temporal resolution, but a single microelectrode used to detect neurotransmitters in the brain limits spatial resolution which limits the ability to characterize the range and interaction of neurotransmitter release in the brain. Therefore, multi-electrode measurements are under development for simultaneous detection in different regions in the brain.[99,119–121] For example, Wightman's group implanted multiple CFMEs in different hemispheres of the brain to

simultaneously detect dopamine *in vivo*, and they found the coordination of dopamine transients across hemispheres.[122] Sombers' group also used two different enzyme-coated CFME to simultaneously detect electrically-stimulated glucose and lactate with FSCV.[123] Further, Ewing's group used microelectrode arrays (MEA) combined with amperometry to measure dopamine in a single cell.[124] In addition, some research groups enhanced the density of detection sites by fabricating 16 microelectrodes to simultaneously monitor neurotransmitter in the brain.[125,126] Graybiel's group used a chronically-implanted electrode array to monitor dopamine in the brain.[127,128] Multi-electrode detection enhances the density of detection sites and also enables simultaneous detection on multiple compounds. However, multi-electrode detection has not been applied to adenosine measurement. Multiple channel detection will be useful for rapid adenosine measurement in the brain to characterize spatial resolution, and Chapter 5 will introduce the distance characterization on rapid adenosine release in brain slices using dual-channel FSCV.

1.3.5 Genetically-encoded sensors

Genetically-encoded sensors have become popular recently because of their high spatial resolution and selectivity. By using genetic engineering tools, part of the specific G protein-coupled receptor (GPCR) is replaced with a conformationally sensitive circularly permutated GFP (cpGFP).[129] The engineered protein inherits the binding affinity and pharmacological properties, which are important for endogenously released transmitter detection. Combined with fluorescence imaging, genetically-encoded sensors show high selectivity and spatial resolution to monitor neurotransmitter release. Because the signal detection comes from the binding between neurotransmitters and the modified GPCRs, this technique enables the direct detection of nonelectroactive species such as ACh and enhances the selectivity of catecholamine detection, which is a limitation with electrochemistry. Recently, multiple types of genetically encoded sensors have been developed for *in vivo* and *ex vivo*

experiments. For example, genetically encoded ACh sensors, $GRAB_{ACh2.0}$ was successfully applied in the brain for *in vivo* and *ex vivo* Ach studies.[130] Furthermore, Yulong Li's group optimized the ACh sensor ($GRAB_{ACh3.0}$) that showed better performance for Ach detection. GRAB sensors were successfully designed and used for dopamine, serotonin, adenosine, and glutamate detection in the rodent brain.[20,102,131–133]

Although genetically-encoded sensor measurements are visible and more selective in the brain, there are still some limitations due to how they were designed. Because the fluorescence signal comes from specific receptor binding, pharmacology experiments that target the same receptors are competitive with the aimed neurotransmitters and influence fluorescence results. Another drawback is the time resolution of clearance. The GRAB sensors are designed to have a strong binding affinity in order to have a high sensitivity, and the high K_{on} rate results in slower neurotransmitter clearance from the sensor, which limits the temporal resolution. In addition, fluorescence-based sensors are limited by color (normally only green or red), which makes it difficult for the GRAB sensors to simultaneously measure different neurotransmitters. The combination of GRAB sensors and FSCV will provide multiple analyte simultaneous detection in real-time with good spatial resolution, and the multiplex techniques will be able to monitor the interaction between different neurotransmitters in the future. GRAB sensors will provide the ability to image active sites and the detect nonelectroactive neurotransmitters. Meanwhile, FSCV provides fast temporal responses with both concentration information and multiple neurotransmitter detection. Chapter 6 proposes the future direction of this work and combines these techniques for multiple neurotransmitter detection.

1.4 Carbon-based microelectrode optimization

Caron fiber microelectrodes combined with FSCV have been used to probe neurochemical dynamics *in vivo* for decades.[98] They show good sensitivity and the 7 µm diameter of a CFME has less damage in the tissue. However, a CFME still possess several

limitations. The sensitivity of microelectrodes still need to improve to detect lower concentrations of neurotransmitters or neuropeptides.[99] Further, the selectivity of CFMEs is limited due to the similar CVs of different neurotransmitters. Biofouling is another common problem for neurochemical detection in complex tissues that limits the electrode surface area available and disturbs electron transfer kinetics, which reduces the sensitivity and accurate detection during *in vivo* measurements. The size of CFMEs is another hinderance, and new CFMEs will need to approach nanometer ranges for synaptic measurements. Thus, there are several strategies to optimize carbon-based microelectrodes to enhance their detection performance, such as carbon nanomaterials grown on micro-sized metal wires, 3D printed microelectrodes, and nanomaterial-coated CFMEs.

1.4.1 Carbon-based nanomaterials on metal wires

The advantage of growing carbon nanomaterials on an electrode via chemical vapor deposition (CVD) is that the pure nanoparticles can fully and evenly cover the electrode surface. Different types of microelectrodes by directly growing carbon nanoparticles on metal wires to improve dopamine detection. For example, carbon nanotubes (CNTs) and carbon nanospikes (CNSs) have been directly grown on metal wires and fabricated as cylinder microelectrodes for dopamine detection with FSCV.[134,135] The larger surface area and increased surface roughness enhance their performance for dopamine detection compared to a CFME.[136] In addition, the metal wire tip can reach nano-scale sizes by electrochemical etching, and carbon nanospikes can be fabricated with this method.[137] 3D printing techniques have also been developed to reach micro and even nanoscale resolution, and they allow different shape designs. After printing and carbonizing the polymer, the printed electrode provides good electrochemical performance for dopamine detection *in vitro* and *in vivo*.[138] All these carbon-based electrodes show good performance and further applications for neurotransmitter detection. However, their

fabrication steps are still more complicated than CFMEs, and they require expensive instruments, which currently limit their development and mass fabrication.

1.4.2 Surface treatment techniques to improve microelectrode performance

Additionally, there are other surface treatments that can be applied directly onto the microelectrode to improve its performance.[99,139] Many of these methods etch the carbon surface to generate more defect sites for dopamine adsorption and enhance its sensitivity. Alternatively, etching is also used to achieve a smaller electrode size, such as a nano-sized needle. For example, applying a constant 2.0 V potential on a CFME in KOH solution significantly enhances dopamine sensitivity due to increased oxygen functional groups on the electrode surface.[140] In addition, the base treatment also peels off the electrode surface, which can be useful for surface cleaning after the electrode is fouled in tissue experiments. The Sombers' group also used base treatments to etch the CFME to fabricate nano-sized carbon fiber electrodes, and the tip could be etched to several hundreds of nanometer in diameter.[141] The size of a flame-etched CFMEs also reaches several hundreds of nanometers, and these nanoelectrodes have been successfully used for single-cell measurement.[114,115,142] Oxygen plasma treatment is another useful technique that increases oxygen functional groups on the surface to improve sensitivity. For example, CNT yarn microelectrodes enhance dopamine sensitivity by three-fold after oxygen plasma etching with a microwave plasma system with oxygen gas flow.[143]

1.4.3 Carbon Nanomaterial-coated CFMEs to improve performance

Carbon nanomaterials and metal nanomaterials are mainly used for CFME modification to enhance the electrode's performance. The nanoparticles on the electrode surface increase the surface area and available reactive sites for electroactive analyte adsorption to improve the sensitivity of microelectrodes in FSCV. For example, gold and platinum nanoparticles were recently coated on CFMEs and showed increased surface area and a higher density of states on the electrode surface, which increased the sensitivity and electron transfer rate for dopamine

compared to bare CFMEs.[144] However, the toxicity of metal nanoparticles in live tissue is still not fully clear, and it might not as safe as carbon-based nanomaterials. Therefore, in this section, carbon-based nanomaterials are mainly discussed for improving CFME performance. The methods of coating nanomaterials on a CFME are relatively easier than growing nanomaterials on a metal wire, but the surface coverage and the amount of coating are difficult to control.

Carbon nanomaterials such as graphene, carbon nanotubes (CNTs), and nanodiamond are broadly used for electrode and sensor modifications. Figure 1.7 shows the structure of some commonly used carbon nanomaterials. CNTs are considered as graphene rolled into a tube structure, and they have been used for surface coating on conventional electrodes such as glassy carbon and carbon-fiber microelectrodes to enhance the electrode performance.[145] CNTs provide more surface area and roughness to the electrode and also improve electrode kinetics due to their electrocatalytic effects.[146] The electrocatalytic effects of CNTs might come from small metal particles, like Ni, that remain during CNT synthesis. Besides CNTs, carbon nanohorns (CNHs) are another similar carbon nanomaterial that can be electrodeposited onto a CFME. Our lab showed that CNHs modified CFMEs enhance dopamine sensitivity over two-fold.[147]

Diamond is a different type of stable, sp^3 carbon that acts as an insulator.[148,149] However, by doping defects on the diamond structure, diamond derivates provide some unique electrochemical properties. For example, boron-doped diamonds (BDDs) are broadly used as a standard electrode in electrochemistry due to the stability and wide potential window of diamonds.[150] In addition, the diamond structure is mainly H-terminated, and fewer surface functional groups enhance the anti-fouling property on diamond electrodes. Further, nanodiamond is a nano-sized diamond that is sp^3 hybridized with sp^2 defects and some oxygen-functional groups.[151] The defects and sp^2 nature of nanodiamond improve the electrochemical performance compared to BDD electrodes, and their ability to disperse in water makes it easier

to coat them on an electrode's surface. Our lab previously drop-casted nanodiamond on CFMEs, which provided higher sensitivity for dopamine detection and better anti-fouling property compared to a bare CFME.[152]

Carbon quantum dots (CQD) or graphene quantum dots (GQD) are sp^3-carbon nanoparticles that contain multiple oxygen functional groups with spherical structures.[148,153] The high surface area and abundant oxygen functional groups provide good sensitivity for dopamine detection, and electrodes modified by CQD improved the sensitivity and electrocatalytic properties for dopamine detection.[154]

Graphene is a 2D structured carbon nanomaterial that is considered a single layer of graphite.[155] Due to the difficulty of obtaining a single-layer structure, multiple layers that are less than 10 layers of graphene are also regarded as graphene materials. Pure graphene has very good conductivity because of the sp^2 hybridized carbon, and the large π-π stacking force makes graphene easy to aggregate. Moreover, multiple-layer graphene has many edge-planes, which could be oxidized to generate defects, and these defects are good for dopamine detection in electrochemistry.[156–158] Therefore, graphene and its derivatives, like graphene oxide, are popular for electrode surface treatment. For example, reduced graphene oxide (rGO) has been used as an electrode coating to enhance sensitivity.[159,160] Also, graphene oxide (GO) is broadly used for enzyme immobilization on biosensor fabrications.[108,157] Graphene oxide is a potential nanomaterial for CFME modification because it has more functional groups for dopamine adsorption, good conductivity, and a huge surface area. The abundant oxygen functional groups also improve the hydrophilicity of GO, and its ability to disperse in water simplifies the electrode coating process.

In summary, previous research indicates that nanomaterial modified CFME provide better performance for dopamine detection by increasing the surface area with defects as functional groups. However, no directly coated GO on CFME has been investigated. Chapter 5

will discuss how different coating methods influence the GO modified CFME surface and optimize the GO/CFME to improve dopamine detection in a flow cell and mouse brain slice.

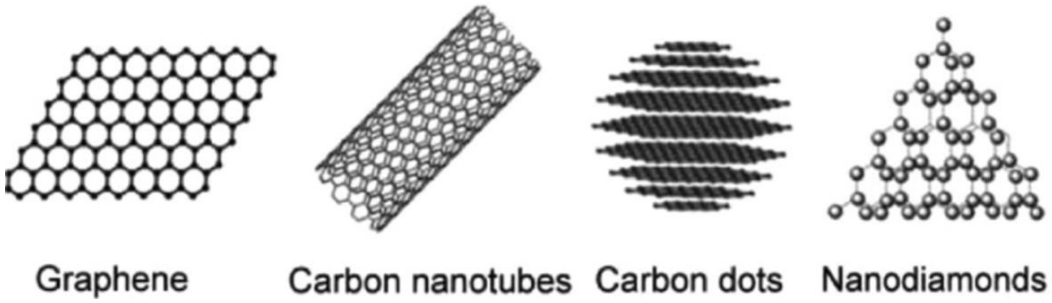

Figure 1.7 Structure of carbon nanomaterials. Graphene, carbon nanotube (CNT), carbon quantum dots (CQD), and Nanodiamond.[148]

1.5 Overview of the dissertation

FSCV combined with CFMEs has been used for real-time neurotransmitter detection for several decades; however, there are still some limitations such as the microelectrode's performance and poor spatial resolution. This dissertation explores different methods that characterize the mechanisms of rapid adenosine in mouse brain slices and investigates improvements to the microelectrode to enhance its performance.

For several years, our lab has investigated the mechanisms of rapid adenosine release in the mouse brain, but we still need more characterizations to understand the role of rapid adenosine in the brain. Traditionally, pharmacology studies are applied in brain slices to characterize the mechanisms of adenosine release. However, some of the drugs are not perfectly selective and might inhibit or stimulate undesired receptors. Therefore, this dissertation uses different types of knockout mice models to investigate rapid adenosine neuromodulation pathways in mouse brain. Chapter 2 investigates how adenosine A_1 and A_{2A} receptors modulate rapid adenosine release in mouse brain slices using global A_1 knockout mice and A_{2A} knockout mice (wild type C57BL/6J (WT) mice were used in control experiments). The results indicate

that A_1 and A_{2A} receptors modulate spontaneous adenosine in a different way, but they do not influence the amount of mechanically-stimulated adenosine release. Chapter 3 explores the extent to which the Pannexin 1 channel acts as a source of rapid adenosine release using Pannexin 1 knockout mice. A non-specific inhibitor of pannexin and connexin channels, carbenoxolone, is applied on WT mice to determine the other gap junction proteins' influence on rapid adenosine release. Pannexin 1 channels do not impact spontaneous adenosine release, but partially influence the concentration of mechanically-stimulated adenosine release in the CA1 region.

Second, in order to characterize the range of rapid adenosine release that could potentially affect the brain, dual-channel FSCV was applied to simultaneously monitor rapid adenosine in the CA1 region at different distances. Chapter 4 shows how simultaneous detection characterizes the range of rapid adenosine neuromodulation. Mechanically-stimulated adenosine was detectable within a 200 μm range, but spontaneous adenosine release was random and localized in the CA1 region. Only few spontaneous adenosine events might release coordinately.

Finally, carbon nanomaterial coatings were applied to enhance the microelectrode's performance for neurotransmitter detection. Chapter 5 compares different coating methods to optimize graphene-oxide (GO) modified CFME for dopamine detection. GO particles increase the surface area and provide more oxygen functional groups to enhance dopamine adsorption. Drop casting, dip coating, and electrodeposition are three basic coating methods for nanomaterial coating. For GO modified CFME, electrodeposition shows the best reproducibility and produces relatively smooth coating. In contrast, with drop casting, it is difficult to coat a single layer on the surface, and GO particles easily aggregate due to π-π stacking. The aggregation of GO on the surface slows down electron transfer kinetics and generates more noise. Therefore, the optimized application method is electrodeposition of GO directly on the

CFME, which provides a 2-fold sensitivity increase for dopamine detection. Moreover, the modified microelectrode is able to be applied in mouse brain slices for dopamine detection.

Overall, this dissertation uses different experimental designs to investigate the mechanisms of rapid adenosine release in a mouse brain slice model, and also optimizes the carbon-fiber microelectrode by using carbon nanomaterial modification that is applied in a brain slice for real-time dopamine detection. In the future, different types of carbon-based microelectrodes could be applied in a brain slice to simultaneously monitor dopamine release via multiple channel FSCV, and this comparison in complex tissue will provide more useful information on different microelectrodes for further applications. In addition, chapter 6 also introduces the future direction of multiplexing analytical tools to simultaneously monitor neurotransmitters in the brain. Combining FSCV with GRAB sensors will not only expand their ability to monitor neurotransmitter interactions, but also enhance spatial resolution. It is difficult to characterize how rapid adenosine modulates other neurotransmitter release in the brain via a single analytical tool (FSCV or GRAB sensors). However, simultaneous detection with multiplexed analytical tools will reveal more information on neurotransmitter interactions in the brain in real-time. By understanding the mechanisms of rapid adenosine release, new therapies that affect adenosine neuromodulation can be investigated in the future to treat several debilitating neurological diseases.

1.6 References

(1) Fredholm, B. B.; Chen, J. F.; Cunha, R. A.; Svenningsson, P.; Vaugeois, J. M. Adenosine and Brain Function. *Int. Rev. Neurobiol.* **2005**, *63*, 191–270. https://doi.org/10.1016/S0074-7742(05)63007-3.

(2) Cunha, R. A. Adenosine as a Neuromodulator and as a Homeostatic Regulator in the Nervous System: Different Roles, Different Sources and Different Receptors. *Neurochem. Int.* **2001**, *38* (2), 107–125. https://doi.org/10.1016/S0197-0186(00)00034-6.

(3) Cunha, R. A. How Does Adenosine Control Neuronal Dysfunction and Neurodegeneration? *J. Neurochem.* **2016**, *139* (6), 1019–1055. https://doi.org/10.1111/jnc.13724.

(4) Fredholm, B. B. Chapter 11 Adenosine and Neuroprotection. In *Neuroprotective Agents and Cerebral Ischaemia*; Green, A. R., Cross, A. J., Eds.; International Review of Neurobiology; Academic Press, 1996; Vol. 40, pp 259–280. https://doi.org/https://doi.org/10.1016/S0074-7742(08)60723-0.

(5) Stenberg, D.; Litonius, E.; Halldner, L.; Johansson, B.; Fredholm, B. B.; Porkka-Heiskanen, T. Sleep and Its Homeostatic Regulation in Mice Lacking the Adenosine A1 Receptor. *J. Sleep Res.* **2003**, *12* (4), 283–290. https://doi.org/10.1046/j.0962-1105.2003.00367.x.

(6) Ledent, C.; Vaugeois, J.-M.; Schiffmann, S. N.; Pedrazzini, T.; Yacoubi, M. El; Vanderhaeghen, J.-J.; Costentin, J.; Heath, J. K.; Vassart, G.; Parmentier, M. Aggressiveness, Hypoalgesia and High Blood Pressure in Mice Lacking the Adenosine A2a Receptor. *Nature* **1997**, *388* (6643), 674–678. https://doi.org/10.1038/41771.

(7) O'Regan, M. Adenosine and the Regulation of Cerebral Blood Flow. *Neurol. Res.* **2005**, *27* (2), 175–181. https://doi.org/10.1179/016164105X21931.

(8) Sollevi, A. Adenosine for Pain Control. *Acta Anaesthesiol. Scand. Suppl.* **1997**, *110*, 135–136. https://doi.org/10.1111/j.1399-6576.1997.tb05532.x.

(9) Kalinchuk, A. V.; Urrila, A. S.; Alanko, L.; Heiskanen, S.; Wigren, H. K.; Suomela, M.; Stenberg, D.; Porkka-Heiskanen, T. Local Energy Depletion in the Basal Forebrain Increases Sleep. *Eur. J. Neurosci.* **2003**, *17* (4), 863–869. https://doi.org/10.1046/j.1460-9568.2003.02532.x.

(10) Augusto, E.; Matos, M.; Sévigny, J.; El-Tayeb, A.; Bynoe, M. S.; Müller, C. E.; Cunha, R. a; Chen, J.-F. Ecto-5'-Nucleotidase (CD73)-Mediated Formation of Adenosine Is Critical for the Striatal Adenosine A2A Receptor Functions. *J. Neurosci.* **2013**, *33* (28), 11390–11399. https://doi.org/10.1523/JNEUROSCI.5817-12.2013.

(11) Boison, D. Adenosine as a Neuromodulator in Neurological Diseases. *Curr. Opin. Pharmacol.* **2008**, *8* (1), 2–7. https://doi.org/https://doi.org/10.1016/j.coph.2007.09.002.

(12) Cunha, R. A. Neuroprotection by Adenosine in the Brain: From A1 Receptor Activation to A2A Receptor Blockade. *Purinergic Signalling*. 2005, pp 111–134. https://doi.org/10.1007/s11302-005-0649-1.

(13) Drury, A. N.; Szent-Györgyi, A. The Physiological Activity of Adenine Compounds with Especial Reference to Their Action upon the Mammalian Heart. *J. Physiol.* **1929**, *68* (3), 213–237. https://doi.org/10.1113/jphysiol.1929.sp002608.

(14) Berne, R. M. Cardiac Nucleotides in Hypoxia: Possible Role in Regulation of Coronary Blood Flow. *Am. J. Physiol. Content* **1963**, *204* (2), 317–322. https://doi.org/10.1152/ajplegacy.1963.204.2.317.

(15) Nesbitt, K. M.; Jaquins-Gerstl, A.; Skoda, E. M.; Wipf, P.; Michael, A. C. Pharmacological Mitigation of Tissue Damage during Brain Microdialysis. *Anal. Chem.* **2013**, *85* (17), 8173–8179. https://doi.org/10.1021/ac401201x.

(16) Sharma, R.; Engemann, S. C.; Sahota, P.; Thakkar, M. M. Effects of Ethanol on Extracellular Levels of Adenosine in the Basal Forebrain: An in Vivo Microdialysis Study in Freely Behaving Rats. *Alcohol. Clin. Exp. Res.* **2010**, *34* (5), 813–818. https://doi.org/10.1111/j.1530-0277.2010.01153.x.

(17) Mitchell, J. B.; Lupica, C. R.; Dunwiddie, T. V. Activity-Dependent Release of Endogenous Adenosine Modulates Synaptic Responses in the Rat Hippocampus. *J. Neurosci.* **1993**, *13* (8), 3439–3447. https://doi.org/10.1523/jneurosci.13-08-03439.1993.

(18) Nguyen, M. D.; Venton, B. J. Fast-Scan Cyclic Voltammetry for the Characterization of Rapid Adenosine Release. *Comput. Struct. Biotechnol. J.* **2015**, *13*, 47–54. https://doi.org/10.1016/j.csbj.2014.12.006.

(19) Llaudet, E.; Botting, N. P.; Crayston, J. A.; Dale, N. A Three-Enzyme Microelectrode Sensor for Detecting Purine Release from Central Nervous System. *Biosens. Bioelectron.* **2003**, *18* (1), 43–52. https://doi.org/https://doi.org/10.1016/S0956-5663(02)00106-9.

(20) Wu, Z.; Cui, Y.; Wang, H.; Song, K.; Yuan, Z.; Dong, A.; Wu, H.; Wan, Y.; Pan, S.; Peng, W.; Jing, M.; Xu, M.; Luo, M.; Li, Y. *A GRAB Sensor Reveals Activity-Dependent Non-Vesicular Somatodendritic Adenosine Release*; 2020. https://doi.org/10.1101/2020.05.04.075564.

(21) Latini, S.; Pedata, F. Adenosine in the Central Nervous System: Release Mechanisms and Extracellular Concentrations. *J. Neurochem.* **2001**, *79* (3), 463–484. https://doi.org/10.1046/j.1471-4159.2001.00607.x.

(22) Park, J.; Gupta, R. Adenosine Metabolism, Adenosine Kinase, and Evolution. In *Adenosine: A Key Link between Metabolism and Brain Activity*; 2013; pp 23–54. https://doi.org/10.1007/978-1-4614-3903-5_2.

(23) Pedata, F.; Corsi, C.; Melani, A.; Bordoni, F.; Latini, S. Adenosine Extracellular Brain Concentrations and Role of A2A Receptors in Ischemia. *Ann. New York Acad. Sci.* **2001**, *939* (1), 74–84.

(24) Lloyd, H. G. E.; Fredholm, B. B. Involvement of Adenosine Deaminase and Adenosine Kinase in Regulating Extracellular Adenosine Concentration in Rat Hippocampal Slices. *Neurochem. Int.* **1995**, *26* (4), 387–395. https://doi.org/10.1016/0197-0186(94)00144-J.

(25) Masino, S.; Bioson, D. *Adenosine : A Key Link between Metabolism and Brain Activity*; Springer US, 2013; Vol. 148.

(26) Westfall, D. P.; Todorov, L. D.; Mihaylova-Todorova, S. T. ATP as a Cotransmitter in Sympathetic Nerves and Its Inactivation by Releasable Enzymes. *J. Pharmacol. Exp. Ther.* **2002**, *303* (2), 439–444. https://doi.org/10.1124/jpet.102.035113.

(27) Street, S. E.; Walsh, P. L.; Sowa, N. A.; Taylor-Blake, B.; Guillot, T. S.; Vihko, P.; Wightman, R. M.; Zylka, M. J. PAP and NT5E Inhibit Nociceptive Neurotransmission by Rapidly Hydrolyzing Nucleotides to Adenosine. *Mol. Pain* **2011**, *7*, 1–15.

https://doi.org/10.1186/1744-8069-7-80.

(28) Cunha, R. A. Regulation of the Ecto-Nucleotidase Pathway in Rat Hippocampal Nerve Terminals. *Neurochem. Res.* **2001**, *26* (8–9), 979–991. https://doi.org/10.1023/A:1012392719601.

(29) Schock, S. C.; LeBlanc, D.; Hakim, A. M.; Thompson, C. S. ATP Release by Way of Connexin 36 Hemichannels Mediates Ischemic Tolerance in Vitro. *Biochem. Biophys. Res. Commun.* **2008**, *368* (1), 138–144. https://doi.org/10.1016/j.bbrc.2008.01.054.

(30) Thompson, R. J.; MacVicar, B. Connexin and Pannexin Hemichannels of Neurons and Astrocytes. *Channels* **2008**, *2* (2), 81–86. https://doi.org/10.4161/chan.2.2.6003.

(31) Sebastião, A. M.; Ribeiro, J. A. Neuromodulation and Metamodulation by Adenosine: Impact and Subtleties upon Synaptic Plasticity Regulation. *Brain Res.* **2015**, *1621*, 102–113. https://doi.org/10.1016/j.brainres.2014.11.008.

(32) Borea, P. A.; Varani, K.; Gessi, S.; Merighi, S.; Vincenzi, F. *The Adenosine Receptors*; The Receptors; Springer International Publishing, 2018.

(33) Fredholm, B. B.; Arslan, G.; Halldner, L.; Kull, B.; Schulte, G.; Wasserman, W. Structure and Function of Adenosine Receptors and Their Genes. *Naunyn. Schmiedebergs. Arch. Pharmacol.* **2000**, *362* (4–5), 364–374. https://doi.org/10.1007/s002100000313.

(34) Borea, P. A.; Gessi, S.; Merighi, S.; Vincenzi, F.; Varani, K. Pathological Overproduction: The Bad Side of Adenosine. *Br. J. Pharmacol.* **2017**, *174* (13), 1945–1960. https://doi.org/10.1111/bph.13763.

(35) Dunwiddie, T. V; Masino, S. a. The Role and Regulation of Adenosine in the Central Nervous System. *Annu. Rev. Pharmacol. Toxicol.* **2001**, *41* (1), 145–174.

(36) Thompson, S. M.; Haas, H. L.; Gähwiler, B. H. Comparison of the Actions of Adenosine at Pre- and Postsynaptic Receptors in the Rat Hippocampus in Vitro. *J. Physiol.* **1992**, *451* (1), 347–363. https://doi.org/10.1113/jphysiol.1992.sp019168.

(37) Reppert, S. M.; Weaver, D. R.; Stehle, J. H.; Rivkees, S. A. Molecular Cloning and Characterization of a Rat A1-Adenosine Receptor That Is Widely Expressed in Brain and Spinal Cord. *Mol. Endocrinol.* **1991**, *5* (8), 1037–1048. https://doi.org/10.1210/mend-5-8-1037.

(38) Cunha, R. A. Neuroprotection by Adenosine in the Brain: From A1 Receptor Activation to A2A Receptor Blockade. *Purinergic Signal.* **2005**, *1* (2), 111–134. https://doi.org/10.1007/s11302-005-0649-1.

(39) Ross, A. E.; Venton, B. J. Adenosine Transiently Modulates Stimulated Dopamine Release in the Caudate-Putamen via A1 Receptors. *J. Neurochem.* **2015**, *132*, 51–60. https://doi.org/10.1111/jnc.12946.

(40) Nguyen, M. D.; Wang, Y.; Ganesana, M.; Venton, B. J. Transient Adenosine Release Is Modulated by NMDA and GABAB Receptors. *ACS Chem. Neurosci.* **2017**, *8* (2), 376–385. https://doi.org/10.1021/acschemneuro.6b00318.

(41) Hartwick, A. T. E.; Lalonde, M. R.; Barnes, S.; Baldridge, W. H. Adenosine A1-Receptor Modulation of Glutamate-Induced Calcium Influx in Rat Retinal Ganglion Cells. *Investig. Ophthalmol. Vis. Sci.* **2004**, *45* (10), 3740–3748. https://doi.org/10.1167/iovs.04-0214.

(42) Pan, W. J.; Osmanović, S. S.; Shefner, S. A. Characterization of the Adenosine A1 Receptor-Activated Potassium Current in Rat Locus Ceruleus Neurons. *J. Pharmacol. Exp. Ther.* **1995**, *273* (1), 537–544.

(43) Fretwell, L.; Dickenson, J. M. Role of Large-Conductance Ca2+-Activated Potassium Channels in Adenosine A1 Receptor-Mediated Pharmacological Preconditioning in H9c2 Cells. *Eur. J. Pharmacol.* **2009**, *618* (1–3), 37–44. https://doi.org/10.1016/j.ejphar.2009.07.008.

(44) de Mendonça, A.; Sebastião, A. M.; Ribeiro, A. J. Inhibition of NMDA Receptor-Mediated Currents in Isolated Rat Hippocampal Neurones by Adenosine A1 Receptor Activation. *Neuroreport* **1995**, *6* (8), 1097–1100.

(45) Moreau, J.-L.; Huber, G. Central Adenosine A2A Receptors: An Overview. *Brain Res. Rev.* **1999**, *31* (1), 65–82. https://doi.org/https://doi.org/10.1016/S0165-0173(99)00059-4.

(46) Chen, J.; Moratalla, R.; Impagnatiello, F.; Grandy, D. K.; Cuellar, B.; Rubinstein, M.; Beilstein, M. A.; Hackett, E.; Fink, J. S.; Low, M. J.; Ongini, E.; Schwarzschild, M. A. The Role of the D2 Dopamine Receptor (D2R) in A2A Adenosine Receptor (A2AR)-Mediated Behavioral and Cellular Responses as Revealed by A2A and D2 Receptor Knockout Mice. *PNAS* **2001**, *98* (4), 1970–1975.

(47) Popoli, P.; Betto, P.; Reggio, R.; Ricciarello, G. Adenosine A2A Receptor Stimulation Enhances Striatal Extracellular Glutamate Levels in Rats. *Eur. J. Pharmacol.* **1995**, *287* (2), 215–217. https://doi.org/https://doi.org/10.1016/0014-2999(95)00679-6.

(48) Schiffmann, S. N.; Fisone, G.; Moresco, R.; Cunha, R. A.; Ferré, S. Adenosine A2A Receptors and Basal Ganglia Physiology. *Prog. Neurobiol.* **2007**, *83* (5), 277–292. https://doi.org/10.1016/j.pneurobio.2007.05.001.

(49) Hettinger, B. D.; Lee, A.; Linden, J.; Rosin, D. L. Ultrastructural Localization of Adenosine A2A Receptors Suggests Multiple Cellular Sites for Modulation of GABAergic Neurons in Rat Striatum. *J. Comp. Neurol.* **2001**, *431* (3), 331–346. https://doi.org/10.1002/1096-9861(20010312)431:3<331::AID-CNE1074>3.0.CO;2-W.

(50) Koga, K.; Jenner, P.; Hakko, K.; Company, K. The Role of Adenosine A2a Receptors in Regulating GABAergic Synaptic Transmission in Striatal Medium Spiny Neurons. *Prog. Neurobiol.* **1996**, *76* (2), 605–611.

(51) Cunha, R. A.; Johansson, B.; Fredholm, B. B.; Alexandre Ribeiro, J.; Sebastião, A. M. Adenosine A2A Receptors Stimulate Acetylcholine Release from Nerve Terminals of the Rat Hippocampus. *Neurosci. Lett.* **1995**, *196* (1), 41–44. https://doi.org/https://doi.org/10.1016/0304-3940(95)11833-I.

(52) El Yacoubi, M.; Ledent, C.; Ménard, J. F.; Parmentier, M.; Costentin, J.; Vaugeois, J. M. The Stimulant Effects of Caffeine on Locomotor Behaviour in Mice Are Mediated through Its Blockade of Adenosine A(2A) Receptors. *Br. J. Pharmacol.* **2000**, *129* (7), 1465–1473. https://doi.org/10.1038/sj.bjp.0703170.

(53) Baldwin, S. A.; Beal, P. R.; Yao, S. Y. M.; King, A. E.; Cass, C. E.; Young, J. D. The Equilibrative Nucleoside Transporter Family, SLC29. *Pflugers Arch. Eur. J. Physiol.* **2004**, *447* (5), 735–743. https://doi.org/10.1007/s00424-003-1103-2.

(54) Thorn, J. A.; Jarvis, S. M. Adenosine Transporters. *Gen. Pharmacol.* **1996**, *27* (4), 613–620. https://doi.org/10.1016/0306-3623(95)02053-5.

(55) Bruzzone, R.; Hormuzdi, S. G.; Barbe, M. T.; Herb, A.; Monyer, H. Pannexins, a Family of Gap Junction Proteins Expressed in Brain. *Proc. Natl. Acad. Sci.* **2003**, *100* (23), 13644–13649. https://doi.org/10.1073/pnas.2233464100.

(56) Bond, S. R.; Lau, A.; Penuela, S.; Sampaio, A. V.; Underhill, T. M.; Laird, D. W.; Naus, C. C. Pannexin 3 Is a Novel Target for Runx2, Expressed by Osteoblasts and Mature Growth Plate Chondrocytes. *J. Bone Miner. Res.* **2011**, *26* (12), 2911–2922. https://doi.org/10.1002/jbmr.509.

(57) Chiu, Y.-H.; Jin, X.; Medina, C. B.; Leonhardt, S. A.; Kiessling, V.; Bennett, B. C.; Shu, S.; Tamm, L. K.; Yeager, M.; Ravichandran, K. S.; Bayliss, D. A. A Quantized Mechanism for Activation of Pannexin Channels. *Nat. Commun.* **2017**, *8*, 14324. https://doi.org/10.1038/ncomms14324.

(58) Bao, L.; Locovei, S.; Dahl, G. Pannexin Membrane Channels Are Mechanosensitive Conduits for ATP. *FEBS Lett.* **2004**, *572* (1–3), 65–68. https://doi.org/10.1016/j.febslet.2004.07.009.

(59) Wang, Y.; Venton, B. J. Caffeine Modulates Spontaneous Adenosine and Oxygen Changes during Ischemia and Reperfusion. *ACS Chem. Neurosci.* **2019**, *10* (4), 1941–1949. https://doi.org/10.1021/acschemneuro.8b00251.

(60) Lin, Y.; Phillis, J. W. Deoxycoformycin and Oxypurinol: Protection against Focal Ischemic Brain Injury in the Rat. *Brain Res.* **1992**, *571* (2), 272–280. https://doi.org/https://doi.org/10.1016/0006-8993(92)90665-V.

(61) Dale, N.; Frenguelli, B. Release of Adenosine and ATP During Ischemia and Epilepsy. *Curr. Neuropharmacol.* **2009**, *7* (3), 160–179. https://doi.org/10.2174/157015909789152146.

(62) During, M. J.; Spencer, D. D. Adenosine: A Potential Mediator of Seizure Arrest and Postictal Refractoriness. *Ann. Neurol.* **1992**, *32* (5), 618–624. https://doi.org/10.1002/ana.410320504.

(63) Li, T.; Ren, G.; Lusardi, T.; Wilz, A.; Lan, J. Q.; Iwasato, T.; Itohara, S.; Simon, R. P.; Boison, D. Adenosine Kinase Is a Target for the Prediction and Prevention of Epileptogenesis in Mice. *J. Clin. Invest.* **2008**, *118* (2), 571–582. https://doi.org/10.1172/JCI33737.

(64) Fedele, D. E.; Gouder, N.; Güttinger, M.; Gabernet, L.; Scheurer, L.; Rülicke, T.; Crestani, F.; Boison, D. Astrogliosis in Epilepsy Leads to Overexpression of Adenosine Kinase, Resulting in Seizure Aggravation. *Brain* **2005**, *128* (10), 2383–2395. https://doi.org/10.1093/brain/awh555.

(65) Gouder, N.; Fritschy, J.-M.; Boison, D. Seizure Suppression by Adenosine A1 Receptor Activation in a Mouse Model of Pharmacoresistant Epilepsy. *Epilepsia* **2003**, *44* (7), 877–885. https://doi.org/10.1046/j.1528-1157.2003.03603.x.

(66) Nampiaparampil, D. E. Prevalence of Chronic Pain after Traumatic Brain Injury: A Systematic Review. *JAMA* **2008**, *300* (6), 711–719. https://doi.org/10.1001/jama.300.6.711.

(67) Moore, E. L.; Terryberry-Spohr, L.; Hope, D. A. Mild Traumatic Brain Injury and Anxiety Sequelae: A Review of the Literature. *Brain Inj.* **2006**, *20* (2), 117–132. https://doi.org/10.1080/02699050500443558.

(68) Bruns, J. J.; Hauser, W. A. The Epidemiology of Traumatic Brain Injury: A Review. *Epilepsia* **2003**, *44* (s10), 2–10. https://doi.org/10.1046/j.1528-1157.44.s10.3.x.

(69) Verma, A.; Anand, V.; Verma, N. P. Sleep Disorders in Chronic Traumatic Brain Injury. *J. Clin. sleep Med. JCSM Off. Publ. Am. Acad. Sleep Med.* **2007**, *3* (4), 357–362.

(70) Lusardi, T. Adenosine Neuromodulation and Traumatic Brain Injury. *Curr. Neuropharmacol.* **2009**, *7* (3), 228–237. https://doi.org/10.2174/157015909789152137.

(71) Jenner, P.; Mori, A.; Hauser, R.; Morelli, M.; Fredholm, B. B.; Chen, J. F. Adenosine, Adenosine A2A Antagonists, and Parkinson's Disease. *Parkinsonism Relat. Disord.* **2009**, *15* (6), 406–413. https://doi.org/https://doi.org/10.1016/j.parkreldis.2008.12.006.

(72) Schwarzschild, M. A.; Agnati, L.; Fuxe, K.; Chen, J.-F.; Morelli, M. Targeting Adenosine A2A Receptors in Parkinson's Disease. *Trends Neurosci.* **2006**, *29* (11), 647–654. https://doi.org/10.1016/j.tins.2006.09.004.

(73) Fuxe, K.; Marcellino, D.; Genedani, S.; Agnati, L. Adenosine A(2A) Receptors, Dopamine D(2) Receptors and Their Interactions in Parkinson's Disease. *Mov. Disord.* **2007**, *22* (14), 1990–2017. https://doi.org/10.1002/mds.21440.

(74) Jacobson, K. A.; Gao, Z.-G. Adenosine Receptors as Therapeutic Targets. *Nat. Rev. Drug Discov.* **2006**, *5* (3), 247–264. https://doi.org/10.1038/nrd1983.

(75) Kumar, A.; Singh, A.; Ekavali. A Review on Alzheimer's Disease Pathophysiology and Its Management: An Update. *Pharmacol. Reports* **2015**, *67* (2), 195–203. https://doi.org/https://doi.org/10.1016/j.pharep.2014.09.004.

(76) Sadigh-Eteghad, S.; Sabermarouf, B.; Majdi, A.; Talebi, M.; Farhoudi, M.; Mahmoudi, J. Amyloid-Beta: A Crucial Factor in Alzheimer's Disease. *Med. Princ. Pract.* **2015**, *24* (1), 1–10. https://doi.org/10.1159/000369101.

(77) Arendash, G. W.; Schleif, W.; Rezai-Zadeh, K.; Jackson, E. K.; Zacharia, L. C.; Cracchiolo, J. R.; Shippy, D.; Tan, J. Caffeine Protects Alzheimer's Mice against Cognitive Impairment and Reduces Brain β-Amyloid Production. *Neuroscience* **2006**, *142* (4), 941–952. https://doi.org/https://doi.org/10.1016/j.neuroscience.2006.07.021.

(78) Dall'Igna, O. P.; Fett, P.; Gomes, M. W.; Souza, D. O.; Cunha, R. A.; Lara, D. R. Caffeine and Adenosine A2a Receptor Antagonists Prevent β-Amyloid (25–35)-Induced Cognitive Deficits in Mice. *Exp. Neurol.* **2007**, *203* (1), 241–245. https://doi.org/https://doi.org/10.1016/j.expneurol.2006.08.008.

(79) Lee, H. T.; Xu, H.; Nasr, S. H.; Schnermann, J.; Emala, C. W. A1 Adenosine Receptor Knockout Mice Exhibit Increased Renal Injury Following Ischemia and Reperfusion. *Am. J. Physiol. - Ren. Physiol.* **2004**, *286* (2 55-2), 298–306. https://doi.org/10.1152/ajprenal.00185.2003.

(80) McGaraughty, S.; Jarvis, M. F. Purinergic Control of Neuropathic Pain. *Drug Dev. Res.* **2006**, *67* (4), 376–388. https://doi.org/10.1002/ddr.20101.

(81) Huffman, M. L.; Venton, B. J. Carbon-Fiber Microelectrodes for in Vivo Applications. *Analyst* **2009**, *134* (1), 18–24. https://doi.org/10.1039/b807563h.

(82) Pajski, M. L.; Venton, B. J. Adenosine Release Evoked by Short Electrical Stimulations in Striatal Brain Slices Is Primarily Activity Dependent. *ACS Chem. Neurosci.* **2010**, *1* (12), 775–787. https://doi.org/10.1021/cn100037d.

(83) Pajski, M. L.; Venton, B. J. The Mechanism of Electrically Stimulated Adenosine Release Varies by Brain Region. **2013**, 167–174. https://doi.org/10.1007/s11302-012-9343-2.

(84) Ross, A. E.; Nguyen, M. D.; Privman, E.; Venton, B. J. Mechanical Stimulation Evokes Rapid Increases in Extracellular Adenosine Concentration in the Prefrontal Cortex. *J. Neurochem.* **2014**, *130* (1), 50–60. https://doi.org/10.1111/jnc.12711.

(85) Wang, Y.; Venton, B. J. Comparison of Spontaneous and Mechanically-Stimulated Adenosine Release in Mice. *Neurochem. Int.* **2019**, *124* (December 2018), 46–50. https://doi.org/10.1016/j.neuint.2018.12.007.

(86) Street, S. E.; Kramer, N. J.; Walsh, P. L.; Taylor-Blake, B.; Yadav, M. C.; King, I. F.; Vihko, P.; Mark Wightman, R.; Millán, J. L.; Zylka, M. J. Tissue-Nonspecific Alkaline Phosphatase Acts Redundantly with PAP and NT5E to Generate Adenosine in the Dorsal Spinal Cord. *J. Neurosci.* **2013**, *33* (27), 11314–11322. https://doi.org/10.1523/JNEUROSCI.0133-13.2013.

(87) Cechova, S.; Venton, B. J. Transient Adenosine Efflux in the Rat Caudate-Putamen. *J. Neurochem.* **2008**, *105* (4), 1253–1263. https://doi.org/10.1111/j.1471-4159.2008.05223.x.

(88) Cechova, S.; Elsobky, A. M.; Venton, B. J. A1 Receptors Self-Regulate Adenosine Release in the Striatum: Evidence of Autoreceptor Characteristics. *Neuroscience* **2010**, *171* (4), 1006–1015. https://doi.org/10.1016/j.neuroscience.2010.09.063.

(89) Wang, Y.; Copeland, J.; Shin, M.; Chang, Y.; Venton, B. J. CD73 or CD39 Deletion Reveals Different Mechanisms of Formation for Spontaneous and Mechanically-Stimulated Adenosine Release and Sex Specific Compensations in ATP Degradation. *ACS Chem. Neurosci.* **2020**, *11* (6), 919–928. https://doi.org/10.1021/acschemneuro.9b00620.

(90) Lee, S. T.; Venton, B. J. Regional Variations of Spontaneous, Transient Adenosine Release in Brain Slices. *ACS Chem. Neurosci.* **2018**, *9* (3), 505–513. https://doi.org/10.1021/acschemneuro.7b00280.

(91) Nguyen, M. D.; Lee, S. T.; Ross, A. E.; Ryals, M.; Choudhry, V. I.; Venton, B. J. Characterization of Spontaneous, Transient Adenosine Release in the Caudate-Putamen and Prefrontal Cortex. *PLoS One* **2014**, *9* (1), e87165. https://doi.org/10.1371/journal.pone.0087165.

(92) Wang, Y.; Venton, B. J. Correlation of Transient Adenosine Release and Oxygen Changes in the Caudate-Putamen. *J. Neurochem.* **2017**, *140* (1), 13–23. https://doi.org/10.1111/jnc.13705.

(93) Nguyen, M. D.; Wang, Y.; Ganesana, M.; Venton, B. J. Transient Adenosine Release Is Modulated by NMDA and GABA B Receptors. *ACS Chem. Neurosci.* **2017**, *8* (2), 376–385. https://doi.org/10.1021/acschemneuro.6b00318.

(94) Borgus, J. R.; Puthongkham, P.; Venton, B. J. Complex Sex and Estrous Cycle Differences in Spontaneous Transient Adenosine. *J. Neurochem.* **2020**, No. January, 1–14. https://doi.org/10.1111/jnc.14981.

(95) Koos, B. J.; Kruger, L.; Murray, T. F. Source of Extracellular Brain Adenosine during Hypoxia in Fetal Sheep. *Brain Res.* **1997**, *778* (2), 439–442. https://doi.org/10.1016/S0006-8993(97)01207-9.

(96) Justice, J. B. Quantitative Microdialysis of Neurotransmitters. *J. Neurosci. Methods* **1993**, *48* (3), 263—276. https://doi.org/10.1016/0165-0270(93)90097-b.

(97) Chefer, V. I.; Thompson, A. C.; Zapata, A.; Shippenberg, T. S. Overview of Brain Microdialysis. *Curr. Protoc. Neurosci.* **2009**, *47* (1), 7.1.1-7.1.28. https://doi.org/https://doi.org/10.1002/0471142301.ns0701s47.

(98) Venton, B. J.; Cao, Q. Fundamentals of Fast-Scan Cyclic Voltammetry for Dopamine Detection. *Analyst* **2020**. https://doi.org/10.1039/C9AN01586H.

(99) Puthongkham, P.; Venton, B. J. Recent Advances in Fast-Scan Cyclic Voltammetry. *Analyst* **2020**, *145* (4), 1087–1102. https://doi.org/10.1039/C9AN01925A.

(100) Swamy, B. E. K.; Venton, B. J. Subsecond Detection of Physiological Adenosine Concentrations Using Fast-Scan Cyclic Voltammetry. *Anal. Chem.* **2007**, *79* (2), 744–750. https://doi.org/10.1021/ac061820i.

(101) Dunham, K. E.; Venton, B. J. Improving Serotonin Fast-Scan Cyclic Voltammetry Detection: New Waveforms to Reduce Electrode Fouling. *Analyst* **2020**, *145* (22), 7437–7446. https://doi.org/10.1039/d0an01406k.

(102) Wan, J.; Peng, W.; Li, X.; Qian, T.; Song, K.; Zeng, J.; Deng, F.; Hao, S.; Feng, J.; Zhang, P.; Zhang, Y.; Zou, J.; Pan, S.; Shin, M.; Venton, B. J.; Zhu, J. J.; Jing, M.; Xu, M.; Li, Y. A Genetically Encoded Sensor for Measuring Serotonin Dynamics. *Nat. Neurosci.* **2021**, *24* (5), 746–752. https://doi.org/10.1038/s41593-021-00823-7.

(103) Lin, L.; Gupta, S.; Zheng, W. S.; Si, K.; Zhu, J. J. Genetically Encoded Sensors Enable Micro- and Nano-Scopic Decoding of Transmission in Healthy and Diseased Brains. *Mol. Psychiatry* **2021**, *26* (2), 443–455. https://doi.org/10.1038/s41380-020-00960-8.

(104) Wan, J.; Peng, W.; Li, X.; Qian, T.; Song, K.; Zeng, J.; Deng, F.; Hao, S.; Feng, J.; Zhang, P.; Zhang, Y.; Zou, J.; Pan, S.; Shin, M.; Venton, B. J.; Zhu, J. J.; Jing, M.; Xu, M.; Li, Y. A Genetically Encoded Sensor for Measuring Serotonin Dynamics. *Nat. Neurosci.* **2021**, *24* (5), 746–752. https://doi.org/10.1038/s41593-021-00823-7.

(105) Melani, A.; De Micheli, E.; Pinna, G.; Alfieri, A.; Corte, L. Della; Pedata, F. Adenosine Extracellular Levels in Human Brain Gliomas: An Intraoperative Microdialysis Study. *Neurosci. Lett.* **2003**, *346* (1), 93–96. https://doi.org/https://doi.org/10.1016/S0304-3940(03)00596-2.

(106) Kennedy, R. T. Emerging Trends in in Vivo Neurochemical Monitoring by Microdialysis. *Curr. Opin. Chem. Biol.* **2013**, *17* (5), 860–867. https://doi.org/https://doi.org/10.1016/j.cbpa.2013.06.012.

(107) Bucher, E. S.; Wightman, R. M. Electrochemical Analysis of Neurotransmitters. **2015**, 239–263. https://doi.org/10.1146/annurev-anchem-071114-040426.

(108) Unnikrishnan, B.; Palanisamy, S.; Chen, S. A Simple Electrochemical Approach to Fabricate a Glucose Biosensor Based on Graphene – Glucose Oxidase Biocomposite. *Biosens. Bioelectron.* **2013**, *39*, 70–75. https://doi.org/10.1016/j.bios.2012.06.045.

(109) Khan, A.; Khan, A. A. P.; Asiri, A. M.; Rub, M. A.; Azum, N.; Rahman, M. M.; Khan, S. B.; Ghani, S. A. A New Trend on Biosensor for Neurotransmitter Choline/Acetylcholine - An Overview. *Appl. Biochem. Biotechnol.* **2013**, *169* (6), 1927–1939. https://doi.org/10.1007/s12010-013-0099-0.

(110) Moon, J. M.; Thapliyal, N.; Hussain, K. K.; Goyal, R. N.; Shim, Y. B. Conducting Polymer-Based Electrochemical Biosensors for Neurotransmitters: A Review. *Biosens. Bioelectron.* **2018**, *102* (December 2017), 540–552. https://doi.org/10.1016/j.bios.2017.11.069.

(111) Sinha, K.; Das Mukhopadhyay, C. Quantitative Detection of Neurotransmitter Using Aptamer: From Diagnosis to Therapeutics. *J. Biosci.* **2020**, *45* (1), 1–12. https://doi.org/10.1007/s12038-020-0017-x.

(112) Ganesana, M.; Trikantzopoulos, E.; Maniar, Y.; Lee, S. T.; Venton, B. J. Development of a Novel Micro Biosensor for in Vivo Monitoring of Glutamate Release in the Brain. *Biosens. Bioelectron.* **2019**, *130* (January), 103–109. https://doi.org/10.1016/j.bios.2019.01.049.

(113) Ewing, A. G.; Hu, K.; Jia, R.; Hatamie, A.; Le Vo, K. L.; Mirkin, M. V. Correlating Molecule Count and Release Kinetics with Vesicular Size Using Open Carbon Nanopipettes. *J. Am. Chem. Soc.* **2020**, *142* (40), 16910–16914. https://doi.org/10.1021/jacs.0c07169.

(114) Hatamie, A.; Ren, L.; Zhang, X.; Ewing, A. G. Vesicle Impact Electrochemical Cytometry to Determine Carbon Nanotube-Induced Fusion of Intracellular Vesicles. *Anal. Chem.* **2021**. https://doi.org/10.1021/acs.analchem.1c01462.

(115) Hatamie, A.; Ren, L.; Dou, H.; Gandasi, N. R.; Rorsman, P.; Ewing, A. Nanoscale Amperometry Reveals That Only a Fraction of Vesicular Serotonin Content Is Released During Exocytosis from Beta Cells. *Angew. Chemie* **2021**, *133* (14), 7671–7674. https://doi.org/10.1002/ange.202015902.

(116) Jackson, B. P.; Dietz, S. M.; Wightman, R. M. Fast-Scan Cyclic Voltammetry of 5-Hydroxytryptamine. *Anal. Chem.* **1995**, *67* (6), 1115–1120.

(117) Ross, A. E.; Venton, B. J. Sawhorse Waveform Voltammetry for Selective Detection of Adenosine, ATP, and Hydrogen Peroxide. *Anal. Chem.* **2014**, *86* (15), 7486–7493. https://doi.org/10.1021/ac501229c.

(118) Takmakov, P.; Zachek, M. K.; Keithley, R. B.; Bucher, E. S.; McCarty, G. S.; Wightman, R. M. Characterization of Local PH Changes in Brain Using Fast-Scan Cyclic Voltammetry with Carbon Microelectrodes. *Anal. Chem.* **2010**, *82* (23), 9892–9900. https://doi.org/10.1021/ac102399n.

(119) Demuru, S.; Nela, L.; Marchack, N.; Holmes, S. J.; Farmer, D. B.; Tulevski, G. S.; Lin, Q.; Deligianni, H. Scalable Nanostructured Carbon Electrode Arrays for Enhanced Dopamine Detection. *ACS Sensors* **2018**, *3* (4), 799–805. https://doi.org/10.1021/acssensors.8b00043.

(120) Koehne, J. E.; Marsh, M.; Boakye, A.; Douglas, B.; Kim, I. Y.; Chang, S.-Y.; Jang, D.-P.; Bennet, K. E.; Kimble, C.; Andrews, R.; Meyyappan, M.; Lee, K. H. Carbon Nanofiber Electrode Array for Electrochemical Detection of Dopamine Using Fast Scan Cyclic Voltammetry. *Analyst* **2011**, *136* (9), 1802–1805. https://doi.org/10.1039/c1an15025a.

(121) Parent, K. L.; Hill, D. F.; Crown, L. M.; Wiegand, J. P.; Gies, K. F.; Miller, M. A.; Atcherley, C. W.; Heien, M. L.; Cowen, S. L. Platform to Enable Combined Measurement of Dopamine and Neural Activity. *Anal. Chem.* **2017**, *89* (5), 2790–2799. https://doi.org/10.1021/acs.analchem.6b03642.

(122) Zachek, M. K.; Takmakov, P.; Park, J.; Wightman, R. M.; McCarty, G. S. Simultaneous

Monitoring of Dopamine Concentration at Spatially Different Brain Locations in Vivo. *Biosens. Bioelectron.* **2010**, *25* (5), 1179–1185. https://doi.org/https://doi.org/10.1016/j.bios.2009.10.008.

(123) Forderhase, A. G.; Styers, H. C.; Lee, C. A.; Sombers, L. A. Simultaneous Voltammetric Detection of Glucose and Lactate Fluctuations in Rat Striatum Evoked by Electrical Stimulation of the Midbrain. *Anal. Bioanal. Chem.* **2020**, *412*, 6611–6624. https://doi.org/10.1007/s00216-020-02797-0.

(124) Zhang, B.; Heien, M. L. A. V.; Santillo, M. F.; Mellander, L.; Ewing, A. G. Temporal Resolution in Electrochemical Imaging on Single PC12 Cells Using Amperometry and Voltammetry at Microelectrode Arrays. *Anal. Chem.* **2011**, *83* (2), 571–577. https://doi.org/10.1021/ac102502g.

(125) Schwerdt, H. N.; Kim, M. J.; Amemori, S.; Homma, D.; Yoshida, T.; Shimazu, H.; Yerramreddy, H.; Karasan, E.; Langer, R.; Graybiel, A. M.; Cima, M. J. Subcellular Probes for Neurochemical Recording from Multiple Brain Sites. *Lab Chip* **2017**, *17* (6), 1104–1115. https://doi.org/10.1039/c6lc01398h.

(126) Wigström, J.; Dunevall, J.; Najafinobar, N.; Lovrić, J.; Wang, J.; Ewing, A. G.; Cans, A. S. Lithographic Microfabrication of a 16-Electrode Array on a Probe Tip for High Spatial Resolution Electrochemical Localization of Exocytosis. *Anal. Chem.* **2016**, *88* (4), 2080–2087. https://doi.org/10.1021/acs.analchem.5b03316.

(127) Feingold, J.; Desrochers, T. M.; Fujii, N.; Harlan, R.; Tierney, P. L.; Shimazu, H.; Amemori, K. I.; Graybiel, A. M. A System for Recording Neural Activity Chronically and Simultaneously from Multiple Cortical and Subcortical Regions in Nonhuman Primates. *J. Neurophysiol.* **2012**, *107* (7), 1979–1995. https://doi.org/10.1152/jn.00625.2011.

(128) Schwerdt, H. N.; Zhang, E.; Kim, M. J.; Yoshida, T.; Stanwicks, L.; Amemori, S.; Dagdeviren, H. E.; Langer, R.; Cima, M. J.; Graybiel, A. M. Cellular-Scale Probes Enable Stable Chronic Subsecond Monitoring of Dopamine Neurochemicals in a Rodent Model. *Commun. Biol.* **2018**, *1* (1), 144. https://doi.org/10.1038/s42003-018-0147-y.

(129) Wang, H.; Jing, M.; Li, Y. Lighting up the Brain: Genetically Encoded Fluorescent Sensors for Imaging Neurotransmitters and Neuromodulators. *Curr. Opin. Neurobiol.* **2018**, *50*, 171–178. https://doi.org/10.1016/j.conb.2018.03.010.

(130) Jing, M.; Zhang, P.; Wang, G.; Feng, J.; Mesik, L.; Zeng, J.; Jiang, H.; Wang, S.; Looby, J. C.; Guagliardo, N. A.; Langma, L. W.; Lu, J.; Zuo, Y.; Talmage, D. A.; Role, L. W.; Barrett, P. Q.; Zhang, L. I.; Luo, M.; Song, Y.; Zhu, J. J.; Li, Y. A Genetically Encoded Fluorescent Acetylcholine Indicator for in Vitro and in Vivo Studies. *Nat. Biotechnol.* **2018**, *36* (8). https://doi.org/10.1038/nbt.4184.

(131) Sun, F.; Zeng, J.; Jing, M.; Zhou, J.; Feng, J.; Owen, S. F.; Luo, Y.; Li, F.; Wang, H.; Yamaguchi, T.; Yong, Z.; Gao, Y.; Peng, W.; Wang, L.; Zhang, S.; Du, J.; Lin, D.; Xu, M.; Kreitzer, A. C.; Cui, G.; Li, Y. A Genetically Encoded Fluorescent Sensor Enables Rapid and Specific Detection of Dopamine in Flies, Fish, and Mice. *Cell* **2018**, *174* (2), 481-496.e19. https://doi.org/10.1016/j.cell.2018.06.042.

(132) Marvin, J. S.; Borghuis, B. G.; Tian, L.; Cichon, J.; Harnett, M. T.; Akerboom, J.; Gordus, A.; Renninger, S. L.; Chen, T. W.; Bargmann, C. I.; Orger, M. B.; Schreiter, E. R.; Demb, J. B.; Gan, W. B.; Hires, S. A.; Looger, L. L. An Optimized Fluorescent Probe for Visualizing Glutamate Neurotransmission. *Nat. Methods* **2013**, *10* (2), 162–170.

https://doi.org/10.1038/nmeth.2333.

(133) Sun, F.; Zhou, J.; Dai, B.; Qian, T.; Zeng, J.; Li, X.; Zhuo, Y.; Zhang, Y.; Wang, Y.; Qian, C.; Tan, K.; Feng, J.; Dong, H.; Lin, D.; Cui, G.; Li, Y. Next-Generation GRAB Sensors for Monitoring Dopaminergic Activity in Vivo. *Nat. Methods* **2020**, *17* (11), 1156–1166. https://doi.org/10.1038/s41592-020-00981-9.

(134) Yang, C.; Jacobs, C. B.; Nguyen, M. D.; Ganesana, M.; Zestos, A. G.; Ivanov, I. N.; Puretzky, A. A.; Rouleau, C. M.; Geohegan, D. B.; Venton, B. J. Carbon Nanotubes Grown on Metal Microelectrodes for the Detection of Dopamine. *Anal. Chem.* **2016**, *88* (1), 645–652. https://doi.org/10.1021/acs.analchem.5b01257.

(135) Zestos, A. G.; Yang, C.; Jacobs, C. B.; Hensley, D.; Jill, B.; Ridge, O.; Ridge, O.; States, U. Carbon Nanospikes Grown on Metal Wires as Microelectrode Sensors for Dopamine. *Analyst* **2015**, *140* (21), 7283–7292. https://doi.org/10.1039/c5an01467k.Carbon.

(136) Cao, Q.; Hensley, D. K.; Lavrik, N. V; Venton, B. J. Carbon Nanospikes Have Better Electrochemical Properties than Carbon Nanotubes Due to Greater Surface Roughness and Defect Sites. *Carbon N. Y.* **2019**, *155*, 250–257. https://doi.org/https://doi.org/10.1016/j.carbon.2019.08.064.

(137) Cao, Q.; Shin, M.; Lavrik, N. V.; Venton, B. J. 3D-Printed Carbon Nanoelectrodes for in Vivo Neurotransmitter Sensing. *Nano Lett.* **2020**, *20* (9), 6831–6836. https://doi.org/10.1021/acs.nanolett.0c02844.

(138) Yang, C.; Cao, Q.; Puthongkham, P.; Lee, S. T.; Ganesana, M.; Lavrik, N. V.; Venton, B. J. 3D-Printed Carbon Electrodes for Neurotransmitter Detection. *Angew. Chemie - Int. Ed.* **2018**, *57* (43), 14255–14259. https://doi.org/10.1002/anie.201809992.

(139) Cao, Q.; Puthongkham, P.; Venton, B. J. Review: New Insights into Optimizing Chemical and 3D Surface Structures of Carbon Electrodes for Neurotransmitter Detection. *Anal. Method* **2019**, *11*, 247–261. https://doi.org/10.1039/c8ay02472c.

(140) Cao, Q.; Lucktong, J.; Shao, Z.; Chang, Y.; Venton, B. J. Electrochemical Treatment in KOH Renews and Activates Carbon Fiber Microelectrode Surfaces. *Anal. Bioanal. Chem.* **2021**, *413* (27), 6737–6746. https://doi.org/10.1007/s00216-021-03539-6.

(141) Roberts, J. G.; Mitchell, E. C.; Dunaway, L. E.; McCarty, G. S.; Sombers, L. A. Carbon-Fiber Nanoelectrodes for Real-Time Discrimination of Vesicle Cargo in the Native Cellular Environment. *ACS Nano* **2020**, *14* (3), 2917–2926. https://doi.org/10.1021/acsnano.9b07318.

(142) Hu, K.; Le Vo, K. L.; Hatamie, A.; Ewing, A. G. Quantifying Intracellular Single Vesicular Catecholamine Concentration with Open Carbon Nanopipettes to Unveil the Effect of L-DOPA on Vesicular Structure. *Angew. Chemie* **2021**, 1–6. https://doi.org/10.1002/ange.202113406.

(143) Yang, C.; Wang, Y.; Jacobs, C. B.; Ivanov, I. N.; Venton, B. J. O2 Plasma Etching and Antistatic Gun Surface Modifications for CNT Yarn Microelectrode Improve Sensitivity and Antifouling Properties. *Anal. Chem.* **2017**, *89* (10), 5605–5611. https://doi.org/10.1021/acs.analchem.7b00785.

(144) Li, Y.; Keller, A. L.; Cryan, M. T.; Ross, A. E. Metal Nanoparticle Modified Carbon-Fiber Microelectrodes Enhance Adenosine Triphosphate Surface Interactions with Fast-Scan Cyclic Voltammetry. *ACS Meas. Sci. Au* **2021**.

https://doi.org/10.1021/acsmeasuresciau.1c00026.

(145) Yang, C.; Denno, M. E.; Pyakurel, P.; Venton, B. J. Recent Trends in Carbon Nanomaterial-Based Electrochemical Sensors for Biomolecules: A Review. *Anal. Chim. Acta* **2015**, *887*, 17–37. https://doi.org/10.1016/j.aca.2015.05.049.

(146) Swamy, B. E. K.; Venton, B. J. Carbon Nanotube-Modified Microelectrodes for Simultaneous Detection of Dopamine and Serotonin in Vivo. *Analyst* **2007**, *132*, 876–884. https://doi.org/10.1039/b705552h.

(147) Puthongkham, P.; Yang, C.; Venton, B. J. Carbon Nanohorn-Modified Carbon Fiber Microelectrodes for Dopamine Detection. *Electroanalysis* **2018**, *30* (6), 1073–1081. https://doi.org/10.1002/elan.201700667.

(148) Power, A. C.; Gorey, B.; Chandra, S.; Chapman, J. Carbon Nanomaterials and Their Application to Electrochemical Sensors: A Review. *Nanotechnol. Rev.* **2018**, *7* (1), 19–41. https://doi.org/10.1515/ntrev-2017-0160.

(149) Mccreery, R. L. Advanced Carbon Electrode Materials for Molecular Electrochemistry. *Chem. Rev.* **2008**, *108* (7), 2646–2687.

(150) Bennet, K. E.; Tomshine, J. R.; Min, H. K.; Manciu, F. S.; Marsh, M. P.; Paek, S. B.; Settell, M. L.; Nicolai, E. N.; Blaha, C. D.; Kouzani, A. Z.; Chang, S. Y.; Lee, K. H. A Diamond-Based Electrode for Detection of Neurochemicals in the Human Brain. *Front. Hum. Neurosci.* **2016**, *10* (MAR2016), 1–12. https://doi.org/10.3389/fnhum.2016.00102.

(151) Yang, N.; Foord, J. S.; Jiang, X. Diamond Electrochemistry at the Nanoscale: A Review. *Carbon N. Y.* **2016**, *99*, 90–110. https://doi.org/10.1016/j.carbon.2015.11.061.

(152) Puthongkham, P.; Venton, B. J. Nanodiamond Coating Improves the Sensitivity and Antifouling Properties of Carbon Fiber Microelectrodes. *ACS Sensors* **2019**, *4*, 2403–2411. https://doi.org/10.1021/acssensors.9b00994.

(153) Georgakilas, V.; Perman, J. A.; Tucek, J.; Zboril, R. Broad Family of Carbon Nanoallotropes : Classi Fi Cation , Chemistry , and Applications of Fullerenes , Carbon Dots , Nanotubes , Graphene , Nanodiamonds , and Combined Superstructures. *Chem. Rev.* **2015**, *115*, 4744–4822. https://doi.org/10.1021/cr500304f.

(154) Fang, J.; Xie, Z.; Wallace, G.; Wang, X. Co-Deposition of Carbon Dots and Reduced Graphene Oxide Nanosheets on Carbon-Fiber Microelectrode Surface for Selective Detection of Dopamine. *Appl. Surf. Sci.* **2017**, *412*, 131–137. https://doi.org/10.1016/j.apsusc.2017.03.257.

(155) Compton, O. C.; Nguyen, S. T. Graphene Oxide , Highly Reduced Graphene Oxide , and Graphene : Versatile Building Blocks for Carbon-Based Materials **. *Small* **2010**, *6* (6), 711–723. https://doi.org/10.1002/smll.200901934.

(156) Kim, B. F.; Cote, L. J.; Huang, J. Graphene Oxide : Surface Activity and Two-Dimensional Assembly. **2010**, 1954–1958. https://doi.org/10.1002/adma.200903932.

(157) Chen, D.; Feng, H.; Li, J. Graphene Oxide : Preparation , Functionalization , and Electrochemical Applications. *Chem. Rev.* **2012**, *112* (11), 6027–6053. https://doi.org/10.1021/cr300115g.

(158) Banks, C. E.; Compton, R. G. New Electrodes for Old : From Carbon Nanotubes to Edge Plane Pyrolytic Graphite. *Analyst* **2006**, 15–21. https://doi.org/10.1039/b512688f.

(159) Chen, L.; Tang, Y.; Wang, K.; Liu, C.; Luo, S. Direct Electrodeposition of Reduced Graphene Oxide on Glassy Carbon Electrode and Its Electrochemical Application. *Electrochem. commun.* **2011**, *13*, 133–137. https://doi.org/10.1016/j.elecom.2010.11.033.

(160) Devadas, B.; Rajkumar, M.; Chen, S.; Saraswathi, R. Electrochemically Reduced Graphene Oxide / Neodymium Hexacyanoferrate Modified Electrodes for the Electrochemical Detection of Paracetomol. *Int. J. Eletrochemical Sci.* **2012**, *7*, 3339–3349.

Chapter 2

A_1 and A_{2A} receptors modulate spontaneous adenosine but not mechanically-stimulated adenosine in the caudate

Chapter 2 was reprinted from *ACS Chem. Neurosci.* **2020**, 11, 20, 3377–3385.

Abstract

Adenosine is a neuromodulator and rapid increases in adenosine in the brain occur spontaneously or after mechanical stimulation. However, the regulation of rapid adenosine by adenosine receptors is unclear, and understanding it would allow better manipulation of neuromodulation. The two main adenosine receptors in the brain are A_1 receptors, which are inhibitory, and A_{2A} receptors, which are excitatory. Here, we investigated the regulation of spontaneous adenosine and mechanically-stimulated adenosine by adenosine receptors, using global A_1 or A_{2A} knockout mice. Results were compared *in vivo* and in brain slices models. A_1KO mice have increased frequency of spontaneous adenosine events, but no change in the average concentration of an event, while A_{2A}KO mice had no change in frequency but increased average event concentration. Thus, both A_1 and A_{2A} self-regulate spontaneous adenosine release, but A_1 acts on the frequency of events, while A_{2A} receptors regulate concentration. The trends are similar both *in vivo* and slices, so brain slices are a good model system to study spontaneous adenosine release. For mechanically-stimulated adenosine, there was no effect of A_1 or A_{2A} KO *in vivo*, but in brain slices there was a significant increase in concentration evoked in A_1KO mice. Mechanically-stimulated release was largely unregulated by A_1 and A_{2A} receptors, likely because of a different release mechanism than spontaneous adenosine. Thus, A_1 receptors affect the frequency of spontaneous adenosine transients and A_{2A} receptors affect the concentration, so future studies could probe drug treatments targeting A_1 and A_{2A} receptors to increase rapid adenosine neuromodulation.

2.1 Introduction

Adenosine plays an important role in the brain as a neuromodulator and a neuroprotector.[1–10] There are four known adenosine receptors, A_1, A_{2A}, A_{2B} and A_3 receptors, which are G protein-coupled receptors, but A_1 and A_{2A} receptors are the most prevalent receptors responsible for adenosine modulation in the brain.[11–14] A_1 receptors are the most abundant in the brain and inhibit neurotransmission by blocking adenylyl cyclase activity, while A_{2A} receptors, the second most abundant receptor type, are excitatory, activating adenylyl cyclase activity.[15] Adenosine receptors, particularly A_{2A} receptors, are located on blood vessels and modulate blood flow and oxygen consumption.[16,17] Moreover, adenosine receptors are also expressed on many neurons and regulate other neurotransmitters in the brain. For example, A_1 and A_{2A} receptors modulate synaptic release of glutamate, acetylcholine, serotonin, and GABA.[1,2,18–20] A_1 and dopamine D_1 receptors form heteromers as well as A_{2A} and D_2 receptors and they therefore modulate dopamine signaling.[21] However, it is still not clear how adenosine A_1 and A_{2A} receptors self-regulate adenosine release.

Traditionally, concentration changes of extracellular adenosine have been investigated on the minute to hour time scale.[22–24] However, electrophysiology experiments in Dunwiddie's group showed rapid signaling of adenosine, on the timescale of milliseconds to seconds.[25] Spontaneous, transient adenosine signaling was recently measured by fast scan cyclic voltammetry, lasting only few seconds.[9,16,26,27] Transient adenosine is activity dependent, and dependent on CD73, an enzyme that converts AMP to adenosine, suggesting spontaneous adenosine is vesicularly released as ATP and broken down in the extracellular space.[9,22,26,28–33] The frequency of spontaneous release is increased by DPCPX, an A_1 receptor inhibitor[34] and DPCPX also increases electrically-stimulated adenosine release.[35] The A_{2A} receptor antagonist, SCH 442416, eliminated the increase in adenosine and oxygen events during cerebral ischemia/reperfusion (I/R) *in vivo*.[36] Another mode of rapid adenosine release is mechanically-stimulated release, whereby moving a pipette or an electrode in the brain causes rapid

adenosine release.[37] Mechanosensitive adenosine release is not dependent on CD73 and thus it may have a different mechanism of formation than spontaneous adenosine.[29,30,37] Mechanosensitive ATP release has been discovered in the brain due to swelling, mechanical perturbation, and shear stress.[38] Thus, while moving the electrode is an easy way to experimentally cause release, mechanically-stimulated adenosine is biologically relevant to physical damage the brain can suffer, such as from shear stress.[37] While adenosine can also be electrically stimulated, mechanically-stimulated adenosine is more reproducible.[35,39] However, little is known about how adenosine receptors modulate mechanically-stimulated adenosine.

Previous studies used pharmacology to understand the regulation of adenosine by blocking different receptors, but drugs cannot block or excite all receptors, and drugs must cross the blood-brain barrier to be utilized *in vivo*. Thus, genetically-altered mice provide an alternative to understand the global effects of receptors on adenosine regulation. Studies using A_1 knockout (A_1KO) and A_{2A} knockout (A_{2A}KO) mice have revealed the importance of these receptors for adenosine regulation.[40–42] For example, mice lacking adenosine A_1 receptors showed decreased hypoxic neuroprotection and an increased renal injury following ischemia and perfusion.[40,42–44] A_{2A}KO mice have less exploratory activity, more anxiety, and are less sensitive to depressant challenges than wild-type mice; moreover, A_{2A}KO mice have an attenuated response to focal ischemia, suggesting that removing A_{2A} receptors is neuroprotective.[45–47] Adenosine receptor knockout mice were also used to investigate adenosine-dopamine interactions, and A_{2A}-mediated neural functions are partially independent of D_2 receptors.[21,48] However, spontaneous, transient adenosine or mechanically-evoked adenosine events have not been measured in A_1 or A_{2A} KO mice.

In this study, we investigated whether adenosine receptors regulate spontaneous transient adenosine and mechanically-stimulated adenosine release *in vivo* and in brain slices using global knockout mice. Brain slice experiments are a useful biological model that bypasses the blood-brain barrier, however, spontaneous and mechanically-evoked adenosine events

have not been directly compared between brain slice experiment and *in vivo* measurements. Data was collected in the caudate-putamen region in wild-type (C57BL/6), A_1KO, and A_{2A}KO mice. Both *in vivo* and brain slice results show A_1KO mice had an increased frequency of spontaneous adenosine events, without changing the mean concentration of each adenosine transient event. A_{2A}KO mice had no change in spontaneous adenosine event frequency but an increase in concentration. For mechanically-evoked adenosine, there was no significant difference in concentration *in vivo*, but in brain slices, A_1KO mice had a significantly higher concentration compared to wild-type mice. Overall, A_1 and A_{2A} receptors self-regulate spontaneous adenosine but self-regulation is less evident for mechanically-evoked release. Differential regulation of different modes of adenosine release may be useful to develop strategies that specifically target spontaneous adenosine to harness its neuromodulatory effects.

2.2 Experimental Section

2.2.1 Chemicals

Artificial cerebral spinal fluid (aCSF) consisted of 126mM NaCl, 2.5 mM KCl, 1.2 mM NaH_2PO_4, 2.4 mM $CaCl_2$ dihydrate, 1.2 mM $MgCl_2$ hexahydrate, 25 mM $NaHCO_3$, 11 mM glucose, and 15 mM tris(hydroxymethyl) aminomethane and was adjusted to pH 7.4 before the experiment. Adenosine was purchased from Acros organics (Morris Plains, NJ, USA) and dissolved in 0.1 M $HClO_4$ for 10 mM stock solution. Stock solutions was diluted to 1 µM in aCSF for the electrode post calibration after brain slice or *in vivo* experiments.

2.2.2 Electrochemistry

Cylinder carbon-fiber microelectrodes were fabricated as described previously.[49] Briefly, electrodes were made by vacuum-aspirating a T-650 carbon fiber (7 µm diameter, Cytec Engineering Materials, West Patterson, NJ) into a glass capillary and pulling into two electrodes

by an electrode puller (model PE-21, Narishige, Tokyo, Japan). The pulled electrode tip was cut to 50-100 µm long for brain slice experiment and 150-200 µm long for *in vivo* experiment. Cyclic voltammograms were collected using a ChemClamp (Dagan, Minneapolis, MN, USA) with HDCV (UNC Chemistry, Chapel Hill, NC, USA). The electrode was scanned by a triangular waveform from -0.4 V to 1.45 V with a frequency of 10 Hz at 400 V/s. Electrodes were calibrated after the experiment by testing their response to 1 µM adenosine in a flow cell and a calibration value obtained (in nA/ µM) that was used to convert currents to concentrations.

2.2.3 Brain Slice experiments

All animal experiments were approved by the Animal Care and Use Committee of the University of Virginia. C57BL/6 mice (6-8 weeks old, Jackson Lab), A_1 receptor knockout mice and A_{2A} receptor knockout mice (6-8 weeks old, obtained from Dr. S. Jamal Mustafa, West Virginia University) were housed in a vivarium and given food and water *ad libitum*. Mice were anesthetized with isoflurane and beheaded immediately. The mouse brain was removed within 2 min and placed in 0–5°C artificial cerebral spinal fluid (aCSF) for 2 min for recovery. Four hundred-micrometer coronal slices of the caudate–putamen were prepared using a vibratome (LeicaVT1000S, Bannockburn, IL, USA), and transferred to oxygenated aCSF (95% oxygen, 5% CO_2), to recover for an hour before the experiment. aCSF (maintained at 35–37°C) flowed over the brain slices using a perfusion pump (Watson-Marlo 205U, Wilmington, MA, USA) at a rate of 2 mL/min for all experiments. Spontaneous adenosine transients were measured by inserting the electrode about 75 µm into the tissue and collected 1 h data after 10 min equilibrium. Mechanical stimulation experiments were performed by lowering the electrode 50 µm every 30 minutes. The electrode was placed in the caudate-putamen (AP +1.1 mm, ML + 1.5 mm, and DV -3.0 mm, scheme is shown in Figure 1). Only one slice was used per animal, so all n values are different animals.

2.2.4 In vivo experiment

All experiments were approved by Animal Care and Use Committee of the University of Virginia. C57BL/6 mice (6-8 weeks old, Jackson Lab), A_1 receptor knockout mice, and A_{2A} receptor knockout mice (6-8 weeks old, both KO obtained from Dr. S. Jamal Mustafa, West Virginia University)[50,51] were housed in a vivarium and given food and water *ad libitum*. Both of the KO mice are on the C57B background and that is the standard control mouse used for studies of their function.[50,51] Mice were anesthetized by flowing 4% isoflurane in 100% oxygen for induction and maintained with 1.5-3% in 100% oxygen via a facemask (Stoelting, Wood Dale, IL, USA), tail pinch to ensure that anesthesia is complete and sustained. Isoflurane levels were adjusted to until loss of righting reflex was observed. The mouse was laid on a heating pad maintaining the temperature around 37 ºC. The surgical site was shaved, the skull was exposed, and a hole drilled that allowed the placement of the electrode in the caudate-putamen (AP +1.1 mm, ML + 1.5 mm, and DV -3.0 mm, scheme is shown in Figure 1). Bupivacaine (0.10 mL, APP Pharmaceuticals, Schaumburg, IL, USA) was applied under the skin for local anesthesia before drilling the skull. Spontaneous adenosine transient events were measured for 4 h total and mechanically-stimulated adenosine events were measured by lowering the electrode 100 µm every 15 minutes.

2.2.5 Statistics

Spontaneous adenosine transients were identified and characterized by an automated algorithm and adenosine transients were confirmed by an analyst to exclude any signals that were not adenosine, the duration results were determined at half-height of the primary peak.[52] All statistics were performed by using GraphPad 8 (GraphPad Software Inc., San Diego, CA, USA). All data are shown as mean ± SEM. Statistical significance was designated at $p < 0.05$.

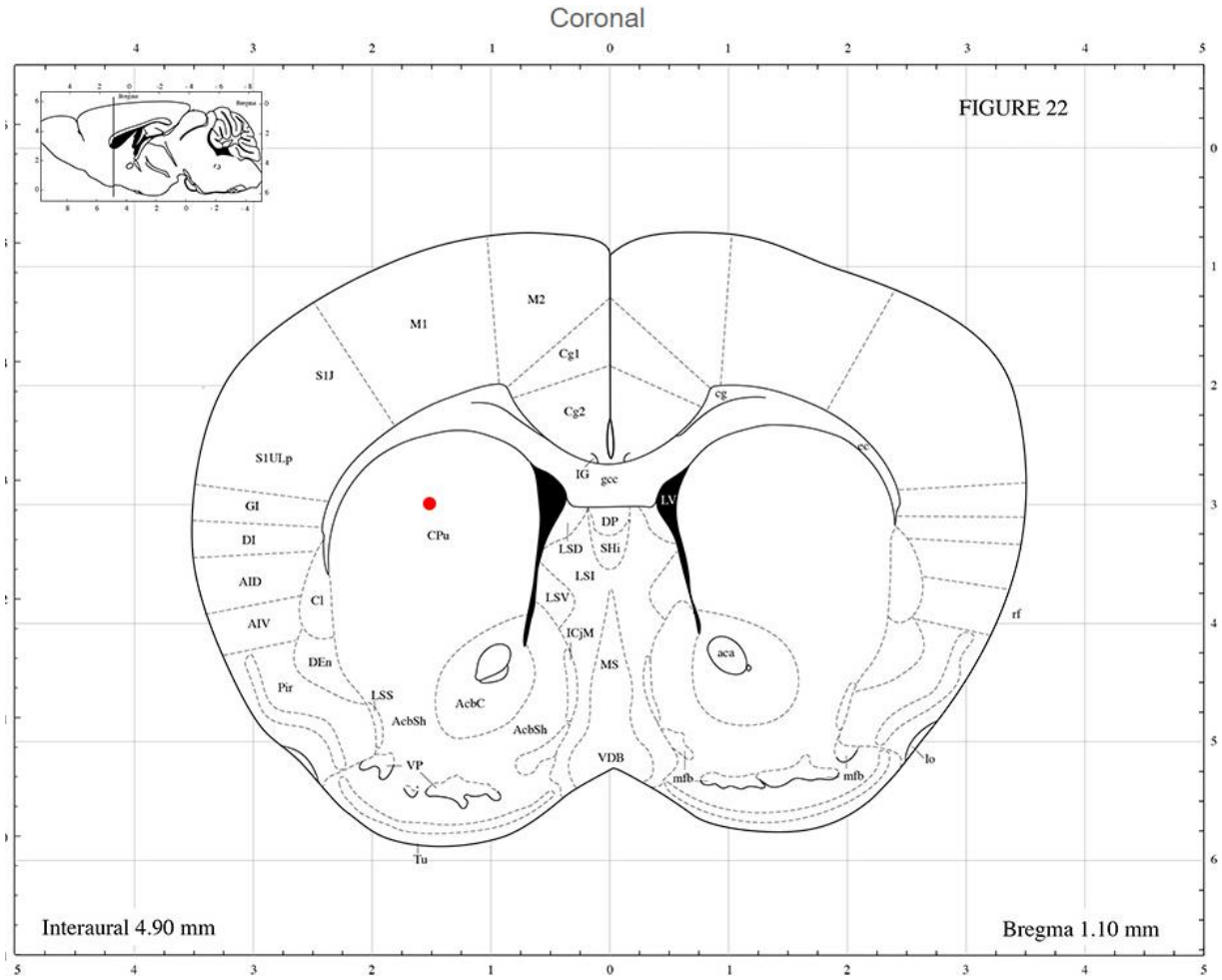

Figure 1 Caudate-putamen (AP +1.1 mm, ML + 1.5 mm, and DV -3.0 mm). The scheme of the position where the electrode was placed *in vivo* and brain slices.

2.3 Results

In this study, spontaneous and mechanically-stimulated adenosine release were compared in wild type mice (C57BL/6), A_1KO, and A_{2A}KO mice. All experiments were performed in the caudate-putamen, which has abundant A_1 and A_{2A} receptors,[53] and two model systems were compared: brain slices and anesthetized mice. The hypothesis is that the frequency or concentration of adenosine will change in the knockout mice if A_1 or A_{2A} receptors self-regulate adenosine.

2.3.1 Spontaneous Adenosine Release

2.3.1.1 Brain slice measurements

Brain slice experiments are easier than *in vivo* studies, especially for pharmacology studies, where there is no blood-brain barrier.[22,26] Figure 2 shows example color plots for spontaneous adenosine release in brain slices of control, A_1KO and A_{2A}KO mice. The color plots display the results in 3 dimensions, with potential on the y-axis, time on the x-axis, and current in false color. The green/purple circles in the center represent the primary adenosine oxidation peak (at 1.4 V), and the green/purple circles slightly below (at 1.0 V) is the secondary oxidation peak of adenosine. The concentration vs time graphs on top plot show the change of primary adenosine peak, which is converted to concentration using a calibration factor. Starred peaks were identified as spontaneous adenosine release via our automated algorithm.[52] Wild type (Fig. 2A) has fewer events than either A_1KO (Fig. 2B) or A_{2A}KO (Fig. 2C), and A_1KO has the highest number of spontaneous adenosine events.

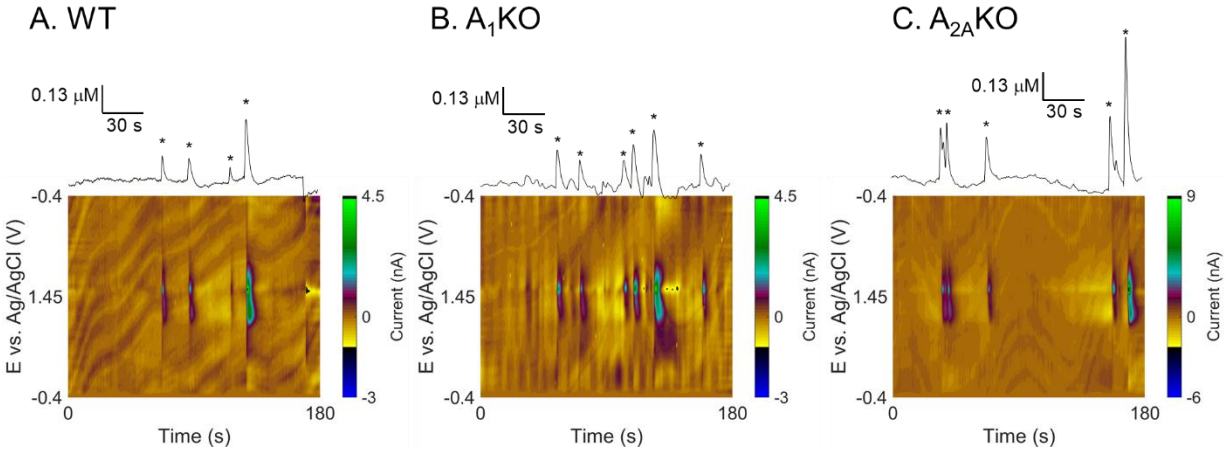

Figure 2 Examples of spontaneous adenosine release in brain slices. Top: concentration vs time trace, with stars indicating the peak was identified as spontaneous adenosine release by our automated algorithm. Bottom: 3-D color plot of spontaneous adenosine release in three different types of mice. A. Wild type, B: A_1KO, and C: A_{2A}KO.

Figure 3 compares average data for spontaneous adenosine events in brain slices among different genotype mice. Figure 3A shows the number of spontaneous events for one-hour measurement and there is a significant main effect of genotype (One-way ANOVA, p=

0.023, n=8-9 brain slices); A_1KO mice have significantly more spontaneous events than wild type mice (Tukey's multiple comparisons, $p<0.05$). However, the number of spontaneous adenosine events is not significantly different between wild type and A_{2A}KO mice (Tukey's multiple comparisons, $p>0.9999$). Inter-event time is the time between two consecutive transients and is a measure of the frequency of adenosine events. Figure 3B shows the distribution of inter-event times in a histogram, with relative frequency of each bin on the y-axis and inter-event time on the x-axis (times were binned in 50 s bins). There is a main effect of genotype (Kruskal-Wallis test, $p<0.0001$, n=8-9 brain slices), with a higher frequency of events in A_1KO mice than wild type mice or A_{2A}KO mice (Dunn's multiple comparisons test, A_1KO vs WT: $p=0.0019$, A_1KO vs A_{2A}KO: $p<0.0001$). There is no significant difference in inter-event time distribution between WT and A_{2A}KO mice ($p>0.99$). Figure 3C shows the mean concentration of the first 10 spontaneous adenosine events from every slice (the first 10 are used in order to avoid the overrepresentation of some animals which have more transients). There is a significant main effect of genotype (One-way ANOVA, $p=0.0004$, n=80 transients/genotype) with A_{2A}KO mice having a significantly higher concentration than wild type or A_1KO mice (Tukey's multiple comparisons, WT vs A_{2A}KO: $p=0.0016$, A_{2A}KO vs A_1KO: $p=0.0019$) but there is no significant difference between wild type and A_1KO mice ($p=0.99$). Fig. 3D shows duration, which is defined as peak width at half height, and there is a main effect of genotype (One-way ANOVA, $p=0.026$, n=8-9 brain slices). A_{2A}KO mice have a shorter average duration compared to the other two genotypes (Tukey's multiple comparison, A_{2A}KO vs WT $p=0.0463$, A_{2A}KO vs A_1KO $p=0.043$) and there is no significant difference between WT and A_1KO ($p=0.99$). The concentration and duration distributions also proved that A_{2A}KO mice have a higher concentration and shorter duration (Figure 4).

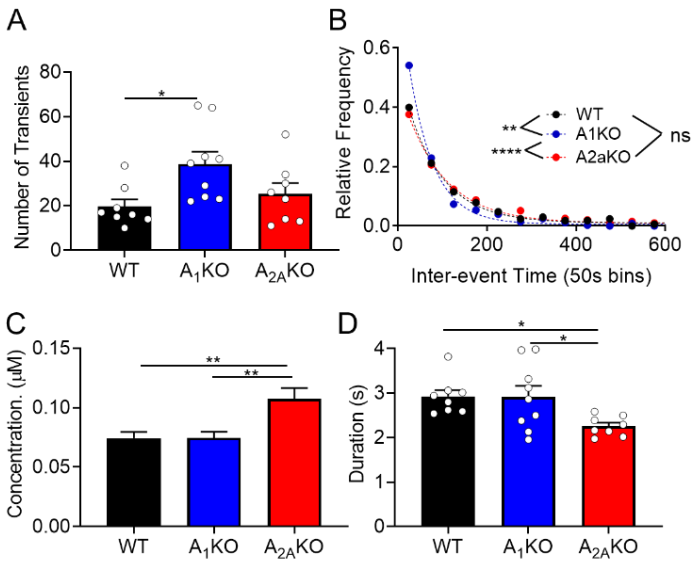

Figure 3. Spontaneous adenosine measurement in brain slices. A. Number of spontaneous adenosine events varies by genotype (One-way ANOVA, overall p=0.023, n=8-9 brain slices, 1 slice per animal). B. Inter-event time histogram (50 s bins) of all adenosine transients (Kruskal-Wallis test, overall p<0.0001). C. Mean concentration of first 10 spontaneous adenosine release in every slice. (One-way ANOVA, Tukey's multiple comparisons, overall p=0.0004, 80 transients in each genotype, **p<0.01, n=8 brain slices, 1 slice per animal) D. Average duration of spontaneous adenosine release (One-way ANOVA, Tukey's multiple comparisons, overall p=0.026) *p<0.05, **p<0.01, ***p<0.001, ****p<0.0001, error bars are SEM. WT=wild type C57BL/6 mice.

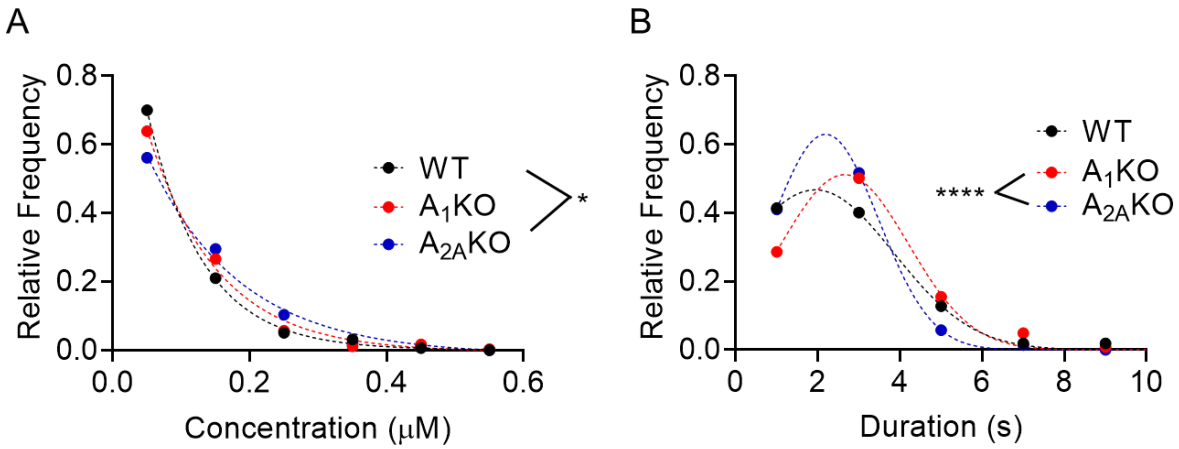

Figure 4 Spontaneous adenosine concentration (A) and duration (B) distribution in brain slice. (A) The concentration histogram of spontaneous adenosine in all genotypes. (0.1 μM bins) of all adenosine transients (Kruskal-Wallis test, overall p=0.0124). (B) The duration histogram of spontaneous adenosine in all genotypes. (2 s bins) of all adenosine transients (Kruskal-Wallis test, overall p<0.0001). *p<0.05, ****p<0.0001, n=8 slices, one slice per animal.

2.3.1.2 *In vivo* measurements

In order to confirm that the brain slice model is reliable for spontaneous adenosine measurements, we also measured spontaneous adenosine release *in vivo* in anesthetized mice. Since experiments can last longer *in vivo*, spontaneous adenosine was measured for four hours in each mouse.

Figure 5 shows examples of spontaneous adenosine measurements *in vivo*. In the example data, the number of transients is higher in A_1KO mice than WT or A_{2A}KO mice, and the concentration of adenosine transients in A_{2A}KO mice is higher than the other two genotype mice. The trend for number of transients in WT mice is the same for *in vivo* measurements as in brain slice measurements, with fewer transients in WT mice and more transients in A_1KO. However, *in vivo* data has higher concentration adenosine events than the brain slice experiment. Moreover, the number of spontaneous adenosine is more stable *in vivo* during the entire duration of the experiment, but most spontaneous adenosine in brain slice experiment happens during the first 30-45 minutes because of the difficulty of synthesis in brain slices.[22] In slices, adenosine synthesis is not as well maintained without the addition of adenine and ribose, but adenine can't be added in FSCV experiments because it is electroactive, so experiments are kept to one hour.[54]

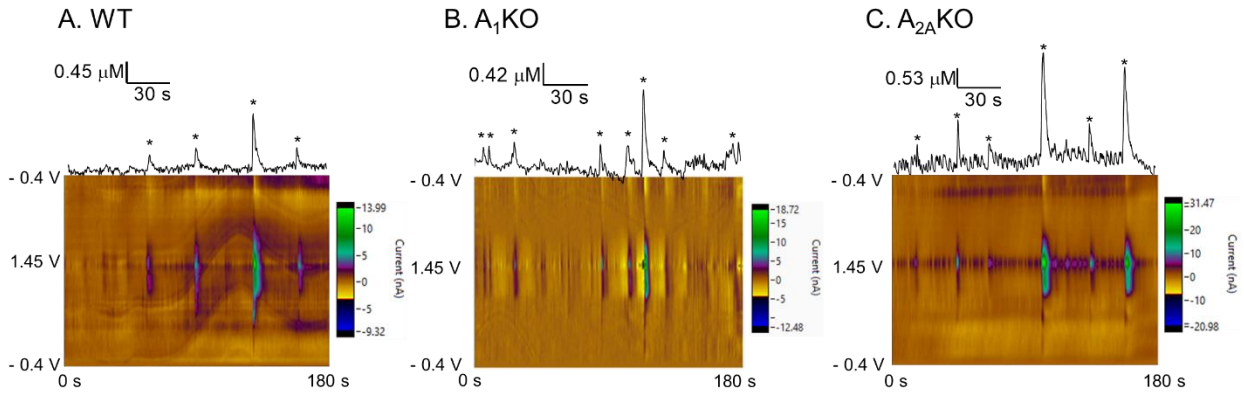

Figure 5 Examples of spontaneous adenosine release *in vivo*. Top concentration vs time traces, with stars indicating the peak was identified as spontaneous adenosine release by our automated algorithm. Bottom: 3-D color plots of spontaneous adenosine release. A. Wild type, B: A_1KO, and C: A_{2A}KO.

Figure 6 shows averaged results of spontaneous adenosine measurements. For the average number of spontaneous adenosine events (Fig. 6A), there is a significant main effect of genotype on the number of transients (One-way ANOVA, main effect p=0.0026, n=8 animals). A_1KO mice have a significantly higher number of events compared to wild type mice (Tukey's multiple comparisons test, p=0.0019) but were not statistically different than A_{2A}KO (p=0.074). The average number of spontaneous adenosine events in A_{2A}KO mice is not significantly different than wild type mice (p=0.24). Figure 6B shows the distribution of inter-event times, with data binned in 50 s intervals and there is a main effect of genotype on inter-event time (Kruskal-Wallis test, p<0.0001, n=8 animals). A_1KO mice have a significantly different distribution compared to WT and A_{2A}KO mice and A_{2A}KO are also different than WT (Dunn's multiple comparisons test, p<0.0001, n=8 animals). The inter-event time in A_1KO is much shorter than the other two types of mice, indicating the frequency of events is higher. Figure 6C shows the mean concentration of the first 60 spontaneous adenosine events from each animal (to use the same number from each to avoid overrepresentation), and there is a significant main effect of genotype (One-way ANOVA, p<0.0001, n=8 animals). A_{2A}KO mice have a significantly higher concentration than wild type or A_1KO mice (Tukey's multiple comparisons test, both p<0.0001), but there is no difference between wild type and A_1KO mice (p>0.99). Thus, A_{2A} receptors influence the concentration of individual transient adenosine events. Furthermore, there was a main effect of genotype on duration (Fig. 6D, One-way ANOVA, p=0.017, n=8 animals), and the average duration of each event in A_{2A}KO mice is shorter (Tukey's multiple comparisons test, p=0.015). There was no significant difference between wild type and A_1KO mice (p=0.10) or A_1KO and A_{2A}KO mice (p=0.62). Differences in duration are slight because the temporal resolution of FSCV is only 0.1 s. Figure 7 presents the concentration and duration histograms of spontaneous adenosine in all genotypes, and the distributions also proves that A_{2A}KO have a higher concentration and shorter duration.

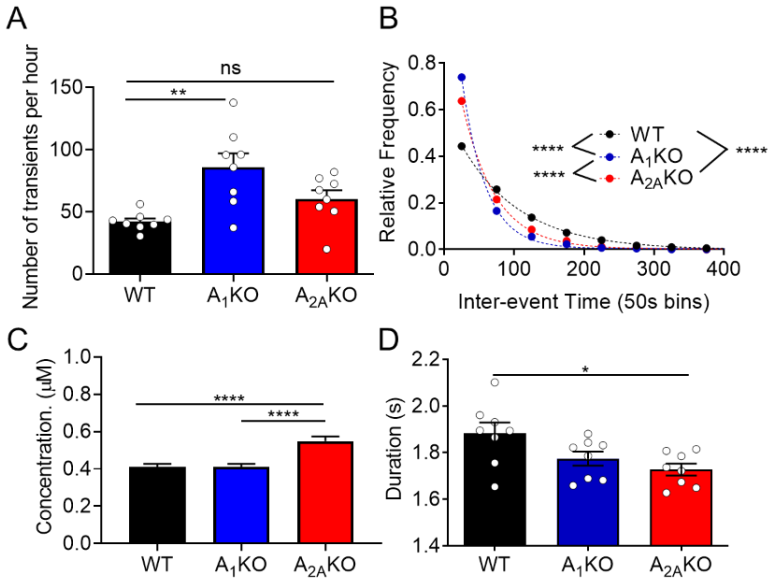

Figure 6 Spontaneous adenosine release *in vivo*. A. Number of spontaneous adenosine events per hour (One-way ANOVA, overall p=0.0026, n=8 animals). B. Inter-event time histogram (50 s bins) of all adenosine transients (Kruskal-Wallis test, overall p<0.0001, n=8 animals) C. Mean concentration of first 60 spontaneous adenosine release (One-way ANOVA, overall p<0.0001, n=8 animals). D. Average duration of spontaneous adenosine release (One-way ANOVA, Tukey's multiple comparisons, overall p=0.017, n=8 animals), *p<0.05, **p<0.01, ****p<0.0001, error bars are SEM. WT=wild type C57BL/6 mice.

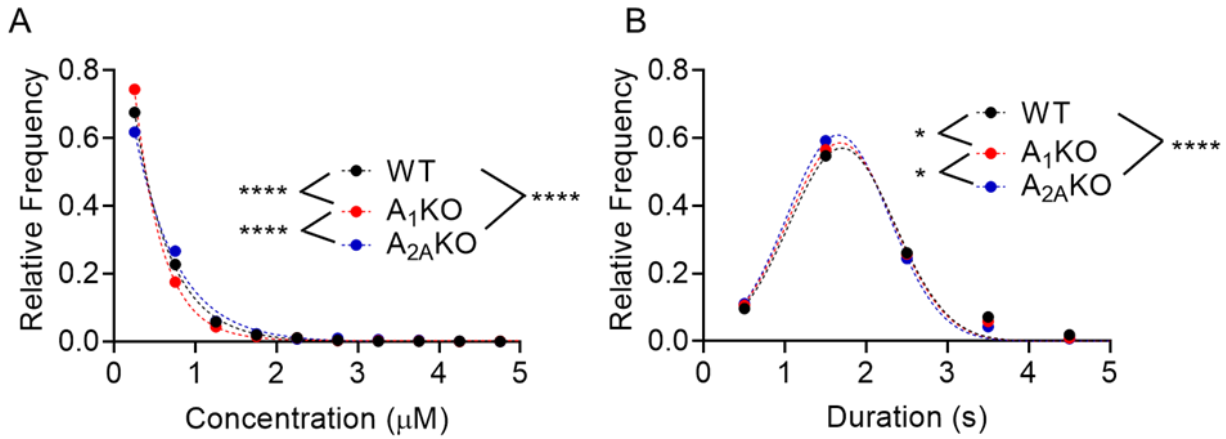

Figure 7 Spontaneous adenosine concentration (A) and duration (B) distribution *in vivo*. (A) The concentration histogram of spontaneous adenosine in all genotypes. (0.5 μM bins) of all adenosine transients (Kruskal-Wallis test, overall p<0.0001). (B) The duration histogram of spontaneous adenosine in all genotypes. (1 s bins) of all adenosine transients (Kruskal-Wallis test, overall p<0.0001).*p<0.05, ****p<0.0001, n=8 animals.

2.3.2 Mechanically-Stimulated Adenosine Release

2.3.2.1 Brain slice measurements

Mechanically-stimulated adenosine was measured in brain slices by lowering the electrode 50 μm three times per slice. Because slices are only 400 μm thick and measurements are generally performed in the middle to avoid dead layers on the edges, moving the electrode ~150 um is about the maximum possible. Separate slices were used, not the same slices where spontaneous events were measured, because slices have a limited time for viability.

Figure 8A shows example results of mechanically-stimulated adenosine. The CV shape and the current do not change for three mechanical stimulations in a one-hour period. Figure 8B is the current vs time trace for the stimulations in Figure 8A. Both the rise time and the duration of these 3 stimulated adenosine traces were similar and relatively stable. Figure 8C compares the average concentration by genotype and there is a main effect of genotype (One-way ANOVA, Tukey's multiple comparisons, $p<0.0001$, n=8 slices). The concentration in A_1KO mice is significantly higher than the other two genotypes ($p<0.0001$), but wild type mice and A_{2A}KO mice are not significantly different in concentration ($p=0.85$). Figure 8D compares duration using $t_{1/2}$ of the primary oxidation peak and there is a significant effect of genotype on duration (One-way ANOVA, $p=0.025$, n=8 slices). Wild-type mice have a significantly longer duration compared to A_1KO (Tukey's multiple comparisons, $p=0.019$). A_1KO mice had the fastest clearance among these three types of mice, but duration was not significantly different from A_{2A}KO mice ($p=0.64$).

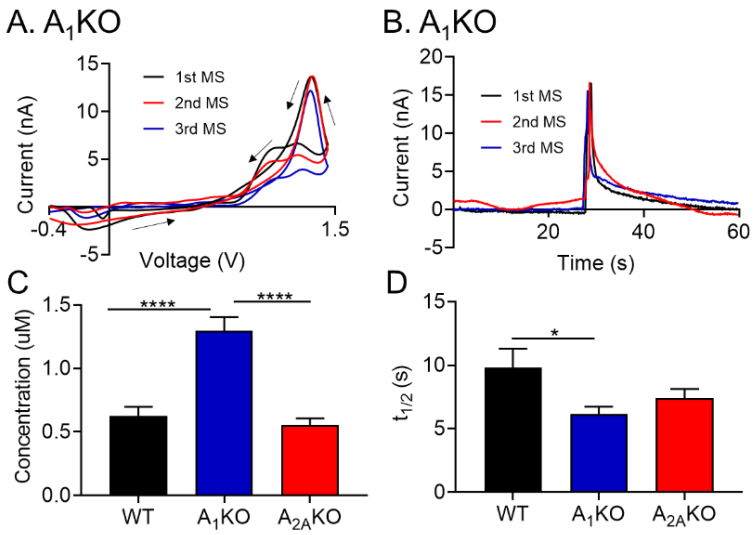

Figure 8 Mechanically-stimulated adenosine in brain slices. A. Example CV of stimulated adenosine release in A_1KO mice brain slice, where the electrode was lowered 50 µm every 15 minutes three times. MS=mechanical stimulation. The black arrows mean the direction of the CV scanning. B. Current vs Time of the primary oxidation peak for same stimulations in A_1KO mice as 5A. C. Average concentration of each stimulation (One-way ANOVA, Tukey's multiple comparisons, overall $p<0.0001$, n=8 slices, 1 slice per animal). D. Average duration ($t_{1/2}$) varies by genotype. (One-way ANOVA, Tukey's multiple comparisons, overall $p=0.025$, n=8 slices, 1 slice per animal.) *$p<0.05$, ****$p<0.0001$, error bars are SEM.

2.3.2.2 *In vivo* measurements.

Mechanical stimulation was also performed *in vivo* by lowering the electrode 4 times, every 15 minutes. These experiments were performed in the same animals as spontaneous adenosine, after the 4 hours of spontaneous data collection. Figure 9 shows the data by stimulation number and the concentration and duration of every mechanical stimulation is stable *in vivo* for multiple stimulations (Figure 9A-9F). Figure 10A shows an example of mechanically-evoked adenosine release in A_1KO mice *in vivo*, with a large adenosine event that begins with the mechanical stimulation at 30 s. The top cyclic voltammogram proves adenosine is detected and the concentration vs time curve shows the response is rapid and cleared within 60 s. *In vivo*, mechanically-evoked adenosine release is larger and longer in duration than spontaneous adenosine release. Figure 10B shows that the average concentration of mechanically-stimulated release is not significantly different by genotype (One-way ANOVA, $p=0.31$, n=8 animals per genotype). For duration, there are no significant differences among the three

genotypes of mice (Fig 6C, One-way ANOVA, p=0.74, n=8 animals per genotype). Overall, knocking out A_1 or A_{2A} receptors does not change the concentration or duration of mechanically-stimulated adenosine *in vivo*.

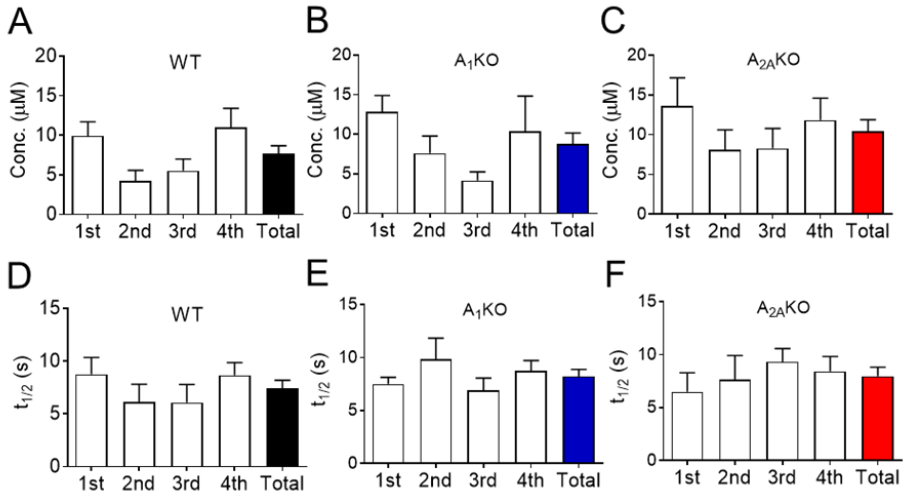

Figure 9. Mechanically-stimulated adenosine measurement *in vivo.* A-C. Adenosine concentration of each mechanical stimulation (A. Wild type, B. A_1KO, C. A_{2A}KO). Total means the average adenosine concentration from the 4 times stimulation. D-F. $t_{1/2}$ of mechanically-stimulated adenosine release (D. Wild type, E. A_1KO, F. A_{2A}KO). Total means the average $t_{1/2}$ of four stimulations.

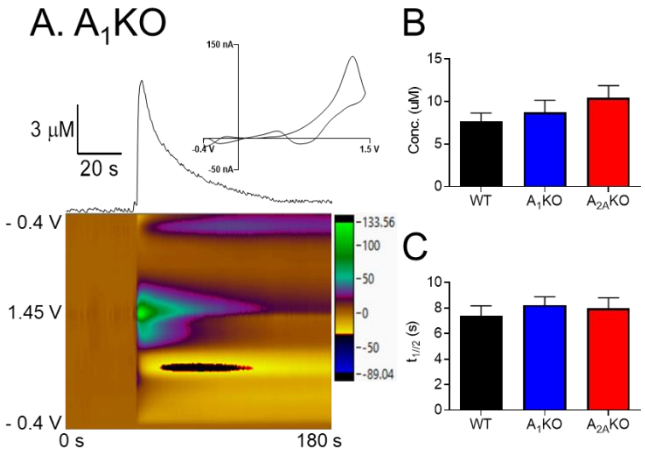

Figure 10. Mechanically-stimulated adenosine measurement *in vivo*. A. Example data of mechanical stimulation in A_1KO mice. Bottom figure is the color plot of the measurement by FSCV (x-axes is time, y-axes is potential and the color differences represent current). Top left is concentration vs time curve of the primary peak, top right is the cyclic voltammogram of adenosine at 30 s. B. Comparison of mechanically-stimulated adenosine concentration shows no difference by genotype (One-way ANOVA, Tukey's multiple comparisons, overall p=0.31, n=8 animals). C. Comparison of $t_{1/2}$ shows no differences genotypes (One-way ANOVA, Tukey's multiple comparisons, overall p=0.74, n=8 animals).

2.4 Discussion

In this study, we investigated the role of A_1 and A_{2A} receptors to regulate spontaneous and mechanically-stimulated adenosine release both *in vivo* and in brain slices. Deletion of A_1 receptors increased the frequency of spontaneous adenosine events but did not change the concentration of the events. Knockout of A_{2A} receptors did not influence the frequency of spontaneous adenosine events but increased the concentration of each event. Brain slice and *in vivo* data had the same trends for spontaneous adenosine release, showing that brain slices are a good model system. For mechanically-stimulated adenosine, the concentration of adenosine was higher in A_1KO mice in the brain slice model, but not *in vivo*. There was no effect of A_{2A} receptors on mechanically-stimulated adenosine. Thus, A_1 and A_{2A} receptors have greater effects on spontaneous adenosine release, and serve to differentially regulate frequency and concentration. This knowledge of adenosine receptor regulation of adenosine signaling is important for future development of drug treatments targeting A_1 and A_{2A} receptors to regulate rapid adenosine release and harness its rapid mode of neuromodulation.

2.4.1 A_1 receptors regulate spontaneous adenosine frequency

A_1 receptors are the most abundant adenosine receptors in the brain and inhibit adenylyl cyclase activity.[53] A_1 receptors are located presynaptically[1,21,55] and can inhibit vesicular release, including that of glutamate and ATP.[10] The mechanism of spontaneous adenosine formation is through the rapid breakdown of extracellular ATP,[30] and thus regulation of ATP release will also regulate adenosine formation. In addition, previous studies demonstrated DPCPX, an A_1 receptor antagonist, regulated the frequency of spontaneous adenosine events, but not the concentration of adenosine release.[32,34,56]

Here, we studied global deletion knockout mice, where the receptor is fully deleted, to better understand the effects of A_1 receptors on spontaneous adenosine. A_1 receptor KO mice

have previously been used to determine the effects of A_1 receptors in regulating sleep[57] and seizures after traumatic brain injury.[58] The hypothesis is that deleting inhibitory A_1 receptors would remove presynaptic inhibition of adenosine release and increase the frequency of adenosine transients. Indeed, in both brain slices and *in vivo*, there was a significantly higher number of spontaneous adenosine events in A_1KO mice compared to wild type. Deletion of A_1 receptors only increased the frequency of spontaneous adenosine, but did not affect the average concentration or the duration. A_1 receptors regulate the frequency of exocytotic events, and global deletion therefore allows more exocytosis, causing more adenosine events. However, the loading of the vesicles remains the same so the average concentration is not affected. Previous studies have shown that spontaneous adenosine is regulated by the frequency of release, particularly when pharmacological agents are given to block A_1, $GABA_B$, or NMDA receptors.[32,34] Mice with global deletions of CD39 or CD73, the enzymes that breakdown extracellular ATP, also had lower frequency of release, but little to no effect on concentration.[30,34,56] Therefore, A_1 receptors, acting presynaptically, regulate the frequency of spontaneous adenosine release, and this mechanism could be explored in the future as a method of harnessing the rapid neuromodulatory properties of adenosine.

2.4.2 A_{2A} receptors regulate the concentration but not the frequency of spontaneous adenosine

A_{2A} receptors are the second most abundant adenosine receptors in the brain, and are expressed at high levels in the caudate-putamen region.[1,53,59,60] A_{2A} receptors are excitatory receptors that stimulate adenylyl cyclase activity to increase cAMP. A_{2A}KO mice have been widely used for behavioral or pharmacology research; for example, A_{2A}KO attenuates brain injury in mice, A_{2A}KO mice are less sensitive in depression tests, and deletion of A_{2A} receptors influences anxiety in mice.[44,47,61,62] A_{2A} receptors are most densely located post-synaptically in the striatum.[63] However, A_{2A} receptors are also located presynaptically, where they control the

release of glutamate[64,65] by tightly interacting with A_1 and other receptors.[66] Moreover, A_{2A} receptors are engaged in neuromodulation in the caudate.[67–71] Here, A_{2A}KO mice had no change in frequency of spontaneous events, suggesting that presynaptic A_{2A} receptors do not control the frequency of spontaneous adenosine events. A_{2A} receptors do not regulate baseline neurotransmitter release but do regulate faster events related to long-term potentiation (LTP)[67] however the lack of A_{2A} receptors does not change adenosine frequency and so spontaneous adenosine release does not appear linked to LTP processes.

The main effect observed in A_{2A}KO mice is that the average concentration of each adenosine event was larger. There are a few possible explanations for this increase in concentration. A_{2A}KO may enhance the breakdown of ATP to extracellular adenosine by enzymes such as CD73, because CD73 is colocalized with A_{2A} receptors in the caudate putamen and activation of A_{2A} receptors requires CD73.[72] Therefore, knocking out A_{2A} receptors may change the expression of CD73, which could result in a higher extracellular adenosine concentration. Another possible mechanism is compensation by adenosine A_{2B} receptors, which are also excitatory. A_{2B} receptor expression is 4.5 fold higher in A_{2A}KO mice than wild type mice.[50] The regulation of spontaneous adenosine concentration by A_{2B} receptors is not known, but could be investigated as a compensatory mechanism.

The duration of spontaneous adenosine in A_{2A}KO mice is also significantly shorter than wild type mice both *in vivo* and in brain slice (Fig. 3D, 6D). A_{2A} receptors may regulate adenosine deaminase or adenosine kinase, the main metabolic enzymes which are responsible for fast extracellular breakdown of adenosine.[26] For example, A_{2A} receptors are affected by adenosine deaminase binding and A_{2A}KO could increase adenosine deaminase activity, which speeds up spontaneous adenosine clearance. Spontaneous adenosine is also cleared by equilibrative nucleoside transporters (ENTs),[26,73] and these ENTs are modulated by A_{2A} receptors to control the extracellular adenosine level in rat hippocampus.[26,74] Future studies

could study adenosine clearance in A_{2A}KO mice with pharmacology to determine the mechanism of clearance.

2.4.3 Mechanically stimulated adenosine is not dependent on A1 or A2A receptors

Moving an electrode in a brain slice causes mechanically-stimulated adenosine without causing significant tissue damage.[37] Mechanical stimulation is therefore a way of causing shear stress in the brain, without killing the cells. The mechanism of formation of mechanically-stimulated release is different than spontaneous adenosine release, as it is not dependent on the adenosine breakdown enzymes CD39 or CD73, implying that it is not due to extracellular breakdown of ATP.[30] Thus, we hypothesized that regulation of mechanically-stimulated release by A_1 and A_{2A} receptors would be different than regulation of spontaneous adenosine release. In A_1 and A_{2A}KO mice, there were no changes in mechanically-stimulated concentration or duration *in vivo*. However, in brain slices, the concentration was significantly higher in A_1KO mice and the duration was significantly lower (Fig. 8C, 8D). These data are the only data from brain slices and *in vivo* which do not agree, as all other data showed the same trends. The reason might be that smaller concentrations are elicited in brain slices in WT, and thus larger concentrations in A_1KO are easier to observe. Larger concentrations are expected if you remove inhibition. However, the *in vivo* data do not show that trend, and stimulations are large for all genotypes, likely due to robust pools of adenosine maintained by synthesis. The source of mechanically-stimulated release is less understood. There is some evidence for exocytosis, as tetrodotoxin or EDTA decrease the concentration of mechanically-stimulated adenosine, suggesting it is activity dependent.[25,37,39] However, other studies suggest it could be regulated by hemichannels such as pannexins or connexins, which are mechanosensitive.[75] Thus, regulation may not be through presynaptic mechanisms and the overall results here suggest mechanically-stimulated release is not as strongly regulated by A_1 and A_{2A} receptors. The data also support that A_1 and A_{2A} drugs would preferentially regulate spontaneous and not

mechanically-stimulated adenosine release, allowing a way to tap into the rapid neuromodulatory properties of spontaneous release.

2.5 Conclusions

In this paper, we investigated the role of adenosine receptors to regulate spontaneous adenosine and mechanically-stimulated adenosine by using knockout mice. A_1KO mice have an increased frequency of spontaneous adenosine, but no change in concentration, both *in vivo* and in brain slices. A_1 receptors act as presynaptic inhibitors, inhibiting exocytotic events that cause spontaneous adenosine. Deletion of A_{2A} receptors resulted in higher concentrations of spontaneous adenosine, which may be related to interplay of A_{2A} receptors with adenosine breakdown enzymes or compensation by A_{2B} receptors. *In vivo*, mechanically-stimulated adenosine concentration is not dependent on A_1 or A_{2A} receptors, suggesting it is regulated differently than spontaneous release. This differential regulation of release is important because it could lead to specific pharmacological treatments of A_1 or A_{2A} receptors that target manipulation of spontaneous adenosine release but not mechanically-stimulated release.

2.6 References

(1) Cunha, R. A. Neuroprotection by Adenosine in the Brain: From A1 Receptor Activation to A2A Receptor Blockade. *Purinergic Signalling*. 2005, pp 111–134. https://doi.org/10.1007/s11302-005-0649-1.

(2) Cunha, R. A. Adenosine as a Neuromodulator and as a Homeostatic Regulator in the Nervous System: Different Roles, Different Sources and Different Receptors. *Neurochem. Int.* **2001**, *38* (2), 107–125. https://doi.org/10.1016/S0197-0186(00)00034-6.

(3) Shibata, S.; Watanabe, S. A Neuroprotective Effect of Histamine H1 Receptor Antagonist on Ischemia-Induced Decrease in 2-Deoxyglucose Uptake in Rat Hippocampal Slices. *Neurosci. Lett.* **1993**, *151* (2), 138–141. https://doi.org/10.1016/0304-3940(93)90005-6.

(4) Wang, Y.; Venton, B. J. Correlation of Transient Adenosine Release and Oxygen Changes in the Caudate-Putamen. *J. Neurochem.* **2017**, *140* (1), 13–23. https://doi.org/10.1111/jnc.13705.

(5) Porkka-Heiskanen, T.; Strecker, R. E.; Thakkar, M.; Bjørkum, A. A.; Greene, R. W.; McCarley, R. W. Adenosine: A Mediator of the Sleep-Inducing Effects of Prolonged Wakefulness. *Science (80-.).* **1997**, *276* (5316), 1265–1267. https://doi.org/10.1126/science.276.5316.1265.

(6) Koos, B. J.; Kruger, L.; Murray, T. F. Source of Extracellular Brain Adenosine during Hypoxia in Fetal Sheep. *Brain Res.* **1997**, *778* (2), 439–442. https://doi.org/10.1016/S0006-8993(97)01207-9.

(7) Kalinchuk, A. V.; Urrila, A. S.; Alanko, L.; Heiskanen, S.; Wigren, H. K.; Suomela, M.; Stenberg, D.; Porkka-Heiskanen, T. Local Energy Depletion in the Basal Forebrain Increases Sleep. *Eur. J. Neurosci.* **2003**, *17* (4), 863–869. https://doi.org/10.1046/j.1460-9568.2003.02532.x.

(8) Dale, N.; Frenguelli, B. G. Release of Adenosine and ATP during Ischemia and Epilepsy. *Curr.Neuropharmacol.* **2009**, *7* (3), 160–179. https://doi.org/10.2174/157015909789152146 [doi].

(9) Ganesana, M.; Jill Venton, B. Early Changes in Transient Adenosine during Cerebral Ischemia and Reperfusion Injury. *PLoS One* **2018**, *13* (5), 1–18. https://doi.org/10.1371/journal.pone.0196932.

(10) Cunha, R. A. How Does Adenosine Control Neuronal Dysfunction and Neurodegeneration? *J. Neurochem.* **2016**, *139* (6), 1019–1055. https://doi.org/10.1111/jnc.13724.

(11) Fredholm, B. B.; Chen, J. F.; Cunha, R. A.; Svenningsson, P.; Vaugeois, J. M. Adenosine and Brain Function. *Int. Rev. Neurobiol.* **2005**, *63*, 191–270. https://doi.org/10.1016/S0074-7742(05)63007-3.

(12) Carr, R. M., Oranu, A., & Khungar, V. *Nomenclature and Classification of Purinoceptors*; 1994; Vol. 46. https://doi.org/10.1016/j.physbeh.2017.03.040.

(13) Borea, P. A.; Gessi, S.; Merighi, S.; Varani, K. Adenosine as a Multi-Signalling Guardian Angel in Human Diseases: When, Where and How Does It Exert Its Protective Effects? *Trends Pharmacol. Sci.* **2016**, *37* (6), 419–434. https://doi.org/10.1016/j.tips.2016.02.006.

(14) Eltzschig, H. K. Adenosine: An Old Drug Newly Discovered. *Anesthesiology* **2009**, *111* (4), 904–915. https://doi.org/10.1097/ALN.0b013e3181b060f2.

(15) Borea, P. A.; Gessi, S.; Merighi, S.; Vincenzi, F.; Varani, K. Pathological Overproduction: The Bad Side of Adenosine. *Br. J. Pharmacol.* **2017**, *174* (13), 1945–1960. https://doi.org/10.1111/bph.13763.

(16) Ganesana, M.; Lee, S. T.; Wang, Y.; Venton, B. J. Analytical Techniques in Neuroscience: Recent Advances in Imaging, Separation, and Electrochemical Methods. *Anal. Chem.* **2017**, *89* (1), 314–341. https://doi.org/10.1021/acs.analchem.6b04278.

(17) Melani, A.; Pugliese, A. M.; Pedata, F. Chapter Thirteen - Adenosine Receptors in Cerebral Ischemia. In *Adenosine Receptors in Neurology and Psychiatry*; of Neurobiology, A. M. B. T.-I. R., Ed.; Academic Press, 2014; Vol. Volume 119, pp 309–348. https://doi.org/https://doi.org/10.1016/B978-0-12-801022-8.00013-1.

(18) Cunha, R. A.; Almeida, T.; Ribeiro, J. A. Modification by Arachidonic Acid of Extracellular Adenosine Metabolism and Neuromodulatory Action in the Rat Hippocampus. *J. Biol. Chem.* **2000**, *275* (48), 37572–37581. https://doi.org/10.1074/jbc.M003011200.

(19) Lopes, L. V.; Cunha, R. A.; Kull, B.; Fredholm, B. B.; Ribeiro, J. A. Adenosine A2A Receptor Facilitation of Hippocampal Synaptic Transmission Is Dependent on Tonic A1 Receptor Inhibition. *Neuroscience* **2002**, *112* (2), 319–329. https://doi.org/10.1016/S0306-4522(02)00080-5.

(20) Rebola, N.; Oliveira, C. R.; Cunha, R. A. Transducing System Operated by Adenosine A2A Receptors to Facilitate Acetylcholine Release in the Rat Hippocampus. *Eur. J. Pharmacol.* **2002**, *454* (1), 31–38. https://doi.org/10.1016/S0014-2999(02)02475-5.

(21) Fuxe, K.; Ferre, S.; Canals, M.; Torvinen, M.; Terasmaa, A.; Marcellino, D.; Goldberg, S. R.; Staines, W.; Jacobsen, K. X.; Lluis, C.; Woods, A. S.; Agnati, L. F.; Franco, R. Adenosine-Dopamine Interactions Revealed in Knockout Mice. *J. Mol. Neurosci.* **2005**, *26* (2), 209–220. https://doi.org/10.1385/JMN/26.

(22) Lee, S. T.; Venton, B. J. Regional Variations of Spontaneous, Transient Adenosine Release in Brain Slices. *ACS Chem. Neurosci.* **2018**, *9* (3), 505–513. https://doi.org/10.1021/acschemneuro.7b00280.

(23) Pazzagli, M.; Pedata, F.; Pepeu, G. Effect of K+ Depolarization, Tetrodotoxin, and NMDA Receptor Inhibition on Extracellular Adenosine Levels in Rat Striatum. *Eur. J. Pharmacol.* **1993**, *234* (1), 61–65.

(24) Lloyd, H. G. E.; Fredholm, B. B. Involvement of Adenosine Deaminase and Adenosine Kinase in Regulating Extracellular Adenosine Concentration in Rat Hippocampal Slices. *Neurochem. Int.* **1995**, *26* (4), 387–395. https://doi.org/10.1016/0197-0186(94)00144-J.

(25) Mitchell, J. B.; Lupica, C. R.; Dunwiddie, T. V. Activity-Dependent Release of Endogenous Adenosine Modulates Synaptic Responses in the Rat Hippocampus. *J. Neurosci.* **1993**, *13* (8), 3439–3447. https://doi.org/10.1523/jneurosci.13-08-03439.1993.

(26) Nguyen, M. D.; Ross, A. E.; Ryals, M.; Lee, S. T.; Venton, B. J. Clearance of Rapid Adenosine Release Is Regulated by Nucleoside Transporters and Metabolism. *Pharmacol. Res. Perspect.* **2015**, *3* (6), 1–12. https://doi.org/10.1002/prp2.189.

(27) Nguyen, M. D.; Venton, B. J. Fast-Scan Cyclic Voltammetry for the Characterization of Rapid Adenosine Release. *Comput. Struct. Biotechnol. J.* **2015**, *13*, 47–54. https://doi.org/10.1016/j.csbj.2014.12.006.

(28) Yang, C.; Wang, Y.; Jacobs, C. B.; Ivanov, I. N.; Venton, B. J. O2 Plasma Etching and Antistatic Gun Surface Modifications for CNT Yarn Microelectrode Improve Sensitivity and Antifouling Properties. *Anal. Chem.* **2017**, *89* (10), 5605–5611. https://doi.org/10.1021/acs.analchem.7b00785.

(29) Wang, Y.; Venton, B. J. Comparison of Spontaneous and Mechanically-Stimulated Adenosine Release in Mice. *Neurochem. Int.* **2019**, *124* (December 2018), 46–50. https://doi.org/10.1016/j.neuint.2018.12.007.

(30) Wang, Y.; Copeland, J.; Shin, M.; Chang, Y.; Venton, B. J. CD73 or CD39 Deletion Reveals Different Mechanisms of Formation for Spontaneous and Mechanically-Stimulated Adenosine Release and Sex Specific Compensations in ATP Degradation. *ACS Chem. Neurosci.* **2020**, *11* (6), 919–928. https://doi.org/10.1021/acschemneuro.9b00620.

(31) Borgus, J. R.; Puthongkham, P.; Venton, B. J. Complex Sex and Estrous Cycle Differences in Spontaneous Transient Adenosine. *J. Neurochem.* **2020**, e14981.

https://doi.org/10.1111/jnc.14981.

(32) Nguyen, M. D.; Wang, Y.; Ganesana, M.; Venton, B. J. Transient Adenosine Release Is Modulated by NMDA and GABAB Receptors. *ACS Chem. Neurosci.* **2017**, *8* (2), 376–385. https://doi.org/10.1021/acschemneuro.6b00318.

(33) Ross, A. E.; Venton, B. J. Adenosine Transiently Modulates Stimulated Dopamine Release in the Caudate-Putamen via A1 Receptors. *J. Neurochem.* **2015**, *132*, 51–60. https://doi.org/10.1111/jnc.12946.

(34) Nguyen, M. D.; Lee, S. T.; Ross, A. E.; Ryals, M.; Choudhry, V. I.; Venton, B. J. Characterization of Spontaneous, Transient Adenosine Release in the Caudate-Putamen and Prefrontal Cortex. *PLoS One* **2014**, *9* (1), e87165. https://doi.org/10.1371/journal.pone.0087165.

(35) Pajski, M. L.; Venton, B. J. The Mechanism of Electrically Stimulated Adenosine Release Varies by Brain Region. **2013**, 167–174. https://doi.org/10.1007/s11302-012-9343-2.

(36) Wang, Y.; Venton, B. J. Caffeine Modulates Spontaneous Adenosine and Oxygen Changes during Ischemia and Reperfusion. *ACS Chem. Neurosci.* **2019**, *10* (4), 1941–1949. https://doi.org/10.1021/acschemneuro.8b00251.

(37) Ross, A. E.; Nguyen, M. D.; Privman, E.; Venton, B. J. Mechanical Stimulation Evokes Rapid Increases in Extracellular Adenosine Concentration in the Prefrontal Cortex. *J. Neurochem.* **2014**, *130* (1), 50–60. https://doi.org/10.1111/jnc.12711.

(38) Wan, J.; Ristenpart, W. D.; Stone, H. A. Dynamics of Shear-Induced ATP Release from Red Blood Cells. *Proc. Natl. Acad. Sci. U. S. A.* **2008**, *105* (43), 16432–16437. https://doi.org/10.1073/pnas.0805779105.

(39) Pajski, M. L.; Venton, B. J. Adenosine Release Evoked by Short Electrical Stimulations in Striatal Brain Slices Is Primarily Activity Dependent. *ACS Chem. Neurosci.* **2010**, *1* (12), 775–787. https://doi.org/10.1021/cn100037d.

(40) Lee, H. T.; Xu, H.; Nasr, S. H.; Schnermann, J.; Emala, C. W. A1 Adenosine Receptor Knockout Mice Exhibit Increased Renal Injury Following Ischemia and Reperfusion. *Am. J. Physiol. - Ren. Physiol.* **2004**, *286* (2 55-2), 298–306. https://doi.org/10.1152/ajprenal.00185.2003.

(41) Schweda, F.; Wagner, C.; Krämer, B. K.; Schnermann, J.; Kurtz, A. Preserved Macula Densa-Dependent Renin Secretion in A1 Adenosine Receptor Knockout Mice. *Am. J. Physiol. - Ren. Physiol.* **2003**, *284* (4 53-4), 770–777. https://doi.org/10.1152/ajprenal.00280.2002.

(42) Lee, H. T.; Jan, M.; Soo, C. B.; Jin, D. J.; Goubaeva, F. R.; Yang, J.; Kim, M. A1 Adenosine Receptor Knockout Mice Are Protected against Acute Radiocontrast Nephropathy in Vivo. *Am. J. Physiol. - Ren. Physiol.* **2006**, *290* (6), 1367–1375. https://doi.org/10.1152/ajprenal.00347.2005.

(43) Ledent, C.; Vaugeois, J.-M.; Schiffmann, S. N.; Pedrazzini, T.; Yacoubi, M. El; Vanderhaeghen, J.-J.; Costentin, J.; Heath, J. K.; Vassart, G.; Parmentier, M. Aggressiveness, Hypoalgesia and High Blood Pressure in Mice Lacking the Adenosine A2a Receptor. *Nature* **1997**, *388* (6643), 674–678. https://doi.org/10.1038/41771.

(44) Johansson, B.; Halldner, L.; Dunwiddie, T. V; Masino, S. A.; Poelchen, W.; Giménez-Llort, L.; Escorihuela, R. M.; Fernández-Teruel, A.; Wiesenfeld-Hallin, Z.; Xu, X.-J.; Hårdemark,

A.; Betsholtz, C.; Herlenius, E.; Fredholm, B. B. Hyperalgesia, Anxiety, and Decreased Hypoxic Neuroprotection in Mice Lacking the Adenosine A1 Receptor. *Proc. Natl. Acad. Sci.* **2001**, *98* (16), 9407–9412. https://doi.org/10.1073/pnas.161292398.

(45) Yacoubi, M. El; Ledent, C.; Parmentier, M.; Bertorelli, R.; Ongini, E.; Costentin, J.; Vaugeois, J.-M. Adenosine A2A Receptor Antagonists Are Potential Antidepressants: Evidence Based on Pharmacology and A2A Receptor Knockout Mice. *Br. J. Pharmacol.* **2001**, *134* (1), 68–77. https://doi.org/10.1038/sj.bjp.0704240.

(46) Montesinos, M. C.; Desai, A.; Chen, J. F.; Yee, H.; Schwarzschild, M. A.; Fink, J. S.; Cronstein, B. N. Adenosine Promotes Wound Healing and Mediates Angiogenesis in Response to Tissue Injury via Occupancy of A2A Receptors. *Am. J. Pathol.* **2002**, *160* (6), 2009–2018. https://doi.org/10.1016/S0002-9440(10)61151-0.

(47) Chen, J. F.; Huang, Z.; Ma, J.; Zhu, J. M.; Moratalla, R.; Standaert, D.; Moskowitz, M. A.; Fink, J. S.; Schwarzschild, M. A. A(2A) Adenosine Receptor Deficiency Attenuates Brain Injury Induced by Transient Focal Ischemia in Mice. *J. Neurosci.* **1999**, *19* (21), 9192–9200. https://doi.org/10.1523/JNEUROSCI.19-21-09192.1999.

(48) Chen, J.-F.; Moratalla, R.; Impagnatiello, F.; Grandy, D. K.; Cuellar, B.; Rubinstein, M.; Beilstein, M. A.; Hackett, E.; Fink, J. S.; Low, M. J.; Ongini, E.; Schwarzschild, M. A. The Role of the D2 Dopamine Receptor (D2R) in A2A Adenosine Receptor (A2AR)-Mediated Behavioral and Cellular Responses as Revealed by A2A and D2 Receptor Knockout Mice. *Proc. Natl. Acad. Sci.* **2001**, *98* (4), 1970–1975. https://doi.org/10.1073/pnas.98.4.1970.

(49) Huffman, M. L.; Venton, B. J. Electrochemical Properties of Different Carbon-Fiber Microelectrodes Using Fast-Scan Cyclic Voltammetry. *Electroanalysis* **2008**, *20* (22), 2422–2428. https://doi.org/10.1002/elan.200804343.

(50) Teng, B.; Ledent, C.; Mustafa, S. J. Up-Regulation of A2B Adenosine Receptor in A2A Adenosine Receptor Knockout Mouse Coronary Artery. *J. Mol. Cell. Cardiol.* **2008**, *44* (5), 905–914. https://doi.org/10.1016/j.yjmcc.2008.03.003.

(51) El-Awady, M. S.; Rajamani, U.; Teng, B.; Tilley, S. L.; Mustafa, S. J. Evidence for the Involvement of NADPH Oxidase in Adenosine Receptors-Mediated Control of Coronary Flow Using A(1) and A(3) Knockout Mice. *Physiol. Rep.* **2013**, *1* (3), e00070. https://doi.org/10.1002/phy2.70.

(52) Borman, R. P.; Wang, Y.; Nguyen, M. D.; Ganesana, M.; Lee, S. T.; Venton, B. J. Automated Algorithm for Detection of Transient Adenosine Release. *ACS Chem. Neurosci.* **2017**, *8* (2), 386–393. https://doi.org/10.1021/acschemneuro.6b00262.

(53) Borea, P. A.; Varani, K.; Gessi, S.; Merighi, S.; Vincenzi, F. *The Adenosine Receptors*; The Receptors; Springer International Publishing, 2018.

(54) zur Nedden, S.; Doney, A. S.; Frenguelli, B. G. Modulation of Intracellular ATP Determines Adenosine Release and Functional Outcome in Response to Metabolic Stress in Rat Hippocampal Slices and Cerebellar Granule Cells. *J. Neurochem.* **2014**, *128* (1), 111–124. https://doi.org/10.1111/jnc.12397.

(55) Rebola, N.; Pinheiro, P. C.; Oliveira, C. R.; Malva, J. O.; Cunha, R. A. Subcellular Localization of Adenosine A1 Receptors in Nerve Terminals and Synapses of the Rat Hippocampus. *Brain Res.* **2003**, *987* (1), 49–58. https://doi.org/10.1016/S0006-8993(03)03247-5.

(56) Cechova, S.; Elsobky, A. M.; Venton, B. J. A1 Receptors Self-Regulate Adenosine Release in the Striatum: Evidence of Autoreceptor Characteristics. *Neuroscience* **2010**, *171* (4), 1006–1015. https://doi.org/10.1016/j.neuroscience.2010.09.063.

(57) Stenberg, D.; Litonius, E.; Halldner, L.; Johansson, B.; Fredholm, B. B.; Porkka-Heiskanen, T. Sleep and Its Homeostatic Regulation in Mice Lacking the Adenosine A1 Receptor. *J. Sleep Res.* **2003**, *12* (4), 283–290. https://doi.org/10.1046/j.0962-1105.2003.00367.x.

(58) Kochanek, P. M.; Vagni, V. A.; Janesko, K. L.; Washington, C. B.; Crumrine, P. K.; Garman, R. H.; Jenkins, L. W.; Clark, R. S. B.; Homanics, G. E.; Dixon, C. E.; Schnermann, J.; Jackson, E. K. Adenosine A1 Receptor Knockout Mice Develop Lethal Status Epilepticus after Experimental Traumatic Brain Injury. *J. Cereb. Blood Flow Metab.* **2005**, *26* (4), 565–575. https://doi.org/10.1038/sj.jcbfm.9600218.

(59) Rosin, D. L.; Robeva, A.; Woodard, R. L.; Guyenet, P. G.; Linden, J. Immunohistochemical Localization of Adenosine A(2A) Receptors in the Rat Central Nervous System. *J. Comp. Neurol.* **1998**, *401* (2), 163–186. https://doi.org/10.1002/(SICI)1096-9861(19981116)401:2<163::AID-CNE2>3.0.CO;2-D.

(60) Hettinger, B. D.; Lee, A.; Linden, J.; Rosin, D. L. Ultrastructural Localization of Adenosine A2A Receptors Suggests Multiple Cellular Sites for Modulation of GABAergic Neurons in Rat Striatum. *J. Comp. Neurol.* **2001**, *431* (3), 331–346. https://doi.org/10.1002/1096-9861(20010312)431:3<331::AID-CNE1074>3.0.CO;2-W.

(61) El Yacoubi, M.; Ledent, C.; Parmentier, M.; Costentin, J.; Vaugeois, J. M. Adenosine A2A Receptor Knockout Mice Are Partially Protected against Drug-Induced Catalepsy. *Neuroreport* **2001**, *12* (5), 983–986. https://doi.org/10.1097/00001756-200104170-00024.

(62) López-Cruz, L.; Carbó-Gas, M.; Pardo, M.; Bayarri, P.; Valverde, O.; Ledent, C.; Salamone, J. D.; Correa, M. Adenosine A2A Receptor Deletion Affects Social Behaviors and Anxiety in Mice: Involvement of Anterior Cingulate Cortex and Amygdala. *Behav. Brain Res.* **2017**, *321*, 8–17. https://doi.org/10.1016/j.bbr.2016.12.020.

(63) Svenningsson, P.; Le Moine, C.; Fisone, G.; Fredholm, B. B. Distribution, Biochemistry and Function of Striatal Adenosine A(2A) Receptors. *Prog. Neurobiol.* **1999**, *59* (4), 355–396. https://doi.org/10.1016/S0301-0082(99)00011-8.

(64) Rodrigues, R. J.; Alfaro, T. M.; Rebola, N.; Oliveira, C. R.; Cunha, R. A. Co-Localization and Functional Interaction between Adenosine A2A and Metabotropic Group 5 Receptors in Glutamatergic Nerve Terminals of the Rat Striatum. *J. Neurochem.* **2005**, *92* (3), 433–441. https://doi.org/10.1111/j.1471-4159.2004.02887.x.

(65) Köfalvi, A.; Moreno, E.; Cordomí, A.; Cai, N.-S.; Fernández-Dueñas, V.; Ferreira, S. G.; Guixà-González, R.; Sánchez-Soto, M.; Yano, H.; Casadó-Anguera, V.; Cunha, R. A.; Sebastião, A. M.; Ciruela, F.; Pardo, L.; Casadó, V.; Ferré, S. Control of Glutamate Release by Complexes of Adenosine and Cannabinoid Receptors. *BMC Biol.* **2020**, *18* (1), 9. https://doi.org/10.1186/s12915-020-0739-0.

(66) Ciruela, F.; Casadó, V.; Rodrigues, R. J.; Luján, R.; Burgueño, J.; Canals, M.; Borycz, J.; Rebola, N.; Goldberg, S. R.; Mallol, J.; Cortés, A.; Canela, E. I.; López-Giménez, J. F.; Milligan, G.; Lluis, C.; Cunha, R. A.; Ferré, S.; Franco, R. Presynaptic Control of Striatal Glutamatergic Neurotransmission by Adenosine A1–A2A Receptor Heteromers. *J. Neurosci.* **2006**, *26* (7), 2080–2087. https://doi.org/10.1523/JNEUROSCI.3574-05.2006.

(67) D'Alcantara, P.; Ledent, C.; Swillens, S.; Schiffmann, S. N. Inactivation of Adenosine A2A Receptor Impairs Long Term Potentiation in the Accumbens Nucleus without Altering Basal Synaptic Transmission. *Neuroscience* **2001**, *107* (3), 455–464. https://doi.org/10.1016/S0306-4522(01)00372-4.

(68) Rebola, N.; Canas, P. M.; Oliveira, C. R.; Cunha, R. A. Different Synaptic and Subsynaptic Localization of Adenosine A2A Receptors in the Hippocampus and Striatum of the Rat. *Neuroscience* **2005**, *132* (4), 893–903. https://doi.org/10.1016/j.neuroscience.2005.01.014.

(69) Quiroz, C.; Gomes, C.; Pak, A. C.; Ribeiro, J. A.; Goldberg, S. R.; Hope, B. T.; Ferré, S. Blockade of Adenosine A2A Receptors Prevents Protein Phosphorylation in the Striatum Induced by Cortical Stimulation. *J. Neurosci.* **2006**, *26* (42), 10808–10812. https://doi.org/10.1523/JNEUROSCI.1661-06.2006.

(70) Schiffmann, S. N.; Fisone, G.; Moresco, R.; Cunha, R. A.; Ferré, S. Adenosine A2A Receptors and Basal Ganglia Physiology. *Prog. Neurobiol.* **2007**, *83* (5), 277–292. https://doi.org/10.1016/j.pneurobio.2007.05.001.

(71) Morato, X.; Cunha, R. A.; Ciruela, F. G Protein-Coupled Receptor 37 (GPR37) Emerges as an Important Modulator of Adenosinergic Transmission in the Striatum. *Neural Regen. Res.* **2019**, *14* (11), 1912–1914. https://doi.org/10.4103/1673-5374.259610.

(72) Augusto, E.; Matos, M.; Sévigny, J.; El-Tayeb, A.; Bynoe, M. S.; Müller, C. E.; Cunha, R. a; Chen, J.-F. Ecto-5'-Nucleotidase (CD73)-Mediated Formation of Adenosine Is Critical for the Striatal Adenosine A2A Receptor Functions. *J. Neurosci.* **2013**, *33* (28), 11390–11399. https://doi.org/10.1523/JNEUROSCI.5817-12.2013.

(73) Thorn, J. A.; Jarvis, S. M. Adenosine Transporters. *Gen. Pharmacol.* **1996**, *27* (4), 613–620. https://doi.org/10.1016/0306-3623(95)02053-5.

(74) Pinto-Duarte, A.; Coelho, J. E.; Cunha, R. A.; Ribeiro, J. A.; Sebastião, A. M. Adenosine A2A Receptors Control the Extracellular Levels of Adenosine through Modulation of Nucleoside Transporters Activity in the Rat Hippocampus. *J. Neurochem.* **2005**, *93* (3), 595–604. https://doi.org/10.1111/j.1471-4159.2005.03071.x.

(75) Xia, J.; Lim, J. C.; Lu, W.; Beckel, J. M.; Macarak, E. J.; Laties, A. M.; Mitchell, C. H. Neurons Respond Directly to Mechanical Deformation with Pannexin-Mediated ATP Release and Autostimulation of P2X 7 Receptors. *J. Physiol.* **2012**, *590* (10), 2285–2304. https://doi.org/10.1113/jphysiol.2012.227983.

Chapter 3

Pannexin1 channels regulate mechanically-stimulated but not spontaneous adenosine release

Chapter 3 was submitted and under reviewed with *Analytical and Bioanalytical Chemistry.* At the time of submission.

Abstract

Fast-scan cyclic voltammetry is a rapid technique to measure neuromodulators, and using FSCV, two modes of rapid adenosine have been discovered. Spontaneous transients occur randomly in the brain, while mechanical stimulation also causes a rapid adenosine event. Pannexin1 channels are membrane channels that transport ions, including ATP, out of the cell where it is rapidly broken down into adenosine. Pannexin 1 channels (Panx1) have a flickering mode of rapid opening and are also mechanically-stimulated. Here, we test the extent to which pannexin channels, specifically pannexin1 (Panx1) channels, are responsible for rapid adenosine events. Spontaneous adenosine release or mechanosensitive adenosine release were measured using fast-scan cyclic voltammetry in hippocampal (CA1) brain slices. In global Panx1KO mice, there is no significant difference in the frequency or concentration of spontaneous adenosine release, indicating Panx1 is not a release mechanism for spontaneous adenosine. Spontaneous adenosine frequency decreased slightly after administration of a large (100 μM) dose of carbenoxolone, a nonspecific inhibitor of many pannexin and connexin channels, suggesting other channels may play a small role. For mechanically-stimulated adenosine release, the concentration of each adenosine event significantly decreased 30% in Panx1KO mice and the frequency of stimulations that evoked adenosine also decreased. The response was similar in WT mice with carbenoxolone. Thus, Panx1 is a release mechanism for mechanically-stimulated adenosine release, but not the only mechanism. These results demonstrate that pannexin channels differentially regulate rapid adenosine release and could be targeted to differentially affect mechanically-stimulated adenosine due to brain damage.

3.1 Introduction

Rapid adenosine release in the brain plays a role in rapid neuromodulation, and adenosine released during conditions such as ischemia is neuroprotective.[1–3] However, monitoring rapid adenosine release is challenging. Our lab has developed fast-scan cyclic voltammetry for the detection of rapid adenosine release.[4,5] FSCV measurements were useful in identifying two modes of rapid adenosine release: (1) spontaneous adenosine release which lasts only a few seconds and occurs once every few minutes [6,7] and (2) mechanically-stimulated release which lasts 20-30 s.[8,9] Spontaneous events are natural and occur randomly in many brain regions.[10,11] Mechanical stimulation is a model of brain damage and release is likely caused by shear stress in the brain.[12] However, the mechanism of release for each of these modes has not been established, and adenosine may be released in different modes depending on the type of release.[13,14] Rapid electrochemical methods, combined with pharmacology and genetic knockout mice, will allow us to test hypotheses about how adenosine is released.

There are many possible mechanisms for adenosine release. One hypothesis for is that rapid adenosine is formed from the breakdown of exocytotically released ATP.[15] Both spontaneous and mechanically-sensitive adenosine are sensitive to tetrodotoxin (TTX),[7,8] which blocks activity dependent release, suggesting they are due to exocytosis. However, the signals are not completely eliminated with TTX, so other release mechanisms exist. Spontaneous adenosine release is dependent on the enzymes CD73 and CD39, which breakdown ATP to adenosine in the extracellular space, but mechanosensitive adenosine is not dependent on those enzymes.[13] Thus, there are still other mechanisms that need to be identified for rapid adenosine release.

One novel mechanism for possible release of adenosine is membrane hemichannels called connexin and pannexin channels.[16–18] Connexin proteins form gap junctions between cells to allow ionic and metabolic coupling, while pannexin channels are transmembrane anion channels that connect the intracellular space of a cell with the extracellular space.[19] There are

three types of pannexin channels: pannexin 1 (Panx1), pannexin 2 (Panx2), and pannexin 3 (Panx3).[20] Panx1 is the most widely studied channel, and is expressed throughout the body, including in cortical and hippocampal neurons in the brain.[21] Pannexins form anion channels and release ATP in response to calcium propagation.[22] Pannexin1 channels are also mechanosensitive, releasing ATP in response to mechanical stress.[23] Panx1 channels regulate ATP release during apoptosis, permanently opening channels to dump ATP which is a signal for phagocytes to consume the cell.[24] However, Panx1 channels also have a reversible mode of operation in live cells, where the channels rapidly open and close in milliseconds.[25] This faster mode could release ATP rapidly, which would be rapidly degraded to adenosine in the extracellular space.[26] However, pannexin channels have not been characterized as a mechanism for causing rapid adenosine release and FSCV is a good technique to interrogate their effects.

In this work, we investigate the effects of pannexin1 channels to cause spontaneous or mechanically-sensitive adenosine release. In global deletion pannexin 1 knock out mice (Panx1KO), spontaneous adenosine release is unchanged, but mechanically-evoked adenosine is reduced in concentration and frequency. After blocking a broader range of pannexins and connexins with 100 μM carbenoxolone, the frequency of spontaneous adenosine release decreased slightly, and the mechanically-stimulated data with carbenoxolone looked similar to that of Panx1KO. Thus, other hemichannels are not playing a major role in rapid adenosine release. This work demonstrates Panx1 channels are not involved in spontaneous adenosine release but do contribute to mechanically-stimulated release, and Panx1 channels could be a therapeutic target to regulate rapid adenosine release during brain injury.

3.2 Experimental Section

3.2.1 Chemicals

Artificial cerebral spinal fluid (aCSF) is made by 126 mM NaCl, 2.5 mM KCl, 1.2 mM NaH_2PO_4, 1.2 mM $MgCl_2$, 25 mM $NaHCO_3$, 2.4 mM $CaCl_2$ dihydrate, 11 mM glucose, and 15 mM tris(hydroxymethyl)aminomethane and adjusted to pH 7.4. Adenosine (Acros organics, Morris Plains, NJ, U.S.A.) was dissolved in 0.1 M $HClO_4$ for 10 mM stock solution. Stock solutions was diluted to 1 μM in PBS buffer for the electrode post calibration after brain slice experiments. Carbenoxolone (Sigma-Aldrich, St. Louis, MO, United States) was dissolved in aCSF buffer at 100 μM concentration for drug perfusion.

3.2.2 Brain slice experiments

Animal experiments were approved by the Animal Care and Use Committee at the University of Virginia. Panx1 knockout mice were Lox-Cre mice developed from the C57B6 strain (used as WT) and were a gift of the Ravichandran lab at University of Virginia.[27] All the mice we used in the experiments are male. A 6-8 weeks old mouse was anesthetized with isoflurane, euthanized via cervical dislocation, and decapitated. The brain was extracted and placed in chilled, oxygenated, artificial cerebral spinal fluid (aCSF). Slices were transferred to room temperature, oxygenated aCSF, brought up to 37° in a water bath, and allowed to recover for half an hour. Sagittal slices (400 μm thick) were collected using a vibratome from one hemisphere of the brain (Leica VT1000S).[7]

The carbon-fiber microelectrode was inserted 75 μm in the CA1 region of the hippocampus and equilibrated for 10 minutes before data collection. The reference electrode was a Ag/AgCl wire. FSCV was performed using a ChemClamp potentiostat (Dagan, Minneapolis, MN) with a Pine 5 MΩ headstage (Pine Instruments, Durham, NC) and data collected using HDCV software (courtesy of Mark Wightman, UNC). The FSCV waveform was a

triangle waveform from -0.4 V to 1.45 V and back at a scan rate of 400 V/s and repetition rate of 10 Hz. Spontaneous adenosine data was measured for one hour. For mechanically-stimulated adenosine, the electrode was lowered 50 μm quickly to stimulate adenosine and up to 3 stimulations were performed per slice, each 10 minutes apart. For carbenoxolone, aCSF buffer with 100 μM carbenoxolone was perfused for 30 minutes over the brain slice before the adenosine measurements. The electrodes were all post-calibrated in flow cell using 1 μM adenosine with PBS solution after the brain slice experiment. The adenosine concentration in brain slice is proportional to the current.

3.2.3 Statistics

An automated algorithm was used to pick spontaneous, transient adenosine peaks and to find the concentrations, durations, and inter-event times.[28] Durations are the peak width at half height. All bar graphs report means ± standard error of the mean. All statistics were performed using GraphPad Prism 8.

3.3 Results and Discussion

Fig. 1A shows example electrochemical data for wild-type brain slices, in C57B6 mice (the background strain used as a control in all Panx1KO studies). The color plot has applied voltage on the y-axis, time on the x-axis, and current in false color. Adenosine is identified by its two characteristic oxidation peaks in the color plot.[8,28] Concentration vs time traces show current changes at the primary oxidation potential, which is converted to concertation with post-calibration. Peaks identified as adenosine by our automated software are marked with a plus sign.[28] On average, we observed about 40 transients per hour in control mice. The concentration of each spontaneous adenosine event spans a wide range, from 20 nM to 1 μM, but the average is around 120 nM. The inter-event time is the time difference between two

consistent events and one is marked over the trace. The distribution of inter-event time characterizes the frequency of spontaneous adenosine release. Figure 1B shows example data for mechanically-stimulated adenosine. Mechanically-stimulated adenosine has a higher concentration and longer duration than spontaneous adenosine. The width at half-height ($t_{1/2}$) is the duration, which is calculated from the concentration vs time trace.

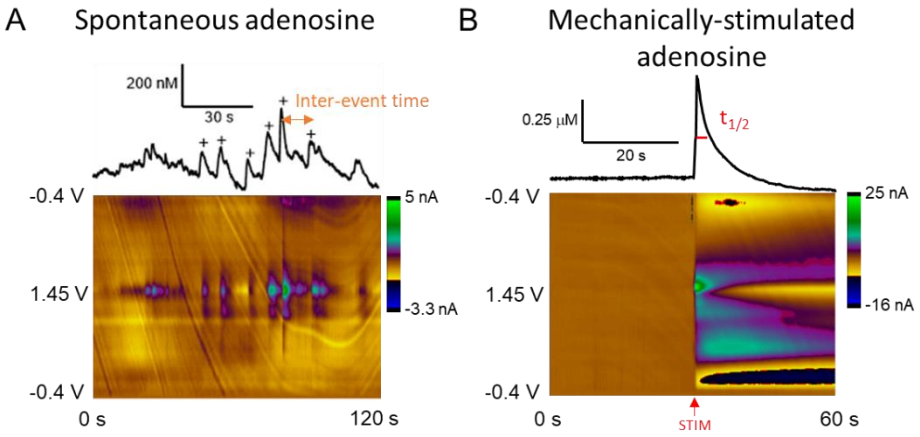

Figure 1. Example FSCV data of rapid adenosine. A. Example color plot of spontaneous adenosine release in wild type mouse brain slices. The color plot shows 2 min. worth of data, and the green/purple spots indicate adenosine. The concentration vs time trace above the color plot shows peaks, and peaks marked with a + are confirmed by our automated detection system. B. Example color plot of mechanically-stimulated adenosine in wild type mouse brain slice. The concentration vs time trace is above, with the red line marking the width at half-height, $t_{1/2}$. The red arrow below the color plot is the time of mechanical stimulation.

3.3.1 Pannexin channels as a possible release mechanism of spontaneous adenosine

Spontaneous adenosine release occurs in mouse brain slices in the CA1 region of the hippocampus frequently, similar to findings *in vivo*.[29] Panx1 global knockout mice were used to probe the extent to which Panx1 was involved in spontaneous adenosine release. Fig. 2 shows an example color plot in Panx1KO. The control animal had 6 events detected during a 2-minute window (Fig. 1A), while the Panx1KO (Fig. 2A) example shows 5 events, which is similar. Carbenoxolone is a broad spectrum pannexin inhibitor that targets many different pannexin and connexin channels.[30] We administered carbenoxolone to WT mice at a high dose of 100 µM to bind target other pannexins and connexins, which are blocked at higher doses.[22] The example

carbenoxolone color plot shows fewer adenosine transients than control or Panx1KO, only 3 (Fig. 1B).

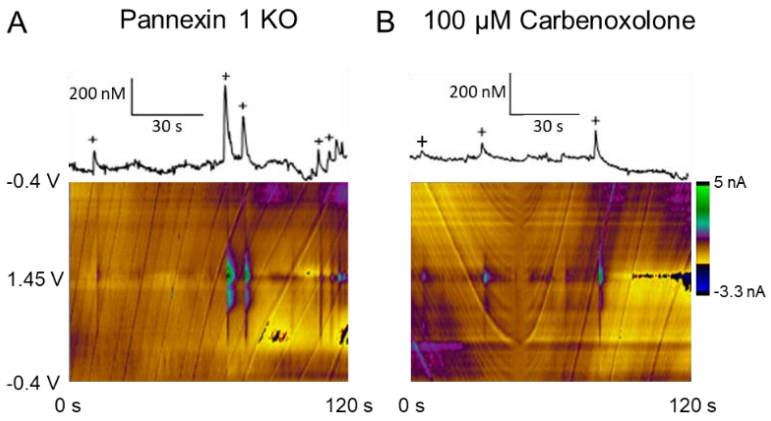

Figure 2. Example color plot of spontaneous adenosine in Panxin1KO mice (A), and carbenoxolone treated wild type mice (B). Above the plots are concentration vs time traces at the primary oxidation potential for adenosine, with confirmed adenosine peaks (by our automated detection system) marked with a '+'.

Figure 3 shows average data for spontaneous adenosine in multiple slices. Fig 3A compares the number of transients detected in one hour of data collection. There is no significant difference in the average number of transients among the three groups of mice (Fig. 3A, one-way ANOVA, p=0.60, n=6-8 slices). Because of high biological variability, even in control animals, it is hard to pick out statistical differences with measures that average over animals. Another measure of frequency is the interevent time, that is the time between two consecutive events. Here, we examine pairs of transients, so n numbers are higher and there is a significant effect of group for interevent frequency (One-Way ANOVA, p= 0.0042, n= 312 transients WT, 238 Panx1KO, 143 CBX). The distribution of interevent times was not significantly different between control and Panx1KO mice (Fig. 3B, Kruskal-Wallis test, p=0.26), but was significantly different between control and carbenoxolone, as the frequency of transients was slower with the drug (p=0.0034). The concentration of each adenosine transient is plotted in Fig. 3C. The average concentration is around 100 nM in all three groups. There was no significant main effect among groups (one-way ANOVA, p=0.64, n=6-8 slices). Overall, there were no significant differences in spontaneous adenosine frequency or concentration between

control and Panx1KO mice, which demonstrates that Panx1 channels are not a mechanism of spontaneous, transient adenosine release.

The hypothesis that pannexin channels are responsible for rapid adenosine release comes from different studies in the literature where pannexin channels rapidly release ATP.[25,31,32] Pannexins are membrane channels that are release ions and small molecules like ATP into the extracellular space[22,23] and are activated by mechanical perturbation, high levels of intracellular calcium, or high extracellular potassium.[23,33] Panx1 are irreversibly opened via caspase cleavage during apoptosis,[24] but adenosine transients are monitored for hours, without visible damage in the region, so apoptosis is not proposed to cause spontaneous adenosine release. Alternatively, pannexin channels undergo rapid opening and closing by activating α1-adrenergic receptors.[25] This behavior, called flickering, is on the millisecond time scale and could potentially cause spontaneous adenosine events. Thus, we hypothesized that pannexin1 channels might be a mechanism for spontaneous, transient adenosine release. However, the lack of effect in Panx1KO mice shows that Panx1 is not the main mechanism of spontaneous adenosine release and the hypothesis was disproved.

One possible problem with genetic KO mice is that they may have compensatory changes, overexpressing other related proteins or channels. For example, an upregulation of Panx3 channels has been found in Panx1KO mice so a potential compensatory role of Panx3 in the Panx1KO mouse model was proposed.[34] Panx1 acts as a feedback response through pre-synaptic activation of A1 receptors, and a compensatory upregulation of metabotropic glutamate receptor 4 expression is proposed in the Panx1KO model.[35] Acetylcholine transmission also increases in Panx1KO mice via a presynaptic regulation modulated by A1 receptor, indicating that A1 receptors may be downregulated in Panx1KO mice.[36,37] Spontaneous adenosine is regulated presynaptically modulated by the A1 receptor, and so changes in A1 receptors in Panx1KO mice could affect spontaneous adenosine release.[7,9] Therefore, we used both a

genetic knockout and complementary pharmacology strategy to verify effects in Panx1KO mice were not just due to compensation.

High dose carbenoxolone treatment slightly decreased the frequency of spontaneous release but did not change the concentration of each event. While the carbenoxolone results suggest there could be a small role of other pannexin or connexin channels, they would not be the major mechanism. We used a high dose of carbenoxolone to block both pannexin channels (IC50 2-5 µM), and connexin channels (IC50 21-34 µM)[38] but carbenoxolone has other targets, including NMDA receptors (IC_{50} 104 µM)[39] which modulate spontaneous adenosine release.[40] While pannexin2 channels that are high expressed in the brain could be examined in future studies,[41] this study shows gap junction channels are not the primary mechanism of spontaneous adenosine release. Instead, the release mechanism of spontaneous release appears is likely activity dependent ATP release, as release is decreased with application of tetrodotoxin, is calcium dependent, and dependent on the ATP breakdown enzymes CD39 and CD73.[7,42] Thus, pannexin1 channels are not a major release mechanism for spontaneous adenosine release, and the flickering patterns previously observed in other cells do not contribute to rapid, spontaneous adenosine release in the hippocampus.

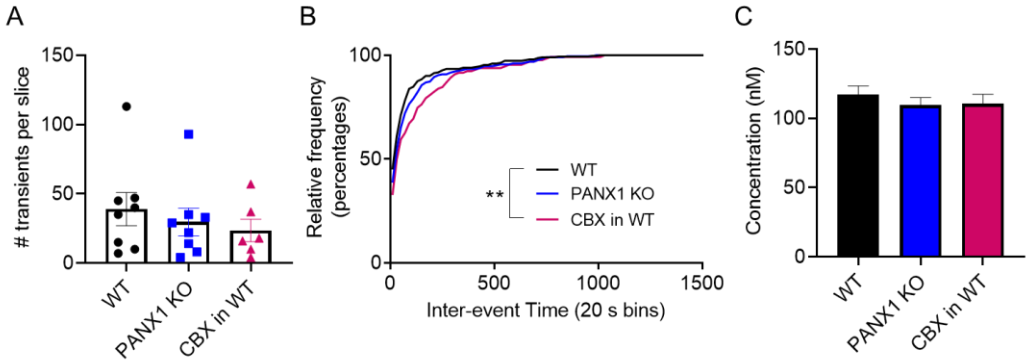

Figure 3. Average data of spontaneous adenosine release. A. Average # of transients per hour is not significantly different among WT and Panx1KO mice CBX treatment (One-way ANOVA multiple comparisons, p = 0.60, n = 6-8 slices). B. There is no change in frequency of transients for Panx1KO mice, but a significant difference between WT and CBX in WT (One-way ANOVA Kruskal-Wallis test, overall p=0.0042, Dunn's multiple comparisons WT vs Panx1KO p=0.26, WT vs CBX in WT p=0.0034). C. There is no change in concentration of each transient in Panx1KO mice or CBX treatment (One-way ANOVA multiple comparisons, p=0.64, n=6-8 slices, one slice

per animal, all mice are male in the experiments, 312 transients WT, 238 Panx1KO, 143 CBX). ** p<0.01

3.3.2 Pannexin channels as a possible release mechanism of mechanosensitive adenosine

Next, we tested the extent to which Panx1 channels control mechanically-stimulated adenosine release. Adenosine was mechanically-stimulated by moving the electrode 50 µm, which causes shear stress, releasing adenosine.[8] The example color plots show adenosine release in WT (Fig. 1B), Panx1KO (Fig 4A), and CBX treated WT mice (Fig 4B). The concentration of mechanically-stimulated adenosine is much bigger than spontaneous adenosine release, around 640 nM on average in WT mice. In addition, mechanical stimulation causes other ionic changes, which produce interfering currents around 0.6 V in the color plot.[43] The example data show that the concentration of the evoked adenosine concentration is smaller in Panx1 mouse and carbenoxolone treated mice.

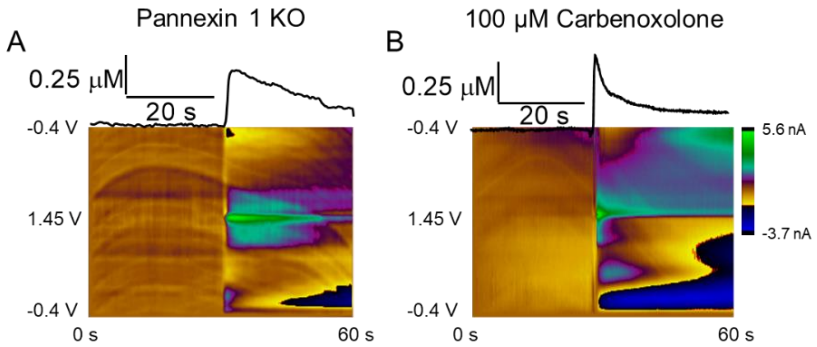

Figure 4. Example color plots of a mechanical stimulation performed by lowering the electrode 50 µm at time 30 s on the plots. A. Panx1KO, B. WT mice with 100 µM carbenoxolone. The top traces are the concentration vs time traces at the primary oxidation potential of adenosine.

Fig. 5 shows average data from 16 brain slices. For averaged concentration data (Fig. 5A), there was a main effect of group (one-way ANOVA, p=0.0005, n=16 slices from 8 male mice in each group) and significant differences between WT and Panx1KO (p=0.0069) and WT and CBX (p=0.0007). For duration (Fig. 5B), there was no significant difference among three groups (one-way ANOVA, p=0.1543, n=16 slices from 8 mice in each group). Fig. 5C plots the percentage of mechanical stimulations that successfully elicited adenosine. For each

stimulation, we simply determined if any adenosine was released, or if there was no evidence of release, and successful stimulation were identified as releasing any level of adenosine, even if it was small. There was a main effect of group (One-Way ANOVA, p=0.0223, n=16 slices from 8 mice) and Panx1KO mice had a significantly lower percent success than WT (p=0.02). In control animals, about 75% of stimulations elicited adenosine, while in Panx1KO it was around 52 % and in CBX treated slices, it was 60%. Thus, mechanically-stimulated release was less frequently evoked in Panx1KO mice and the concentration was lower, indicating that Panx1 channels are a release mechanism for mechanically-stimulated release.

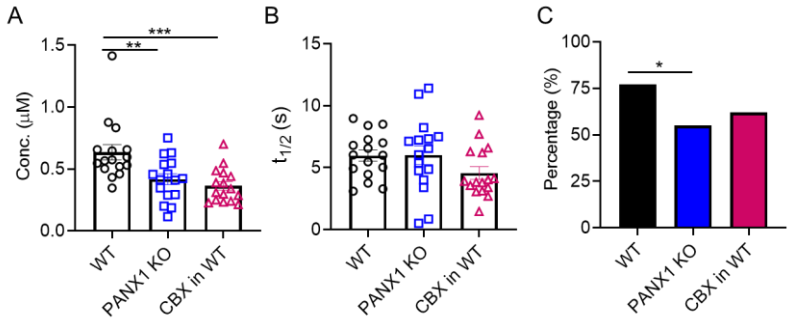

Figure 5. Average data of mechanically-stimulated adenosine release in different type of mice. A. Concentration of each mechanically-stimulated release. (One-way ANOVA, p= 0.0005, Tukey's multiple comparisons, WT vs Panx1KO p=0.0069, WT vs CBX in WT p=0.0007, Panx1 vs CBX in WT p=0.7073, n=8 mice/16 slices per group). B. Duration (width at half height) of mechanically-stimulated adenosine (One-way ANOVA, p= 0.1543, n=8 mice/16 slices per group). C. Percent of mechanical stimulations that evoked adenosine (Kruskal-Wallis test, p=0.0223, n=8 mice/16 slices. Dunn's multiple comparisons, WT vs Panx1KO p=0.02, WT vs CBX in WT p=0.19, Panx1 vs CBX in WT p>0.99,) *p<0.05, **p<0.01, ***p<0.001. Error bars are SEM.

Pannexin1 channels are mechanosensitive, leading to the hypothesis that pannexin channels may be involved in mechanosensitive release.[23] Here, we found the concentration of adenosine release by a mechanical stimulation decreased by about 30% in Panx1KO mice and the success rate for mechanical stimulations to release adenosine decreased about 25%. Thus, pannexin1 channels contribute to mechanosensitive release but are not fully responsible for all the release. Carbenoxolone treated WT mice had similar mechanosensitive release to Panx1KO, implying there are not many other pannexin and connexin channels contributing to

release. Mechanosensitive release is complex and shear stress is expected to play a major role; cells stretch in response to electrode moving which could open pannexin1 channels.[32] But other stresses, such as swelling or pulling could lead to calcium channel activation and activity dependent release as well.[44] Mechanosensitive release is reduced by TTX, but it is not as dependent on CD73 or CD39 as spontaneous release, so there could be mixed mechanisms of pannexin and activity-dependent release.[8,13] These studies identify pannexin1 channels as a release mechanism for mechanically-stimulated adenosine release in the brain for the first time, and this mechanism might be able to be explored as treatment for brain injury. Also, treatments targeting pannexin1 channels for adenosine release will differentially only target mechanosensitive release and not disturb spontaneous events.

3.4 Conclusions

In this study, we examined pannexin channels as a possible mode to release spontaneous and mechanically-stimulated adenosine in the hippocampus CA1. In global Panx1KO mice,[27] there are no changes in spontaneous adenosine release so pannexin1 channels are not contributing to spontaneous adenosine release. A high dose of carbenoxolone that blocks many gap junction proteins did slightly decrease the frequency of adenosine release, suggesting other channels could play a minor role in spontaneous release. For mechanically-stimulated release, Panx1KO mice have smaller concentration transients and mechanical stimulation was less likely to evoke adenosine. However, pannexin channels are not the only release mechanism and CBX studies in WT mice looked similar to Panx1KO mice, suggesting that the remaining mechanosensitive release is not due to other pannexin or connexin channels. Thus, this study shows that Pannexin1 channels are not a release mechanism for spontaneous adenosine but are responsible for some mechanosensitive release. Therefore, Panx1 channels could be targeted to differentially affect adenosine release from shear stress or brain damage,

but targeting them would not affect normal spontaneous release. This better understanding of the mechanism of action will lead to better therapies that specifically target different modes of adenosine release.

3.5 References

(1) Ganesana, M.; Venton, B. J. Early Changes in Transient Adenosine during Cerebral Ischemia and Reperfusion Injury. *PLoS One* **2018**, *13* (5), e0196932. https://doi.org/10.1371/journal.pone.0196932.

(2) Gomes, C. V; Kaster, M. P.; Tome, A. R.; Agostinho, P. M.; Cunha, R. A. Adenosine Receptors and Brain Diseases: Neuroprotection and Neurodegeneration. *Biochim. Biophys. Acta* **2011**, *1808* (5), 1380–1399. https://doi.org/10.1016/j.bbamem.2010.12.001.

(3) Cunha, R. A. Different Cellular Sources and Different Roles of Adenosine: A1 Receptor-Mediated Inhibition through Astrocytic-Driven Volume Transmission and Synapse-Restricted A2A Receptor-Mediated Facilitation of Plasticity. *Neurochem. Int.* **2008**, *52* (1), 65–72. https://doi.org/10.1016/j.neuint.2007.06.026.

(4) Nguyen, M. D.; Venton, B. J. Fast-Scan Cyclic Voltammetry for the Characterization of Rapid Adenosine Release. *Comput. Struct. Biotechnol. J.* **2015**, *13*, 47–54. https://doi.org/10.1016/j.csbj.2014.12.006.

(5) Swamy, B. E. K.; Venton, B. J. Subsecond Detection of Physiological Adenosine Concentrations Using Fast-Scan Cyclic Voltammetry. *Anal. Chem.* **2007**, *79* (2), 744–750. https://doi.org/10.1021/ac061820i.

(6) Nguyen, M. D.; Lee, S. T.; Ross, A. E.; Ryals, M.; Choudhry, V. I.; Venton, B. J. Characterization of Spontaneous, Transient Adenosine Release in the Caudate-Putamen and Prefrontal Cortex. *PLoS One* **2014**, *9* (1), e87165. https://doi.org/10.1371/journal.pone.0087165.

(7) Lee, S. T.; Venton, B. J. Regional Variations of Spontaneous, Transient Adenosine Release in Brain Slices. *ACS Chem. Neurosci.* **2018**, *9* (3), 505–513. https://doi.org/10.1021/acschemneuro.7b00280.

(8) Ross, A. E.; Nguyen, M. D.; Privman, E.; Venton, B. J. Mechanical Stimulation Evokes Rapid Increases in Extracellular Adenosine Concentration in the Prefrontal Cortex. *J. Neurochem.* **2014**, *130* (1), 50–60. https://doi.org/10.1111/jnc.12711.

(9) Chang, Y.; Wang, Y.; Venton, B. J. A1 and A2A Receptors Modulate Spontaneous Adenosine but Not Mechanically Stimulated Adenosine in the Caudate. *ACS Chem. Neurosci.* **2020**, *11* (20), 3377–3385. https://doi.org/10.1021/acschemneuro.0c00510.

(10) Borgus, J. R.; Puthongkham, P.; Venton, B. J. Complex Sex and Estrous Cycle Differences in Spontaneous Transient Adenosine. *J. Neurochem.* **2020**, *153* (2), 216–229. https://doi.org/10.1111/jnc.14981.

(11) Wang, Y.; Venton, B. J. Comparison of Spontaneous and Mechanically-Stimulated

Adenosine Release in Mice. *Neurochem. Int.* **2019**, *124*. https://doi.org/10.1016/j.neuint.2018.12.007.

(12) Wan, J.; Ristenpart, W. D.; Stone, H. A. Dynamics of Shear-Induced ATP Release from Red Blood Cells. *Proc. Natl. Acad. Sci.* **2008**, *105* (43), 16432–16437.

(13) Wang, Y.; Copeland, J.; Shin, M.; Chang, Y.; Venton, B. J. CD73 or CD39 Deletion Reveals Different Mechanisms of Formation for Spontaneous and Mechanically Stimulated Adenosine and Sex Specific Compensations in ATP Degradation. *ACS Chem. Neurosci.* **2020**, *11* (6), 919–928. https://doi.org/10.1021/acschemneuro.9b00620.

(14) Fernández, P.; Perez-Aso, M.; Smith, G.; Wilder, T.; Trzaska, S.; Chiriboga, L.; Franks, A.; Robson, S. C.; Cronstein, B. N.; Chan, E. S. L. Extracellular Generation of Adenosine by the Ectonucleotidases CD39 and CD73 Promotes Dermal Fibrosis. *Am. J. Pathol.* **2013**, *183* (6), 1740–1746. https://doi.org/10.1016/j.ajpath.2013.08.024.

(15) Wall, M.; Dale, N. Activity-Dependent Release of Adenosine: A Critical Re-Evaluation of Mechanism. *Curr. Neuropharmacol.* **2008**, *6* (4), 329–337. https://doi.org/10.2174/157015908787386087.

(16) Lohman, A. W.; Isakson, B. E. Differentiating Connexin Hemichannels and Pannexin Channels in Cellular ATP Release. *FEBS Lett.* **2014**, *588* (8), 1379–1388. https://doi.org/10.1016/j.febslet.2014.02.004.

(17) Wang, J.; Jackson, D. G.; Dahl, G. The Food Dye FD&C Blue No. 1 Is a Selective Inhibitor of the ATP Release Channel Panx1. *J. Gen. Physiol.* **2013**, *141* (5), 649–656. https://doi.org/10.1085/jgp.201310966.

(18) Lopatar, J.; Dale, N.; Frenguelli, B. G. Pannexin-1-Mediated ATP Release from Area CA3 Drives MGlu5-Dependent Neuronal Oscillations. *Neuropharmacology* **2015**, *93*, 219–228. https://doi.org/10.1016/j.neuropharm.2015.01.014.

(19) Thompson, R. J.; MacVicar, B. Connexin and Pannexin Hemichannels of Neurons and Astrocytes. *Channels* **2008**, *2* (2), 81–86. https://doi.org/10.4161/chan.2.2.6003.

(20) Bruzzone, R.; Hormuzdi, S. G.; Barbe, M. T.; Herb, A.; Monyer, H. Pannexins, a Family of Gap Junction Proteins Expressed in Brain. *Proc. Natl. Acad. Sci.* **2003**, *100* (23), 13644–13649. https://doi.org/10.1073/pnas.2233464100.

(21) Ray, A.; Zoidl, G.; Weickert, S.; Wahle, P.; Dermietzel, R. Site-Specific and Developmental Expression of Pannexin1 in the Mouse Nervous System. *Eur. J. Neurosci.* **2005**, *21* (12), 3277–3290. https://doi.org/10.1111/j.1460-9568.2005.04139.x.

(22) Dahl, G.; Qiu, F.; Wang, J. The Bizarre Pharmacology of the ATP Release Channel Pannexin1. *Neuropharmacology* **2013**, *75*, 583–593. https://doi.org/10.1016/j.neuropharm.2013.02.019.

(23) Bao, L.; Locovei, S.; Dahl, G. Pannexin Membrane Channels Are Mechanosensitive Conduits for ATP. *FEBS Lett.* **2004**, *572* (1–3), 65–68. https://doi.org/10.1016/j.febslet.2004.07.009.

(24) Chekeni, F. B.; Elliott, M. R.; Sandilos, J. K.; Walk, S. F.; Kinchen, J. M.; Lazarowski, E. R.; Armstrong, A. J.; Penuela, S.; Laird, D. W.; Salvesen, G. S.; Isakson, B. E.; Bayliss, D. A.; Ravichandran, K. S. Pannexin 1 Channels Mediate “find-Me” Signal Release and Membrane Permeability during Apoptosis. *Nature* **2010**, *467* (7317), 863–867. https://doi.org/10.1038/nature09413.

(25) Chiu, Y.-H.; Jin, X.; Medina, C. B.; Leonhardt, S. A.; Kiessling, V.; Bennett, B. C.; Shu, S.; Tamm, L. K.; Yeager, M.; Ravichandran, K. S.; Bayliss, D. A. A Quantized Mechanism for Activation of Pannexin Channels. *Nat. Commun.* **2017**, *8*, 14324. https://doi.org/10.1038/ncomms14324.

(26) Dunwiddie, T. V; Dlao, L.; Proctor, W. R. Adenine Nucleotides Undergo Rapid, Quantitative Conversion to Adenosine in the Extracellular Space in Rat Hippocampus. *J. Neurosci.* **1997**, *17* (20), 7673–7682. https://doi.org/10.1523/jneurosci.17-20-07673.1997.

(27) Poon, I. K. H.; Chiu, Y. H.; Armstrong, A. J.; Kinchen, J. M.; Juncadella, I. J.; Bayliss, D. A.; Ravichandran, K. S. Unexpected Link between an Antibiotic, Pannexin Channels and Apoptosis. *Nature* **2014**, *507* (7492), 329–334. https://doi.org/10.1038/nature13147.

(28) Borman, R. P.; Wang, Y.; Nguyen, M. D.; Ganesana, M.; Lee, S. T.; Venton, B. J. Automated Algorithm for Detection of Transient Adenosine Release. *ACS Chem. Neurosci.* **2017**, *8* (2), 386–393. https://doi.org/10.1021/acschemneuro.6b00262.

(29) Wang, Y.; Venton, B. J. Comparison of Spontaneous and Mechanically-Stimulated Adenosine Release in Mice. *Neurochem. Int.* **2019**, *124*, 46–50. https://doi.org/https://doi.org/10.1016/j.neuint.2018.12.007.

(30) Xia, J.; Lim, J. C.; Lu, W.; Beckel, J. M.; Macarak, E. J.; Laties, A. M.; Mitchell, C. H. Neurons Respond Directly to Mechanical Deformation with Pannexin-Mediated ATP Release and Autostimulation of P2X $_7$ Receptors. *J. Physiol.* **2012**, *590* (10), 2285–2304. https://doi.org/10.1113/jphysiol.2012.227983.

(31) Ransford, G. A.; Fregien, N.; Qiu, F.; Dahl, G.; Conner, G. E.; Salathe, M. Pannexin 1 Contributes to ATP Release in Airway Epithelia. *Am. J. Respir. Cell Mol. Biol.* **2009**, *41* (5), 525–534. https://doi.org/10.1165/rcmb.2008-0367OC.

(32) Reigada, D.; Lu, W.; Zhang, M.; Mitchell, C. H. Elevated Pressure Triggers a Physiological Release of ATP from the Retina: Possible Role for Pannexin Hemichannels. *Neuroscience* **2008**, *157* (2), 396–404. https://doi.org/10.1016/j.neuroscience.2008.08.036.

(33) Locovei, S.; Wang, J.; Dahl, G. Activation of Pannexin 1 Channels by ATP through P2Y Receptors and by Cytoplasmic Calcium. *FEBS Lett.* **2006**, *580* (1), 239–244. https://doi.org/10.1016/j.febslet.2005.12.004.

(34) Whyte-Fagundes, P.; Kurtenbach, S.; Zoidl, C.; Shestopalov, V. I.; Carlen, P. L.; Zoidl, G. A Potential Compensatory Role of Panx3 in the VNO of a Panx1 Knock out Mouse Model. *Front. Mol. Neurosci.* **2018**, *11* (April), 1–16. https://doi.org/10.3389/fnmol.2018.00135.

(35) Prochnow, N.; Abdulazim, A.; Kurtenbach, S.; Wildförster, V.; Dvoriantchikova, G.; Hanske, J.; Petrasch-Parwez, E.; Shestopalov, V. I.; Dermietzel, R.; Manahan-Vaughan, D.; Zoidl, G. Pannexin1 Stabilizes Synaptic Plasticity and Is Needed for Learning. *PLoS One* **2012**, *7* (12). https://doi.org/10.1371/journal.pone.0051767.

(36) Miteva, A. S.; Gaydukov, A. E.; Shestopalov, V. I.; Balezina, O. P. Mechanism of P2X7 Receptor-Dependent Enhancement of Neuromuscular Transmission in Pannexin 1 Knockout Mice. *Purinergic Signal.* **2018**, *14* (4), 459–469. https://doi.org/10.1007/s11302-018-9630-7.

(37) Miteva, A. S.; Gaydukov, A. E.; Shestopalov, V. I.; Balezina, O. P. The Role of Pannexin

1 in the Purinergic Regulation of Synaptic Transmission in Mouse Motor Synapses. *Biochem. Suppl. Ser. A Membr. Cell Biol.* **2017**, *11* (4), 311–320. https://doi.org/10.1134/S1990747817040067.

(38) Schock, S. C.; LeBlanc, D.; Hakim, A. M.; Thompson, C. S. ATP Release by Way of Connexin 36 Hemichannels Mediates Ischemic Tolerance in Vitro. *Biochem. Biophys. Res. Commun.* **2008**, *368* (1), 138–144. https://doi.org/10.1016/j.bbrc.2008.01.054.

(39) Chepkova, A. N.; Sergeeva, O. A.; Haas, H. L. Carbenoxolone Impairs LTP and Blocks NMDA Receptors in Murine Hippocampus. *Neuropharmacology* **2008**, *55* (2), 139–147. https://doi.org/https://doi.org/10.1016/j.neuropharm.2008.05.001.

(40) Nguyen, M. D.; Wang, Y.; Ganesana, M.; Venton, B. J. Transient Adenosine Release Is Modulated by NMDA and GABAB Receptors. *ACS Chem. Neurosci.* **2017**, *8* (2), 376–385. https://doi.org/10.1021/acschemneuro.6b00318.

(41) Vogt, A.; Hormuzdi, S. G.; Monyer, H. Pannexin1 and Pannexin2 Expression in the Developing and Mature Rat Brain. *Brain Res. Mol. Brain Res.* **2005**, *141* (1), 113–120. https://doi.org/10.1016/j.molbrainres.2005.08.002.

(42) Wang, Y.; Copeland, J.; Shin, M.; Chang, Y.; Venton, B. J. CD73 or CD39 Deletion Reveals Different Mechanisms of Formation for Spontaneous and Mechanically-Stimulated Adenosine Release and Sex Specific Compensations in ATP Degradation. *ACS Chem. Neurosci.* **2020**, *11* (6), 919–928. https://doi.org/10.1021/acschemneuro.9b00620.

(43) Takmakov, P.; Zachek, M. K.; Keithley, R. B.; Bucher, E. S.; McCarty, G. S.; Wightman, R. M. Characterization of Local PH Changes in Brain Using Fast-Scan Cyclic Voltammetry with Carbon Microelectrodes. *Anal. Chem.* **2010**, *82* (23), 9892–9900. https://doi.org/10.1021/ac102399n.

(44) Yamashiro, K.; Fujii, Y.; Maekawa, S.; Morita, M. Multiple Pathways for Elevating Extracellular Adenosine in the Rat Hippocampal CA1 Region Characterized by Adenosine Sensor Cells. *J. Neurochem.* **2017**, *140* (1), 24–36. https://doi.org/10.1111/jnc.13888.

Chapter 4

Dual channel electrochemical measurements reveal rapid adenosine is localized in brain slices

Chapter 4 was reprinted from *ACS Chem. Neurosci.* **2022**, 13, 4, 477–485.

Abstract

Rapid adenosine signaling has been detected spontaneously or after mechanical stimulation in the brain, providing rapid neuromodulation in a local area. To measure rapid adenosine signaling, a single carbon-fiber microelectrode has traditionally been used, which limits spatial resolution and an understanding of regional coordination. In this study, we utilized dual channel FSCV to measure spontaneous or mechanically stimulated adenosine release at two electrodes placed at different spacings in hippocampal CA1 mouse brain slices. For mechanically-stimulated adenosine release, adenosine can be detected up to 150 µm away from where it was stimulated, although the signal is smaller and delayed. While spontaneous adenosine transients were detected at both electrodes, only 10 percent of events were detected concurrently, and that number was similar at 50 µm and 200 µm electrode spacings. Thus, most adenosine transients were not caused by widespread coordination of release. There was no evidence of diffusion of spontaneous transients to a second electrode 50-200 µm away. This study shows that spontaneous adenosine events are very localized, and thus provide only local neuromodulation. Injury, such as mechanical stimulation, allows adenosine to diffuse farther, but neuroprotective effects are still regional. These results provide a better understanding of the spatial and temporal profiles of adenosine available to act at receptors, which is crucial for future studies that design neuroprotective treatments based on rapid adenosine signaling.

4.1 Introduction

Rapid adenosine acts as a neuromodulator, signaling through receptors to modulate blood flow, the sleep-awake cycle, pain and memory.[1–10] Adenosine receptors are located both presynaptically and postsynaptically and adenosine often has an overall inhibitory effect, acting at A_1 receptors to dampen dopamine, glutamate and GABA neurotransmission.[11–14] The hippocampus CA1 region is an important region for adenosine neuromodulation, as adenosine inhibits excitatory synaptic transmission during ischemia. There is a high frequency and concentration of adenosine transient events in the hippocampus CA1 region,[15] and the CA1 may be susceptible to ischemic damage because adenosine transient events do not increase during ischemia.[16] Exogenous adenosine protects hippocampal neurons from death during cerebral ischemic injury,[17] but the endogenous pool of adenosine is depletable in the CA1.[18]

A rapid mode of adenosine release was discovered by electrophysiology,[19] and the Zylka group discovered spontaneous adenosine release in the spinal cord which lasted only few seconds.[20] Our lab used fast-scan cyclic voltammetry (FSCV) to further investigate the mechanisms of spontaneous, transient adenosine release using drugs or genetic knockout mice in the rodent brain.[15,21–25] Mechanical stimulation also releases transient concentrations of adenosine, and these events have a higher concentration and slightly longer duration (about 30 s) than spontaneous adenosine. Mechanically-stimulated adenosine acts via A_1 receptors to decrease stimulated dopamine in the caudate, suggesting it is a rapid neuromodulator.[26] While the temporal dynamics of rapid adenosine neuromodulation have been studied, how far spontaneous or mechanically-stimulated adenosine release can diffuse to signal at receptors is not known, because most measurements are recorded from a single location. Imaging techniques based on G-protein coupled receptors have been used to monitor adenosine recently with better spatial resolution, but they have not been demonstrated to measure rapid adenosine transients.[27] Understanding the range of rapid adenosine release would provide a

better understanding of the temporal and spatial profiles of adenosine neuromodulation in a region.

One strategy to understand spatial signaling in the brain is to measure at multiple electrodes simultaneously.[28] For example, Wightman's group used dual channel FSCV to measure dopamine in different hemispheres of the brain, finding coordination of dopamine transients across hemispheres.[29] Sombers' group also used dual electrodes to measure electrically-stimulated glucose and lactate simultaneously via FSCV after neuronal activation.[30] Electrode arrays have also been developed for detection at multiple brain sites.[28,29,31–33] Ewing's group develop an array with seven CFMEs to monitor dopamine exocytosis from a single PC12 cell.[34] Cima's group measured from 16 sites in the caudate simultaneously to enable high density detection on dopamine neurotransmission.[35] Graybiel's group also used chronically-implanted electrode arrays to monitor dopamine in the brain.[36,37] However, these studies mainly focused on dopamine and the spatial and temporal profiles of adenosine release to act on receptors are not fully understood.

The goal of this study is to investigate the spatial and temporal profile of rapid adenosine signals in the hippocampus CA1 region. We investigated spontaneous and mechanically-stimulated adenosine in brain slice via dual channel FSCV measurements, and this is the first study to detect rapid adenosine events with multiple electrodes. Spontaneous adenosine is randomly released and highly localized. The majority of spontaneous transients were also not due to coordinated firing. Mechanically-stimulated adenosine can diffuse further, and could be detected at 150 μm away from the release site, although the magnitude of the adenosine decreases with distance. The range of signaling by adenosine after mechanical stimulation indicates that injury to the brain causes more regional neuromodulatory effects but spontaneous adenosine is a highly localized modulatory signal likely related to local cell activity. The differences in spatial resolution between the two modes of adenosine signaling provides new

details on differential neuroprotection of adenosine, which could be used to design treatments that take advantage of rapid neuromodulation of adenosine.

4.2 Experimental Section

4.2.1 Chemicals

Artificial cerebral spinal fluid (aCSF) containing 126mM NaCl, 2.5 mM KCl, 1.2 mM NaH_2PO_4, 2.4 mM $CaCl_2 \cdot 2H_2O$, 1.2 mM $MgCl_2 \cdot 6H_2O$, 25mM $NaHCO_3$, 11 mM glucose, and 15 mM Tris(hydroxymethyl) aminomethane was freshly made and adjusted to pH 7.4 before brain slice experiments. All the salts were purchased from Sigma-Aldrich. Adenosine (Acros organics, Morris Plains, NJ, USA) was dissolved in 0.1 M $HClO_4$ for 10 mM adenosine stock solution. A 1 µM adenosine solution was freshly made before flow cell experiment and post calibration by diluting the stock solution.

4.2.2 Electrochemistry

Cylinder carbon-fiber microelectrodes were fabricated by inserting a T-650 carbon fiber (7 µm diameter Cytec Engineering Materials, West Patterson, NJ) into a glass capillary (1.2 mm OD x 0.68 mm ID, 4'', A-M systems), pulling the capillary into two electrodes via an electrode puller (model PE-21, Narishige, Tokyo, Japan).[38] Then, the pulled electrodes were cut to 50-100 µm long under microscope. A WaveNeuro FSCV potentiostat combing with a WaveNeuro Dual Channel Adapter (DCA) (5 MΩ headstage, Pine Research Instrument, Durham, NC) was used for the two-channel fast-scan cyclic voltammetry measurement. A triangular waveform of -0.4 V to 1.45 V at 400 V/s in 10 Hz was applied on both channels.[39] Data collection was accomplished by HDCV software (UNC Chemistry, Chapel Hill, NC, USA).

4.2.3 Brain slice experiment

Brain slice experiments were approved by the Animal Care and Use Committee of the University of Virginia. Wild type mice C57BL/6 mice (6-8 weeks old, Jackson Lab) were housed in the vivarium in the University of Virginia. Mice were anesthetized with isoflurane before decapitalization. The mouse brain was removed within two minutes and transferred into 0-5 °C oxygenated (95% oxygen, 5% CO_2) aCSF for two minutes for recovery. After recovery, the mouse brain was quickly stabilized on the cold slicing stage and sliced into 400 µm thickness via a vibratome (LeicaVT1000S, Bannockburn, IL, USA), then the brain slices were transferred into a room temperature oxygenated aCSF to recover for 30 minutes before the experiment. During the experiment, aCSF (maintained at 35 °C) was consistently perfumed over the brain slice by a perfusion pump (Watson-Marlo 205U, Wilmington, MA, USA) at 2 mL/min. All the brain slices were obtained by coronal slicing the brain.

Mechanically stimulated adenosine was measured in the hippocampus CA1 region (AP: -2.5mm, ML: 2.3 mm, DL: 1.7mm). Two electrodes were inserted about 75 µm deep in the tissue and equilibrium for 15 minutes before the stimulation. The mechanical stimulation was performed by lowering one electrode 50 µm every 10 minutes and collecting two channels simultaneously. Spontaneous adenosine was collected by inserting two electrodes in the CA1 region. After 5-10 minutes of applying the adenosine waveform (Triangular waveform -0.4 V to 1.45 V at 400 V/s for 10 Hz), when the electrode background were stable, spontaneous adenosine events were measured for 1 hour. The electrodes were post calibrated separately in the same flow cell (VICI Valco) using 1 µM adenosine injection.

4.2.4 Statistics

The spontaneous adenosine events were identified and characterized by an image analysis program coded in Matlab, and the identified adenosine transients were confirmed by the author to exclude any signals that were not adenosine.[40] All the statistics were performed by GraphPad 8 (GraphPad Software Inc., San Diego, CA, USA), all the data are shown as mean ± SEM.

4.3 Results

In this study, we used a dual channel FSCV system to characterize the distance over which rapid adenosine can signal by changing the distance of two working electrodes in brain slice. Experiments were performed in the hippocampus CA1 region, which has both spontaneous adenosine transients and strong mechanically-stimulated release.[15,23] The hypothesis was that mechanically stimulated adenosine will diffuse further than spontaneous adenosine because of its higher concentration and duration.

4.3.1 Dual channel adenosine measurements during flow injection analysis

To prove that the two channels have similar responses, we used flow injection analysis to measure 1 µM adenosine at two similar length carbon-fiber microelectrodes. Each channel was tested separately, as only one electrode fits in our flow-injection system. Figure 1A shows example color plots of an adenosine bolus, with channel 0 (CH0) on top and channel 1 (CH1) on bottom. The color plots present the results in three dimensions, with time on the x-axis, potential on the y-axis, and current in false color. The green/purple color circles at around 1.4 V are the primary oxidation peak of adenosine, and the green/purple circles at around 1.0 V are the secondary oxidation peaks of adenosine. From the time trace in the color plot, the peak current at 1.0 V occurs later than the peak at 1.4 V, therefore, the 1.0 V oxidation peak is considered as secondary oxidation of adenosine. Figure 1B shows the background charging current of the two

electrodes, and the two electrodes on the different channels have a similar background shape. Figure 1C shows the background-subtracted cyclic voltammograms (CV) from the two channels. CH1 had a slightly larger background current and a slightly higher Faradaic current for adenosine. The potentials are slightly shifted to later times (i.e. more on the backscan) for CH1, but different electrodes can have different electron transfer kinetics, and these are both clearly CVs for adenosine. Figure 1D shows the current vs time traces, and both channels have a similar square-like shape and rise times. Therefore, the dual channel system has similar results on both channels in the flow cell, confirming both channels work well for adenosine measurements.

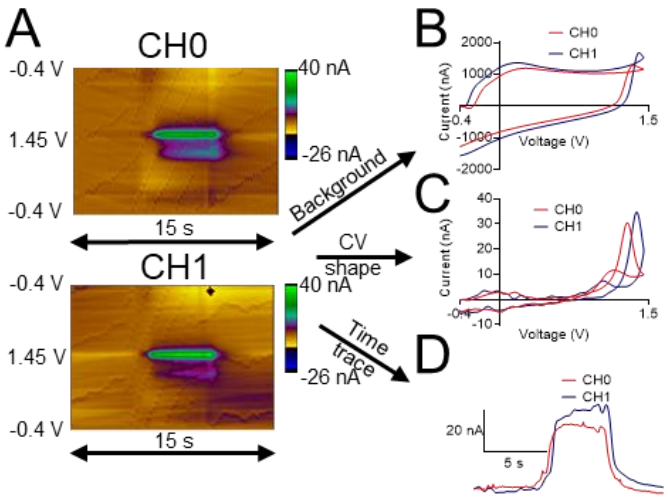

Figure 1 Example of adenosine measurement with dual channel system *in vitro*. A. Example color plots of two channels (top: CH0, bottom: CH1). B. Background charging current of two electrodes. C. Background-subtracted CV of adenosine for each electrode. D. Current vs time trace for the primary adenosine peak from the color plots in figure 1A. Red line was measured on CH0 in HDCV, Blue line measured on CH1.

4.3.2 Dual channel measurements of mechanically-stimulated adenosine release

To understand the range of adenosine signaling in brain slices, we first measured mechanically-stimulated adenosine at two electrodes spaced different distances apart. Figure 2A shows placement of 2 electrodes in a brain slice in the CA1 region. Both electrodes were inserted approximately 75 µm deep and equilibrium for about 10 minutes before experiment.

Mechanically-stimulated adenosine was generated by lowering the one electrode 50 µm in brain slice.[26] The second electrode (called the stable electrode) did not move. Therefore, two electrodes simultaneously detected stimulated adenosine at different sites. The horizontal distance between the electrodes was varied from 50 to 200 µm in order to characterize how far mechanically-stimulated adenosine diffused and could signal in brain tissue.

Figure 2 shows an example of mechanically-stimulated adenosine with two electrodes 50 µm apart. Figure 2B shows the color plots; the top color plot is the electrode which was moved to evoke the stimulation, while the bottom one is the stable electrode. In the color plot, stimulated adenosine is immediately detected on stimulation channel (STIM CH) but is delayed on stable channel (Stable CH) 50 µm away. The current on STIM CH is also higher than Stable CH , as some of the adenosine would be cleared or metabolized before it gets to the stable electrode, or it may diffuse in a different direction.[21] Figure 2C presents the time traces of the adenosine concentration and STIM CH has a has a rapid response after the stimulation. However, the rise in adenosine on the other channel is slower and adenosine stays elevated for a longer time, which indicates the signal in Stable CH is from diffusion of mechanically-stimulated adenosine near the other electrode. Figure 2D displays the CVs of adenosine; the stimulation electrode has a higher peak than the non-stimulation electrode but both are characteristic of adenosine. The differences between mechanically-stimulated adenosine CV extra peak at 0.5 V and the adenosine CV in the flow cell (Figure 1) are due to the ionic changes after lowering the electrode in the tissue.[41,42]

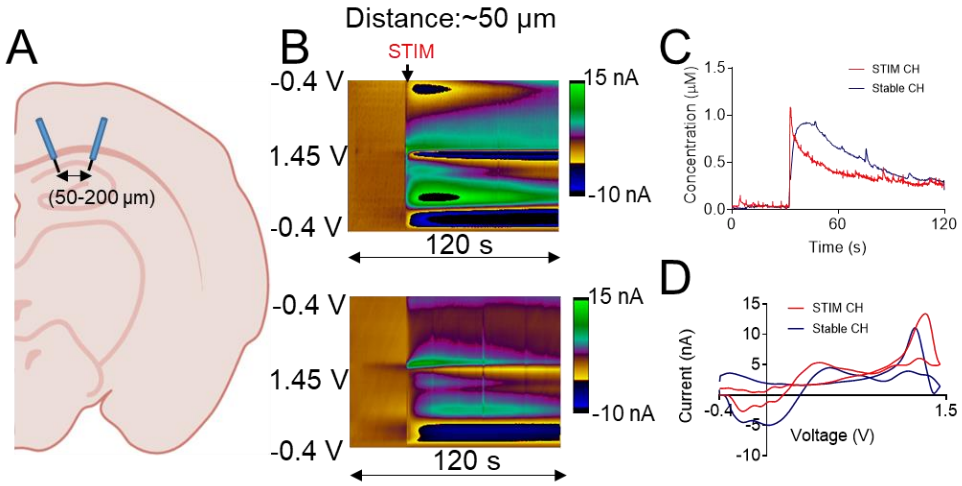

Figure 2 Examples of mechanically stimulated adenosine release with dual channel measurements with 50 µm spacing. A. Brain slice set up for dual channel measurement in CA1 region. The distance of two electrodes was varied from 50 to 200 µm. B. The color plots from the two channels. Top: stimulation channel (STIM CH), where the electrode was lowered for mechanically stimulation. The arrow marks the stimulation time. Bottom: stable channel (Stable CH), the stable electrode implanted 50 µm away. Adenosine is detected after the stimulation on Stable CH, but is smaller than on STIM CH. C. The concentration vs time traces of the primary oxidation peak on the two channels shows a faster rise and decay at STIM CH. D. CV of the adenosine signal in two channels. Red: STIM CH, Blue: Stable CH.

Next, we changed the horizontal spacing of the electrodes, varying it between 50 and 200 µm. To clarify the details of the two electrode positions, we implanted the first electrode in the medial CA1 region under the microscope, and then placed the other electrode laterally to vary the distance of two electrode. The top color plots in Figure 3 are from the stimulating electrodes, while the bottom color plots are the stable electrodes which did not move during the measurement. In order to prove both channels worked in the same way, we did the mechanical stimulation half the time on CH0 and half on CH1 and the results were similar (e.g.: experiments in Fig. 2A and 3B were stimulated on CH0, 3A and 3C were stimulated on CH1). The distance between the 2 electrodes is 100 µm in Fig 3A, 150 µm in Fig 3B, and 200 µm in Fig 3C. With a distance of 100-150 µm, the stable electrode detected adenosine (Figure 3A and 3B), but the signal is smaller and delayed. However, for 200 µm, adenosine was not detected on the stable electrode (Figure 3C). Figure 4 also compared the concentration vs time trends. As the distance between electrodes increases, the concentration of adenosine at the stable electrode

decreases; meanwhile, the rise time at the stable electrode is slower compared to the stimulation channel response. Figure 5 shows the CV of mechanically-stimulated adenosine (from Figure 5A-C); the secondary peak proves the signal is adenosine.

The averaged results in Figure 3D show that the adenosine signal decreases with larger electrode spacing in the hippocampus CA1 region (10 slices from 6 mice). In addition, the time of adenosine signal on the stable electrode is delayed compared to the stimulation site. Figure 3E shows the time delay at the stable electrode increases as the electrode distance increases. Both of the signal decay and time delay show significant difference at different distance (one-way ANOVA Tukey's multiple comparison tests, $p<0.0001$). These data are evidence that adenosine diffuses from the site of the stimulation to the other electrode up to 150 µm.

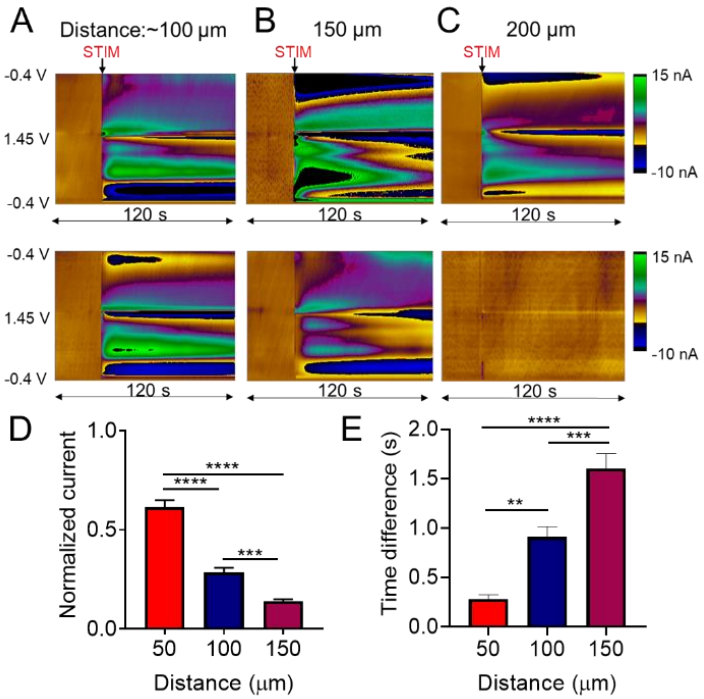

Figure 3. Mechanically-stimulated adenosine measurement with different electrode distance. A-C: Top color plots are STIM CH, bottom color plots are stable CH. A. 100 µm spacing. B. 150 µm spacing. C. 200 µm spacing. D. Difference in measured current at the stable electrode as a function of spacing (One-way ANOVA Tukey's multiple comparisons test, overall $p<0.0001$, $p=0.0002$). Current is normalized to the current measured on the stimulation electrode (which is 1). E. Time difference between the start of the rise in current at the stimulation and stable electrode (One-way ANOVA Tukey's multiple comparisons test, overall $p<0.0001$). D-E. All are 10 slices from 6 male mice, measured in the Hippocampus CA1 region, Error bars are SEM, ** $p<0.01$, *** $p<0.001$, **** $p<0.0001$.

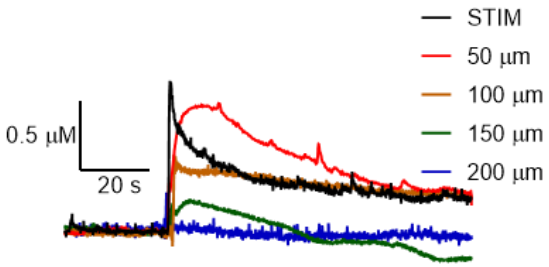

Figure 4 Example of concentration vs time trend of mechanically-stimulated adenosine release at different distances. All the time trends were obtained from the primary peak of adenosine in Figure 2 and Figure 3 color plot data.

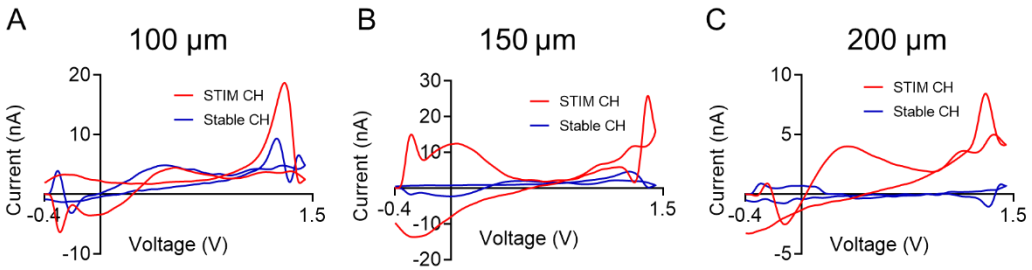

Figure 5 Mechanically-stimulated adenosine CV of Figure 3 color plot examples. A. 100 µm distance, B. 150 µm distance, C. 200 µm distance.

4.3.3 Dual channel measurements of spontaneous adenosine

Spontaneous adenosine release is another mode of rapid adenosine that can be measured in brain slices without a stimulation. [20,43,44] For spontaneous adenosine measurements, the two electrodes were implanted 50 or 200 µm apart in slices of the mouse hippocampus CA1 region, and spontaneous adenosine was measured continuously on both channels for 1h. In around 30% of the experiments, spontaneous adenosine was not detected at both electrodes, and these data were excluded (note, in some of these excluded experiments, adenosine was detected at one electrode, but not the other). Figure 6 shows example color plots for spontaneous adenosine measurement at two electrodes 50 µm apart (Fig. 6A, CH0, Fig 6B, CH1). Concentration vs time traces over the color plots show concentration changes estimated from the adenosine primary oxidation peak potential. The stars on the top mean the peak was identified as adenosine by our automated image analysis program in Matlab.[40] The CV figure on the top right of the color plot represents the spontaneous adenosine, the tiny

secondary peak indicates the transient is not hydrogen peroxide. On the color plots, the white numbers indicate the time the transient begins. The average concentration of events at both electrodes is similar for both channels, as is the frequency of release. The majority of events do not align in time; here, there are two transients that occur at similar times on both channels, around 21 s. The transient at 21 s on CH0 has a smaller concentration than the transient at 20.5 s on CH1. We examined transients that occurred within 2 s of each more carefully to determine if there was evidence of diffusion.

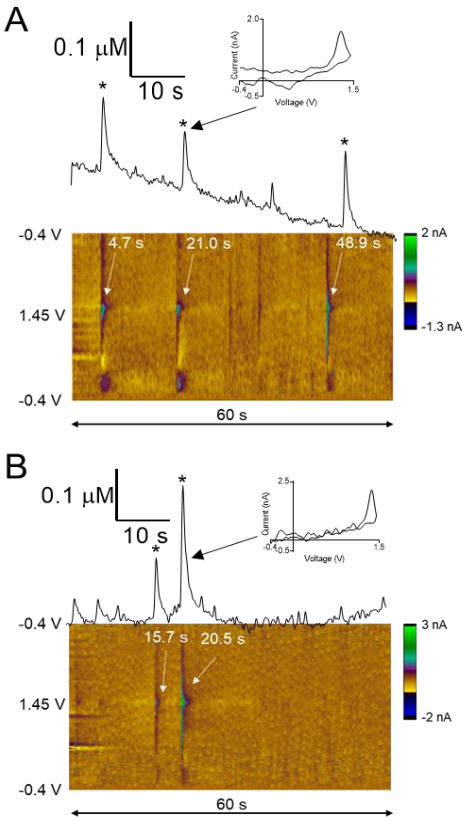

Figure 6 Examples of spontaneous adenosine release in dual channel. A: Channel 0 (CH0). B: Channel 1 (CH1). Top: concentration vs time trace, with stars marking peaks that were identified as spontaneous adenosine with an image analysis program coded in Matlab. A represent CV of spontaneous adenosine from the color plot transients is also presented. Bottom: Color plots in dual channel, with start times of transients indicated.

Figure 7 compares the average data for spontaneous adenosine release at two electrodes at different distances (50 µm and 200 µm). The 200 µm distance was chosen

because mechanically-stimulated adenosine did not diffuse that far. Thus, we hypothesized that spontaneous transients measured on both the channels beyond 200 μm distance would not be due to diffusion. These data were obtained from 8 mouse brain slices from 6 male mice at each distance. Figure 7A shows the average number of transients detected on each channel is not significantly different (Two way-ANOVA, Sidak's multiple comparison test, interaction p=0.84, channel p=0.56, spacing p=0.57, n=8 slices). The average concentration of spontaneous adenosine on each channel is also not significantly different (Figure 7B, two way-ANOVA Sidak's multiple comparison test, interaction p=0.63, channel p=0.35, spacing p=0.21, n=8 slices for each group). The average half time of each transient (7C) is also similar for all channels and spacing (Two way-ANOVA, Sidak's multiple comparison test, interaction p=0.48, channel p=0.68, spacing p=0.79, n=8 slices for each group). Figure 7D compares the distribution of inter-event times (time between two consecutive transients in one channel), and there is an overall significant difference in distribution but no significant differences for the two channels in the same slice (one way-ANOVA multiple comparisons, Kruskal-Wallis test, overall $p<0.0001$, CH0 50 vs CH1 50 p=0.32, CH0 200 vs CH1 200 p=0.2115, n=8 slices). Thus, the distribution of spontaneous adenosine events is similar on both channels. Moreover, the distribution can be fit by a one phase decay which is similar to the previous results in both rat and mouse model, suggesting that spontaneous adenosine events are randomly released in the brain.[21,25] The results in Figure 7 show that there is no significant difference of transient events at different detection sites in the CA1 region: all of the electrodes detect a similar frequency and concentration of spontaneous adenosine release. However, these data do not tell us about coincident release, and so that was examined next.

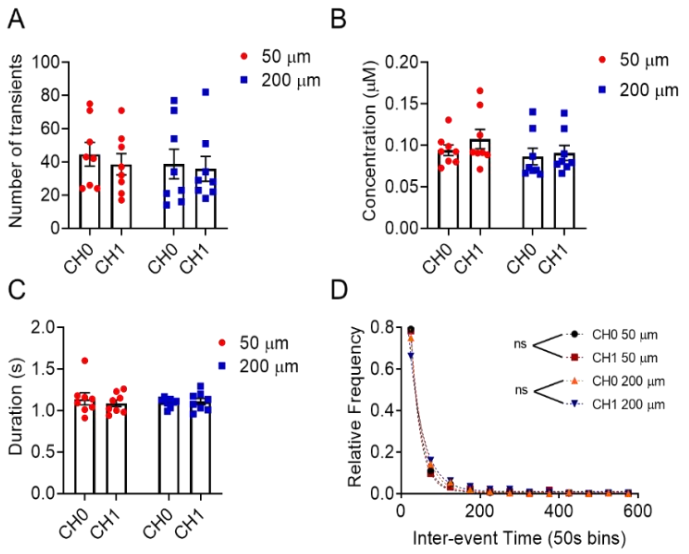

Figure 7 Characterization of spontaneous adenosine at different spacing (50 µm and 200 µm). A. Average number of transients per hour (Two way-ANOVA, Sidak's multiple comparison test, interaction p=0.84, channel p=0.56, spacing p=0.57, n=8 slices). B. Average concentration of transients in each slice (Two way-ANOVA Sidak's multiple comparison test, interaction p=0.63, channel p=0.35, spacing p=0.21, n=8 slices per group). C. Average duration (peak width at half height). Two way-ANOVA, Sidak's multiple comparison test, interaction p=0.48, channel p=0.68, spacing p=0.79, n=8 slices per group. p. D. Inter-event time distribution (50 s bins) of all adenosine transients (One way-ANOVA multiple comparisons, Kruskal-Wallis test, overall p<0.0001). The error bars are SEM.

In order to understand if spontaneous adenosine was detected on both electrodes simultaneously, we investigated the times of all the spontaneous adenosine transients. Table 1 shows aggregate data of coincident transients for both distances. When electrodes were 50 µm apart, about 10.5% of all the transients occurred within 2 s of a transient at the other electrode. Similarly, at 200 µm distance, 10.1% of all transients occurred within 2 s of a transient on the other electrode. To state it another way, about 90% of transients did not occur within 2 s of a transient detected on the other channel, so we considered that 90% of transients were not due to diffusion or coordinated release. If adenosine is diffusing from a point of release to the other electrode, we would expect the first transient to be detected to be a higher concentration so we examined whether the earlier transient had higher release (Table 1). About 50% of the earlier transients were higher concentration and 50% of the later transients were higher concentration, so there is no pattern of higher concentrations at the first transient. These results show that

spontaneous adenosine is randomly released, and the similar release time is likely not due to adenosine diffusion from the electrode to the other.

To understand if the 10% of coincident transients were occurring because of random chance, and not coordination, we also compared the times of transient release from different slices, where there would obviously be no coordination. Table 2 shows the details of the comparison, and about 8% of transients on average were within 2 s of a transient in the other slice. Thus, the 10% numbers we measured with dual channel measurements are similar to the 8% of transients that occurred within 2 s by random chance, and there is likely no coordination between events.

Table 1. Comparison of simultaneously released events (t_{diff} < 2 s)

Spacing	Parameter	Simultaneously released (<2 s)	Higher conc. in earlier release	Higher conc. in later release
50 µm	Number of transients within 2 s	70	38	32
	Percentage	10.5 %	54.3 %	45.7 %
200 µm	Number of transients within 2 s	60	26	34
	Percentage	10.1 %	43.3 %	56.7 %

Table 2 Comparison of simultaneously released adenosine from different slices. (8 slices were compared one by one)

Slice number	Number of transients within 2 s	Percentage (%)
1 vs 2	2	3
1 vs 3	4	5.9
1 vs 4	2	1.9
1 vs 5	10	8.8
1 vs 6	2	2.1
1 vs 7	4	3.4
1 vs 8	0	0
2 vs 3	6	12.0
2 vs 4	8	9.1
2 vs 5	8	8.4
2 vs 6	8	10.5
2 vs 7	6	6.1
2 vs 8	2	4.3
3 vs 4	12	13.3
3 vs 5	6	6.2
3 vs 6	8	10.3
3 vs 7	4	4.0
3 vs 8	4	8.2
4 vs 5	22	16.3
4 vs 6	28	24.1
4 vs 7	12	8.6
4 vs 8	4	4.6
5 vs 6	16	13.0
5 vs 7	16	11.0
5 vs 8	6	6.4
6 vs 7	14	11.0
6 vs 8	6	8.0
7 vs 8	4	4.1
Average	**8 (4 pairs)**	**8.0**

Note: The numbers in first row represents different slices. Data comes from the spontaneous adenosine results in CH0 at 50 µm spacing (8 slices). The average percentage among from the table is 8.0%.

4.4 Discussion

The goal of this study was to understand the spatial and temporal range of adenosine signaling. Mechanically-stimulated adenosine was detected 150 µm away from the stimulation site in the hippocampus CA1 region, indicating that stimulated adenosine affects a portion of the CA1 region after a brain injury. However, spontaneous adenosine did not diffuse even 50 µm, indicating that spontaneous adenosine is extremely localized in the brain. Only 10% of spontaneous adenosine events occurred within 2 seconds of an event on the other channel, indicating most of the transient events are not released in coordination. Thus, using multiple electrodes helps define that an injury to the brain causes more regional neuromodulatory effects but spontaneous adenosine is a highly localized modulatory signal likely related to local cell activity. The short range of rapid adenosine neuromodulation needs to be taken into account when designing treatments that take advantage of rapid adenosine neuromodulation.

4.4.1 Mechanically-stimulated adenosine has a longer spatial range of signaling

Moving an electrode in the brain slice generates sheer stress in the tissue, and this causes ATP release from cells that is rapidly degenerated to adenosine.[26,45] While electrode movement is an artificial stimulus, shear stress occurs in other types of brain injury like traumatic brain injury.[25,45] The high concentration of mechanosensitive adenosine release could act as a neuroprotector to inhibit other neurotransmissions in the brain, which is similar to the role that adenosine plays in brain injury.[46,47] Here, we defined the spatial range of adenosine in tissue due to an injury at a point location. Adenosine signal decreases when the distance between two electrodes increase and then was not detected when the electrode was 200 µm away. Adenosine is cleared by metabolism and taken up by transporters, so the signal decreases with distance.[21] Because we only measured in one direction, we would expect mechanically-stimulated adenosine to influence a sphere with a radius of about 150 µm, which is smaller than the size of the specific CA1 region. The average concentration of mechanically-

stimulated adenosine is 0.5-1 µM at the stimulation and about 0.1 µM at 150 µm away. Considering the high affinity of adenosine A_1 (K_D~70 nM) and A_{2A} receptors (K_D~150 nM), mechanical stimulation would be able to activate these receptors even at 150 mm away from the stimulation.[48,49] Thus, the concentration of mechanically-stimulated adenosine is high enough to activate the most abundant A_1 receptors and inhibit other neurotransmitters to when injury occurs. This spatial resolution provides a better knowledge on how far the stimulated adenosine could potentially modulate other neurotransmitters like dopamine in the brain. There is also a time delay that arises from diffusion. With a diffusion constant of $5*10^{-5}$ cm^2/s, the time delay for 150 µm is expected to be about 2 s, similar to what we measured.[50,51] The duration of the signal is about 30 s which is much longer than the time delay. Therefore, mechanically-stimulated adenosine has a regional influence and would provide neuroprotection within 2 s.

4.4.2 Spontaneous adenosine acts as a localized transient neuromodulator in brain

Spontaneous adenosine release has a more localized spatial profile than mechanically-stimulated release. Most (90%) of events that were detected at an electrode had no corresponding event on the other electrode. If adenosine was diffusing from one electrode to another then the transient detected first would be expected to have the highest concentration. However, results were random with about 50% of earlier transients being larger concentration and 50% of later transients, numbers that did not depend on spacing.[50–53] Thus, there is no evidence that adenosine is diffusing even 50 µm in the brain. While our spatial resolution was limited by our microscope accuracy, closer spacings would be needed to understand the diffusion distance. The magnitude of spontaneous adenosine (0.1 µM) is less than that of mechanically-stimulated adenosine (0.5-1.0 µM), so the diffusion distance is smaller and most of the adenosine is likely cleared or metabolized locally. Spontaneous adenosine is likely formed after breakdown of ATP released from vesicles,[20] so its rapid neuromodulation would be

linked to neuronal activity. Thus, it would have only a very local effect, signaling at receptors in its immediate subregion for only 2 to 3 seconds.

The low percentage of simultaneous spontaneous adenosine release indicates that there is no evidence of widespread coordination of adenosine transients. Instead, the results point towards spontaneous adenosine being randomly released on both channels. Interestingly, the same percentage of coincident events was detected for 50 and 200 µm distances, so if there is coordination, it would be over a 200 µm range. In addition, correlating data from separate slices showed 8% of transients occurred within 2 s of another, our best estimate of what random chance would be. This 8% random chance number is very similar to 10% we measured with dual channel measurements, which suggests there is no coordination. Our results show that different local regions within the CA1 region have similar frequency of spontaneous adenosine release, indicating that when spontaneous adenosine events are detected at electrodes, there are not specific 'hot spots' or 'cold spots' in CA1 region. Therefore, spontaneous adenosine is a random, non-coordinated signal that occurs throughout the CA1 region.

4.4.3 Mechanically-stimulated adenosine and spontaneous adenosine perform different roles in neuromodulation in the brain.

There are two potential reasons that the diffusion impact is different between spontaneous and mechanically-stimulated release. The concentration of mechanically-stimulated adenosine is over 5-fold higher than spontaneous adenosine, and the higher concentration may cause a larger diffusion range, because it will overwhelm local metabolic enzymes and transporters.[54,55] In addition, spontaneous adenosine events only last a few seconds and the shorter duration will allow faster clearance.[21] The two types of adenosine release may also be differently modulated in the brain, which may cause differences in the

range of signaling. For example, studies with genetic knockout mice found that spontaneous adenosine is modulated by A_1 receptors and ATP degeneration enzymes CD39 and CD73 but mechanically-stimulated release was not regulated by adenosine receptors and ATP degeneration enzymes.[24,25,56]

The different range of the modes of rapid adenosine release demonstrate that mechanically-stimulated adenosine and spontaneous adenosine play different roles of neuromodulation. Spontaneous adenosine is more localized, causing neuromodulation only in a very discrete location in the brain for a few seconds, and there is little coordination over the CA1. While these random, localized events change frequency under ischemia or with drugs, they still would be discrete events.[6,57] The frequency of spontaneous adenosine is likely related to cell activity, and thus localized neuromodulation would occur in regions of high activity. Mechanically-stimulated adenosine has a larger concentration and diffusion distance in brain and lasts for about 30 s. Thus, mechanical stress like sheer stress or other brain injury generates a larger adenosine release that acts in a more regional fashion to modulate other neuromodulators such as dopamine release or glutamate release via adenosine receptors.[58–60] The fast response to the stimulation illustrates that mechanically-stimulated adenosine could efficiently cause neuroprotection by inhibiting other neurotransmitters release when the damage or injury comes.[1,61,62] Therefore, understanding the range of adenosine release is important for further characterizations of neuromodulation in real-time.

With the new knowledge on the spatial profile of spontaneous adenosine signaling, we will be able to better understand its rapid, local neuromodulatory effects.[63] For example, knowing that adenosine diffusion after shear stress is limited to 150 µm, treatments may be designed to decrease breakdown and to increase the range of neuromodulation. Also, drugs that increase spontaneous adenosine can be understood to be increasing only a localized neuromodulatory signal and not affecting an entire region. This study used a common dual-

channel potentiostat to measure on 2 channels, but future experiments could expand on these methods. Larger arrays of electrodes with 8 or 16 channels would give more insight into diffusion and coordination of signaling over a wider area.[28,31,32,64] Also, FSCV could be expanded to measure adenosine and other neurotransmitters, such as dopamine, simultaneously to investigate neuromodulation in real time.[58] Thus, there is still much to be learned about the spatial and temporal profiles of adenosine neuromodulation and how these function in healthy and diseased brains.

4.5 Conclusions

In this paper, we investigated the range of mechanically-stimulated adenosine and spontaneous adenosine via dual channel measurements. The results show that spontaneous adenosine acts as a localized rapid neuromodulator in brain and it is randomly released. Mechanically-stimulated adenosine can diffuse 150 µm, indicating it may have influence cells regionally. The random release of spontaneous adenosine indicates that spontaneous adenosine neuromodulation relates to cell activity. Mechanically-stimulated adenosine, on the other hand, relates to the broader range of neuroprotection during the brain injury. Our results indicate more spatial information on real-time rapid adenosine detection, but many rapid interactions based on rapid adenosine neuromodulations and the relationship between these functions in the brain are still needed to be investigate in the future.

4.6 References

(1) Cunha, R. A. Neuroprotection by Adenosine in the Brain: From A1 Receptor Activation to A2A Receptor Blockade. *Purinergic Signalling*. 2005, pp 111–134. https://doi.org/10.1007/s11302-005-0649-1.

(2) Cunha, R. A. How Does Adenosine Control Neuronal Dysfunction and Neurodegeneration? *J. Neurochem.* **2016**, *139* (6), 1019–1055.

https://doi.org/10.1111/jnc.13724.

(3) Cunha, R. A. Adenosine as a Neuromodulator and as a Homeostatic Regulator in the Nervous System: Different Roles, Different Sources and Different Receptors. *Neurochem. Int.* **2001**, *38* (2), 107–125. https://doi.org/10.1016/S0197-0186(00)00034-6.

(4) Shibata, S.; Watanabe, S. A Neuroprotective Effect of Histamine H1 Receptor Antagonist on Ischemia-Induced Decrease in 2-Deoxyglucose Uptake in Rat Hippocampal Slices. *Neurosci. Lett.* **1993**, *151* (2), 138–141. https://doi.org/10.1016/0304-3940(93)90005-6.

(5) Porkka-Heiskanen, T.; Strecker, R. E.; Thakkar, M.; Bjørkum, A. A.; Greene, R. W.; McCarley, R. W. Adenosine: A Mediator of the Sleep-Inducing Effects of Prolonged Wakefulness. *Science (80-.).* **1997**, *276* (5316), 1265–1267. https://doi.org/10.1126/science.276.5316.1265.

(6) Wang, Y.; Venton, B. J. Caffeine Modulates Spontaneous Adenosine and Oxygen Changes during Ischemia and Reperfusion. *ACS Chem. Neurosci.* **2019**, *10* (4), 1941–1949. https://doi.org/10.1021/acschemneuro.8b00251.

(7) Dale, N.; Frenguelli, B. G. Release of Adenosine and ATP during Ischemia and Epilepsy. *Curr.Neuropharmacol.* **2009**, *7* (3), 160–179. https://doi.org/10.2174/157015909789152146 [doi].

(8) Ganesana, M.; Jill Venton, B. Early Changes in Transient Adenosine during Cerebral Ischemia and Reperfusion Injury. *PLoS One* **2018**, *13* (5), 1–18. https://doi.org/10.1371/journal.pone.0196932.

(9) Ganesana, M.; Lee, S. T.; Wang, Y.; Venton, B. J. Analytical Techniques in Neuroscience: Recent Advances in Imaging, Separation, and Electrochemical Methods. *Anal. Chem.* **2017**, *89* (1), 314–341. https://doi.org/10.1021/acs.analchem.6b04278.

(10) Melani, A.; Pugliese, A. M.; Pedata, F. Chapter Thirteen - Adenosine Receptors in Cerebral Ischemia. In *Adenosine Receptors in Neurology and Psychiatry*; of Neurobiology, A. M. B. T.-I. R., Ed.; Academic Press, 2014; Vol. Volume 119, pp 309–348. https://doi.org/https://doi.org/10.1016/B978-0-12-801022-8.00013-1.

(11) Cunha, R. A.; Ribeiro, J. A. Purinergic Modulation of [3H]GABA Release from Rat Hippocampal Nerve Terminals. *Neuropharmacology* **2000**, *39* (7), 1156–1167. https://doi.org/https://doi.org/10.1016/S0028-3908(99)00237-3.

(12) Pinna, A.; Bonaventura, J.; Farré, D.; Sánchez, M.; Simola, N.; Mallol, J.; Lluís, C.; Costa, G.; Baqi, Y.; Müller, C. E.; Cortés, A.; McCormick, P.; Canela, E. I.; Martínez-Pinilla, E.; Lanciego, J. L.; Casadó, V.; Armentero, M. T.; Franco, R. L-DOPA Disrupts Adenosine A2A-Cannabinoid CB1-Dopamine D2 Receptor Heteromer Cross-Talk in the Striatum of Hemiparkinsonian Rats: Biochemical and Behavioral Studies. *Exp. Neurol.* **2014**, *253*, 180–191. https://doi.org/10.1016/j.expneurol.2013.12.021.

(13) Sebastião, A. M.; Ribeiro, J. A. Neuromodulation and Metamodulation by Adenosine: Impact and Subtleties upon Synaptic Plasticity Regulation. *Brain Res.* **2015**, *1621*, 102–113. https://doi.org/10.1016/j.brainres.2014.11.008.

(14) Dunwiddie, T. V; Fredholm, B. B. Adenosine Receptors Mediating Inhibitory Electrophysiological Responses in Rat Hippocampus Are Different from Receptors Mediating Cyclic AMP Accumulation. *Naunyn. Schmiedebergs. Arch. Pharmacol.* **1984**, *326* (4), 294–301. https://doi.org/10.1007/BF00501433.

(15) Lee, S. T.; Venton, B. J. Regional Variations of Spontaneous, Transient Adenosine Release in Brain Slices. *ACS Chem. Neurosci.* **2018**, *9* (3), 505–513. https://doi.org/10.1021/acschemneuro.7b00280.

(16) Ganesana, M.; Venton, B. J. Spontaneous, Transient Adenosine Release Is Not Enhanced in the CA1 Region of Hippocampus during Severe Ischemia Models. *J. Neurochem.* **2021**, in press. https://doi.org/10.1111/jnc.15496.

(17) Seydyousefi, M.; Moghanlou, A. E.; Metz, G. A. S.; Gursoy, R.; Faghfoori, M. H.; Mirghani, S. J.; Faghfoori, Z. Exogenous Adenosine Facilitates Neuroprotection and Functional Recovery Following Cerebral Ischemia in Rats. *Brain Res. Bull.* **2019**, *153* (September), 250–256. https://doi.org/10.1016/j.brainresbull.2019.09.010.

(18) Pearson, T.; Nuritova, F.; Caldwell, D.; Dale, N.; Frenguelli, B. G. A Depletable Pool of Adenosine in Area CA1 of the Rat Hippocampus. *J.Neurosci.* **2001**, *21* (7), 2298–2307.

(19) Mitchell, J. B.; Lupica, C. R.; Dunwiddie, T. V. Activity-Dependent Release of Endogenous Adenosine Modulates Synaptic Responses in the Rat Hippocampus. *J. Neurosci.* **1993**, *13* (8), 3439–3447. https://doi.org/10.1523/jneurosci.13-08-03439.1993.

(20) Street, S. E.; Walsh, P. L.; Sowa, N. A.; Taylor-Blake, B.; Guillot, T. S.; Vihko, P.; Wightman, R. M.; Zylka, M. J. PAP and NT5E Inhibit Nociceptive Neurotransmission by Rapidly Hydrolyzing Nucleotides to Adenosine. *Mol. Pain* **2011**, *7*, 1–15. https://doi.org/10.1186/1744-8069-7-80.

(21) Nguyen, M. D.; Ross, A. E.; Ryals, M.; Lee, S. T.; Venton, B. J. Clearance of Rapid Adenosine Release Is Regulated by Nucleoside Transporters and Metabolism. *Pharmacol. Res. Perspect.* **2015**, *3* (6), 1–12. https://doi.org/10.1002/prp2.189.

(22) Nguyen, M. D.; Wang, Y.; Ganesana, M.; Venton, B. J. Transient Adenosine Release Is Modulated by NMDA and GABAB Receptors. *ACS Chem. Neurosci.* **2017**, *8* (2), 376–385. https://doi.org/10.1021/acschemneuro.6b00318.

(23) Wang, Y.; Venton, B. J. Comparison of Spontaneous and Mechanically-Stimulated Adenosine Release in Mice. *Neurochem. Int.* **2019**, *124* (December 2018), 46–50. https://doi.org/10.1016/j.neuint.2018.12.007.

(24) Wang, Y.; Copeland, J.; Shin, M.; Chang, Y.; Venton, B. J. CD73 or CD39 Deletion Reveals Different Mechanisms of Formation for Spontaneous and Mechanically-Stimulated Adenosine Release and Sex Specific Compensations in ATP Degradation. *ACS Chem. Neurosci.* **2020**, *11* (6), 919–928. https://doi.org/10.1021/acschemneuro.9b00620.

(25) Chang, Y.; Wang, Y.; Venton, B. J. A1and A2AReceptors Modulate Spontaneous Adenosine but Not Mechanically Stimulated Adenosine in the Caudate. *ACS Chem. Neurosci.* **2020**, *11* (20), 3377–3385. https://doi.org/10.1021/acschemneuro.0c00510.

(26) Ross, A. E.; Nguyen, M. D.; Privman, E.; Venton, B. J. Mechanical Stimulation Evokes Rapid Increases in Extracellular Adenosine Concentration in the Prefrontal Cortex. *J. Neurochem.* **2014**, *130* (1), 50–60. https://doi.org/10.1111/jnc.12711.

(27) Peng, W.; Wu, Z.; Song, K.; Zhang, S.; Li, Y.; Xu, M. Regulation of Sleep Homeostasis Mediator Adenosine by Basal Forebrain Glutamatergic Neurons. *Science (80-.).* **2020**, *369* (6508), eabb0556. https://doi.org/10.1126/science.abb0556.

(28) Puthongkham, P.; Venton, B. J. Recent Advances in Fast-Scan Cyclic Voltammetry.

Analyst **2020**, *145* (4), 1087–1102. https://doi.org/10.1039/C9AN01925A.

(29) Zachek, M. K.; Takmakov, P.; Park, J.; Wightman, R. M.; McCarty, G. S. Simultaneous Monitoring of Dopamine Concentration at Spatially Different Brain Locations in Vivo. *Biosens. Bioelectron.* **2010**, *25* (5), 1179–1185. https://doi.org/https://doi.org/10.1016/j.bios.2009.10.008.

(30) Forderhase, A. G.; Styers, H. C.; Lee, C. A.; Sombers, L. A. Simultaneous Voltammetric Detection of Glucose and Lactate Fluctuations in Rat Striatum Evoked by Electrical Stimulation of the Midbrain. *Anal. Bioanal. Chem.* **2020**, *412*, 6611–6624. https://doi.org/10.1007/s00216-020-02797-0.

(31) Koehne, J. E.; Marsh, M.; Boakye, A.; Douglas, B.; Kim, I. Y.; Chang, S.-Y.; Jang, D.-P.; Bennet, K. E.; Kimble, C.; Andrews, R.; Meyyappan, M.; Lee, K. H. Carbon Nanofiber Electrode Array for Electrochemical Detection of Dopamine Using Fast Scan Cyclic Voltammetry. *Analyst* **2011**, *136* (9), 1802–1805. https://doi.org/10.1039/c1an15025a.

(32) Demuru, S.; Nela, L.; Marchack, N.; Holmes, S. J.; Farmer, D. B.; Tulevski, G. S.; Lin, Q.; Deligianni, H. Scalable Nanostructured Carbon Electrode Arrays for Enhanced Dopamine Detection. *ACS Sensors* **2018**, *3* (4), 799–805. https://doi.org/10.1021/acssensors.8b00043.

(33) Parent, K. L.; Hill, D. F.; Crown, L. M.; Wiegand, J. P.; Gies, K. F.; Miller, M. A.; Atcherley, C. W.; Heien, M. L.; Cowen, S. L. Platform to Enable Combined Measurement of Dopamine and Neural Activity. *Anal. Chem.* **2017**, *89* (5), 2790–2799. https://doi.org/10.1021/acs.analchem.6b03642.

(34) Zhang, B.; Heien, M. L. A. V.; Santillo, M. F.; Mellander, L.; Ewing, A. G. Temporal Resolution in Electrochemical Imaging on Single PC12 Cells Using Amperometry and Voltammetry at Microelectrode Arrays. *Anal. Chem.* **2011**, *83* (2), 571–577. https://doi.org/10.1021/ac102502g.

(35) Schwerdt, H. N.; Kim, M. J.; Amemori, S.; Homma, D.; Yoshida, T.; Shimazu, H.; Yerramreddy, H.; Karasan, E.; Langer, R.; Graybiel, A. M.; Cima, M. J. Subcellular Probes for Neurochemical Recording from Multiple Brain Sites. *Lab Chip* **2017**, *17* (6), 1104–1115. https://doi.org/10.1039/C6LC01398H.

(36) Schwerdt, H. N.; Zhang, E.; Kim, M. J.; Yoshida, T.; Stanwicks, L.; Amemori, S.; Dagdeviren, H. E.; Langer, R.; Cima, M. J.; Graybiel, A. M. Cellular-Scale Probes Enable Stable Chronic Subsecond Monitoring of Dopamine Neurochemicals in a Rodent Model. *Commun. Biol.* **2018**, *1* (1), 144. https://doi.org/10.1038/s42003-018-0147-y.

(37) Feingold, J.; Desrochers, T. M.; Fujii, N.; Harlan, R.; Tierney, P. L.; Shimazu, H.; Amemori, K. I.; Graybiel, A. M. A System for Recording Neural Activity Chronically and Simultaneously from Multiple Cortical and Subcortical Regions in Nonhuman Primates. *J. Neurophysiol.* **2012**, *107* (7), 1979–1995. https://doi.org/10.1152/jn.00625.2011.

(38) Huffman, M. L.; Venton, B. J. Electrochemical Properties of Different Carbon-Fiber Microelectrodes Using Fast-Scan Cyclic Voltammetry. *Electroanalysis* **2008**, *20* (22), 2422–2428. https://doi.org/10.1002/elan.200804343.

(39) Swamy, B. E. K.; Venton, B. J. Subsecond Detection of Physiological Adenosine Concentrations Using Fast-Scan Cyclic Voltammetry. *Anal. Chem.* **2007**, *79* (2), 744–750. https://doi.org/10.1021/ac061820i.

(40) Puthongkham, P.; Rocha, J.; Borgus, J. R.; Ganesana, M.; Wang, Y.; Chang, Y.; Gahlmann, A.; Venton, B. J. Structural Similarity Image Analysis for Detection of Adenosine and Dopamine in Fast-Scan Cyclic Voltammetry Color Plots. *Anal. Chem.* **2020**, *92* (15), 10485–10494. https://doi.org/10.1021/acs.analchem.0c01214.

(41) Takmakov, P.; Zachek, M. K.; Keithley, R. B.; Bucher, E. S.; McCarty, G. S.; Wightman, R. M. Characterization of Local PH Changes in Brain Using Fast-Scan Cyclic Voltammetry with Carbon Microelectrodes. *Anal. Chem.* **2010**, *82* (23), 9892–9900. https://doi.org/10.1021/ac102399n.

(42) Phillips, P. E. M.; Robinson, D. L.; Stuber, G. D.; Carelli, R. M.; Wightman, R. M. Real-Time Measurements of Phasic Changes in Extracellular Dopamine Concentration in Freely Moving Rats by Fast-Scan Cyclic Voltammetry. *Methods Mol. Med.* **2003**, *79*, 443–464. https://doi.org/10.1385/1-59259-358-5:443.

(43) Street, S. E.; Kramer, N. J.; Walsh, P. L.; Taylor-Blake, B.; Yadav, M. C.; King, I. F.; Vihko, P.; Mark Wightman, R.; Millán, J. L.; Zylka, M. J. Tissue-Nonspecific Alkaline Phosphatase Acts Redundantly with PAP and NT5E to Generate Adenosine in the Dorsal Spinal Cord. *J. Neurosci.* **2013**, *33* (27), 11314–11322. https://doi.org/10.1523/JNEUROSCI.0133-13.2013.

(44) Nguyen, M. D.; Lee, S. T.; Ross, A. E.; Ryals, M.; Choudhry, V. I.; Venton, B. J. Characterization of Spontaneous, Transient Adenosine Release in the Caudate-Putamen and Prefrontal Cortex. *PLoS One* **2014**, *9* (1), e87165. https://doi.org/10.1371/journal.pone.0087165.

(45) Wan, J.; Ristenpart, W. D.; Stone, H. A. Dynamics of Shear-Induced ATP Release from Red Blood Cells. *Proc. Natl. Acad. Sci. U. S. A.* **2008**, *105* (43), 16432–16437. https://doi.org/10.1073/pnas.0805779105.

(46) Fredholm, B. B. Chapter 11 Adenosine and Neuroprotection. In *Neuroprotective Agents and Cerebral Ischaemia*; Green, A. R., Cross, A. J., Eds.; International Review of Neurobiology; Academic Press, 1996; Vol. 40, pp 259–280. https://doi.org/https://doi.org/10.1016/S0074-7742(08)60723-0.

(47) Lin, Y.; Phillis, J. W. Deoxycoformycin and Oxypurinol: Protection against Focal Ischemic Brain Injury in the Rat. *Brain Res.* **1992**, *571* (2), 272–280. https://doi.org/https://doi.org/10.1016/0006-8993(92)90665-V.

(48) Sheth, S.; Brito, R.; Mukherjea, D.; Rybak, L. P.; Ramkumar, V. Adenosine Receptors: Expression, Function and Regulation. *Int. J. Mol. Sci.* **2014**, *15* (2), 2024–2052. https://doi.org/10.3390/ijms15022024.

(49) Dunwiddie, T. V; Masino, S. a. The Role and Regulation of Adenosine in the Central Nervous System. *Annu. Rev. Pharmacol. Toxicol.* **2001**, *41* (1), 145–174.

(50) Dworkin, M.; Keller, K. H. Solubility and Diffusion Coefficient of Adenosine 3:5 Monophosphate. *J. Biol. Chem.* **1977**, *252* (3), 864–865. https://doi.org/10.1016/s0021-9258(19)75177-1.

(51) Bassingthwaighte, J. B. Interstitial Adenosine: The Measurement, The Interpretation. *J. Mol. Cell. Cardiol.* **1992**, *24* (4), 337–346.

(52) During, M. J.; Spencer, D. D. Adenosine: A Potential Mediator of Seizure Arrest and Postictal Refractoriness. *Ann. Neurol.* **1992**, *32* (5), 618–624.

https://doi.org/10.1002/ana.410320504.

(53) Lindefors, N.; Amberg, G.; Ungerstedt, U. Intracerebral Microdialysis: I. Experimental Studies of Diffusion Kinetics. *J. Pharmacol. Methods* **1989**, *22* (3), 141–156. https://doi.org/10.1016/0160-5402(89)90011-9.

(54) Thorn, J. A.; Jarvis, S. M. Adenosine Transporters. *Gen. Pharmacol.* **1996**, *27* (4), 613–620. https://doi.org/10.1016/0306-3623(95)02053-5.

(55) Cunha, R. A. Regulation of the Ecto-Nucleotidase Pathway in Rat Hippocampal Nerve Terminals. *Neurochem. Res.* **2001**, *26* (8–9), 979–991. https://doi.org/10.1023/A:1012392719601.

(56) Augusto, E.; Matos, M.; Sévigny, J.; El-Tayeb, A.; Bynoe, M. S.; Müller, C. E.; Cunha, R. a; Chen, J.-F. Ecto-5'-Nucleotidase (CD73)-Mediated Formation of Adenosine Is Critical for the Striatal Adenosine A2A Receptor Functions. *J. Neurosci.* **2013**, *33* (28), 11390–11399. https://doi.org/10.1523/JNEUROSCI.5817-12.2013.

(57) Fredholm, B. B.; Chen, J. F.; Cunha, R. A.; Svenningsson, P.; Vaugeois, J. M. Adenosine and Brain Function. *Int. Rev. Neurobiol.* **2005**, *63*, 191–270. https://doi.org/10.1016/S0074-7742(05)63007-3.

(58) Ross, A. E.; Venton, B. J. Adenosine Transiently Modulates Stimulated Dopamine Release in the Caudate-Putamen via A1 Receptors. *J. Neurochem.* **2015**, *132*, 51–60. https://doi.org/10.1111/jnc.12946.

(59) Lopes, L. V.; Cunha, R. A.; Ribeiro, J. A. Cross Talk between A1 and A(2A) Adenosine Receptors in the Hippocampus and Cortex of Young Adult and Old Rats. *J. Neurophysiol.* **1999**, *82* (6), 3196–3203. https://doi.org/10.1152/jn.1999.82.6.3196.

(60) Marchi, M.; Raiteri, L.; Risso, F.; Vallarino, A.; Bonfanti, A.; Monopoli, A.; Ongini, E.; Raiteri, M. Erratum: Effects of Adenosine A 1 and A 2A Receptor Activation on the Evoked Release of Glutamate from Rat Cerebrocortical Synaptosomes (British Journal of Pharmacology (2002) 136 (434-440)). *Br. J. Pharmacol.* **2002**, *137* (2), 294. https://doi.org/10.1038/sj.bjp.0704857.

(61) Boison, D. Adenosine as a Neuromodulator in Neurological Diseases. *Curr. Opin. Pharmacol.* **2008**, *8* (1), 2–7. https://doi.org/https://doi.org/10.1016/j.coph.2007.09.002.

(62) Chen, J. F.; Huang, Z.; Ma, J.; Zhu, J. M.; Moratalla, R.; Standaert, D.; Moskowitz, M. A.; Fink, J. S.; Schwarzschild, M. A. A(2A) Adenosine Receptor Deficiency Attenuates Brain Injury Induced by Transient Focal Ischemia in Mice. *J. Neurosci.* **1999**, *19* (21), 9192–9200. https://doi.org/10.1523/JNEUROSCI.19-21-09192.1999.

(63) Wan, J.; Peng, W.; Li, X.; Qian, T.; Song, K.; Zeng, J.; Deng, F.; Hao, S.; Feng, J.; Zhang, P.; Zhang, Y.; Zou, J.; Pan, S.; Shin, M.; Venton, B. J.; Zhu, J. J.; Jing, M.; Xu, M.; Li, Y. A Genetically Encoded Sensor for Measuring Serotonin Dynamics. *Nat. Neurosci.* **2021**, *24* (5), 746–752. https://doi.org/10.1038/s41593-021-00823-7.

(64) Wigström, J.; Dunevall, J.; Najafinobar, N.; Lovrić, J.; Wang, J.; Ewing, A. G.; Cans, A. S. Lithographic Microfabrication of a 16-Electrode Array on a Probe Tip for High Spatial Resolution Electrochemical Localization of Exocytosis. *Anal. Chem.* **2016**, *88* (4), 2080–2087. https://doi.org/10.1021/acs.analchem.5b03316.

Chapter 5

Optimization of graphene oxide-modified carbon-fiber microelectrode for dopamine detection

Chapter 5 was reprinted from *Anal. Methods*, **2020**, 12, 2893-2902 published by The Royal Society of Chemistry.

Abstract

Graphene oxide (GO) is a carbon-based material that is easily obtained from graphite or graphite oxide. GO has been used broadly for electrochemistry applications and our hypothesis is that GO coating a carbon-fiber microelectrode (CFME) will increase the sensitivity for dopamine by providing more adsorption sites due to the enhancement of oxygen functional groups. Here, we compared drop casting, dip coating, and electrodeposition methods to directly coat commercial GO on CFME surfaces. Dip coating did not result in much GO coating and drop casting resulted in large agglomerations that produced noisy signals and slow rise times. Electrodeposition method with cyclic voltammetry increase the current for dopamine and this method was the most reproducible and had the least noise compared to the other two coating methods. The optimized method used a triangular waveform scanned from -1.2 V to 1.5 V at 100 mV/s for 5 cycles in 0.2 mg/mL GO in water. With fast-scan cyclic voltammetry (FSCV), the optimized GO/CFME enhanced the dopamine oxidation peak two-fold. The sensitivity of the modified electrode is 41±2 nA/μM with a linear range from 25 nM to 1 μM, and a limit of detection of 11 nM. The optimized electrodes were used to detect electrically-stimulated dopamine in brain slices to demonstrate their performance in tissue. Thus, GO can be used to enhance the sensitivity of electrodes for dopamine and improve biological measurements.

5.1 Introduction

Dopamine detection in the brain is important because its dysfunction contributes to serious neurological problems such as drug addiction and Parkinson's disease.[1–3] Dopamine measurement *in vivo* requires real time techniques with high selectivity and sensitivity because of its low concentration and other interferences in brain.[1,4,5] Traditional methods of dopamine detection, such as microdialysis and chronoamperometry, are slower and do not measure in real time.[6] Fast-scan cyclic voltammetry (FSCV) at an implanted carbon-fiber microelectrode (CFME) meets these requirements by providing high temporal resolution and a cyclic voltammogram fingerprint of the species identified.[4,6–8] However, the sensitivity of CFMEs is not high enough to always detect dopamine, particularly in experiments with low numbers of stimulation pulses; thus, strategies to increase sensitivity are advantageous.[9]

Carbon nanomaterial coatings have been implemented to improve the sensitivity of electrodes.[5,10] Carbon nanotubes (CNTs) have been coated or grown on electrodes to enhance the sensitivity and decrease the peak to peak difference (ΔE_p) for dopamine detection.[11–17] In addition, CNT yarns and fibers have been made that have high sensitivity and good temporal resolution.[15,18–20] Graphene has also been widely used to modify electrochemical sensors to improve the sensitivity.[21–23] Other carbon-based nanomaterials have been used to improve the CFME performance, including carbon nanospikes[24,25] and carbon nanofibers.[26,27] Carbon nanohorn-coated CFMEs increase the current of dopamine detection by increasing the electrode surface area and the oxygen functional groups on the electrode.[28] Nanodiamond-coated CFMEs improve the sensitivity and antifouling properties for neurotransmitter detection.[29]

Graphene oxide is another common carbon nanomaterial which is oxidized graphene containing several oxygen functional groups. Graphene oxide (GO) has a high specific surface area, and sp^2-hybridized carbon on the basal plane that provides electronic conductivity.[30] However, due to the random oxidation, oxygen functional groups break up the structure, leading

to structural defects. For example, epoxide groups break the conjugation of the sp^2-hybridized carbon and hydroxyl or carboxylate groups form on the edge plane.[31–35] The defects make GO less conductive compared to graphene and other carbon materials;[30] however, oxygen functional groups on the edge plane are advantageous in other carbon nanomaterials for enhancing adsorption of dopamine, increasing dopamine sensitivity.[22,36] Precise control of oxygenation sites is difficult, however, and orientation of these groups may play a role in sensitivity. Another advantage of these additional oxygen groups is that they make GO more hydrophilic and easier to disperse in water or other organic solvents compared to pure graphene.[35,37,38] Therefore, several easy coating methods can be tested, such as drop casting, dip coating, and electrodeposition.[31] GO-coated electrodes have increased sensitivity relative to bare glassy carbon for dopamine or other compounds, however these experiments were performed with glassy carbon electrodes and tested using traditional cyclic voltammetry.[39,40] Few groups focus on CFME coating, and the only study coating GO on CFMEs, by the Cui group, coated the GO in the polymer PEDOT to enhance the sensitivity of dopamine detection.[21] Direct fabrication of GO-coated CFMEs without polymers will provide a better understanding of how GO enhances the sensitivity for dopamine for possible *in vivo* applications. Moreover, in order to avoid the difficulty of functionalization and structure differences caused by different fabrication methods, we use commercialized graphene oxide powder instead.

In this study, we optimized the direct coating of GO onto CFMEs and then used it for detection of dopamine in tissue. Dip coating, drop casting, and electrodeposition were compared to optimize the GO-coated CFME. The surface coating was evaluated with scanning electron microscopy (SEM) and dip coating provided little coverage, while drop casting caused large agglomerations of GO to attach to the electrode. The electrodeposition method provided superior increases in sensitivity, along with a stable GO coating on the CFME surface. The optimized GO modified CFME (GO/CFME) has a 2-fold current enhancement and was successfully used in mice brain slices to measure electrically stimulated dopamine release.

Overall, GO is a facile, carbon-based material that is easily used for electrode coating to improve the sensitivity of dopamine detection. The improved sensitivity may enable detection of smaller concentrations elicited by small stimulations in the future.

5.2 Experimental Section

5.2.1 Chemicals

Dopamine was purchased from Acros Organics (Morris Plains, NJ). A 10 mM stock solution of dopamine was prepared in 0.1 M $HClO_4$. The working solutions were prepared daily by diluting the stock solution in a phosphate buffer saline (PBS) (131.25 mM NaCl, 3.00 mM KCl, 10 mM NaH_2PO_4, 1.2 mM $MgCl_2$, 2.0 mM Na_2SO_4, and 1.2 mM $CaCl_2$ with pH adjusted to 7.4) to the desired concentration. Graphene oxide powder was purchased from Sigma-Aldrich (St. Louis, MO 63178, USA).

5.2.2 Electrode Fabrication

Carbon-fiber microelectrodes were fabricated by vacuum-aspirating a T-650 carbon fiber (7 µm diameter, Cytec Engineering Materials, West Patterson, NJ) into a glass capillary and pulling into two electrodes by an electrode puller (model PE-21, Narishige, Tokyo, Japan). The pulled electrode tip was cut to 100 µm long and sealed with Epon Resin 828 (Danbury, CT) with 14% (w/w) m-phenylenediamine (Acros Organics, Morris Plains, NH) hardener heated to 80 ºC. The electrodes were dipped into the heated epoxy for 30 s and dipped into acetone solution for 5 s to wash out the epoxy on the carbon fiber surface. Finally, the sealed electrodes were left overnight at room temperature, heated to 100 ºC in an oven for 2 h and then baked at 150 ºC overnight. One molar KCl solution was injected into the capillary to provide the electrical connection between the carbon fiber and the silver wire to the headstage. Graphene oxide solutions were prepared by dissolving the GO powder into DI water with 0.1M NaCl and 0.001M sodium dodecyl sulfate (SDS) to obtain the desired concentration (0.2 mg/mL). The solution was

homogenized by ultrasonic tissue homogenizer (model 150VT, Biologics, Manassas, VA) for 1h before using. The dip coating modified electrodes were fabricated by dipping the electrodes into the prepared GO solution for 5 min or 10 min. Drop casting was performed by dropping 20 µL GO solution to cover the CFME tip on a glass slide on a 65 ºC hot plate. The dropping process was repeated to optimize the amount of GO on the CFME surface via the number of the drops. The electrodepostion method was performed via a potentiostat (Gamry Instruments, Warminster, PA) in an electrochemical cell containing Ag/AgCl reference electrode, Pt counter electrode, and CFME working electrode in the GO dispersion. A repeated cyclic voltammetric waveform was applied and different parameters were optimized, including scan rate, number of cycles, and potential range. All modified electrodes were left overnight at room temperature before being used.

5.2.3 Surface Characterization

Scanning electron microscopy (SEM) images were taken with a Quanta 650 (FEI Company, Hillsboro, OR) at the Nanoscale Materials Characterization Facility, Department of Materials Science and Engineering, University of Virginia. The secondary electron detector images were recorded with an accelerating voltage of 2 kV and a working distance of approximately 10 mm.

5.2.4 Brain slice experiment

All animal experiments were approved by the Animal Care and Use Committee of the University of Virginia. Male C57BL/6 mice (6-8 weeks old, Jackson Labs) were housed in a vivarium and given food and water ad libitum. Mice were anesthetized with isoflurane and beheaded immediately. The mouse brain was removed within 2 min and placed in 0–5°C artificial cerebral spinal fluid (aCSF) for 2 min for recovery. Four hundred-micrometer slices of the caudate–putamen were prepared using a vibratome (LeicaVT1000S, Bannockburn, IL, USA), and transferred to oxygenated aCSF (95% oxygen, 5% CO_2), to recover for an hour

before the experiment. aCSF (maintained at 35–37°C) flowed over the brain slices using a perfusion pump (Watson-Marlo 205U, Wilmington, MA, USA) at a rate of 2 mL/min for all experiments. The distance between the electrode and the stimulated electrode was 50-100 µm. Stimulated release was electrically evoked using biphasic stimulation pulses (300 µA, 5 pulses at 60 Hz).

5.2.5 Electrochemical instrumentation

FSCV experiments were perform with a two-electrode system with a CFME or GO/CFME working electrode and Ag/AgCl reference electrode. A ChemClamp (Dagan, Minneapolis, MN, n=0.01 headstage) was used to connect the electrode and a triangular waveform was applied with a holding potential at -0.4 V, a switching potential at 1.3 V, a scan rate at 400 V/s, and repeated at 10 Hz. The PBS buffer and dopamine solution were injected through the flow cell by an automated two channel syringe pump (Harvard Apparatus, Holliston, MA) at a flow rate of 2 mL/min. The FSCV data were collected with HDCV Analysis software (Department of Chemistry, University of North Carolina at Chapel Hill).

5.2.6 Statistics

All reported values are given as the mean ± standard error of the mean (SEM) for n number of electrodes. Error bars are also SEM. All statistical analyses were performed in GraphPad Prism 8 (GraphPad Software, La Jolla, CA). Statistical significance was defined at $p < 0.05$.

5.3 Results and Discussion

The purpose of this study was to examine graphene oxide coatings of carbon-fiber microelectrodes in order to enhance the detection of dopamine with FSCV. First, we compared three different coating methods: drop casting, dip coating, and electrodeposition. Then, we further optimized electrodeposition method parameters, applying different waveforms. Finally,

the optimized GO modified CFME was used in mice brain slices to measure electrically stimulated dopamine release.

5.3.1 Coating method comparison

First, we compared dip coating, drop casting, and electrodeposition for CFME coating with GO. A 0.2 mg/mL GO solution was used for all coating methods. For dip coating, a bare CFME was dipped into the GO solution for 10 minutes. For drop casting, 20 µL of GO solution was dropped on the electrode tip and the solution evaporated using a hot plate at 70 ºC. This procedure was repeated twice. For the electrodeposition method, a cyclic voltammetry waveform was applied to the CFME while it was in the GO solution, and the potential was ramped from -0.2 V to 1.0 V at 100 mV/s for 10 cycles.

The top row of Fig. 1 shows example FSCV data for each coating method and bare electrodes. Figure 1A shows the background charging current of bare CFMEs and GO/CFMEs. Dip coating or electrodeposition did not enhance the background charging current compared to the bare CFME; however, the background charging current dramatically increased after GO drop casting. Background current is proportional to surface area, so the drop casting method likely deposited a thick layer of GO that increased the area. Fig. 1B compares background subtracted CVs for 1 µM dopamine. The current for the dip coated electrode is similar to the bare electrode, and both the drop casting and electrodeposition electrodes have larger currents than the bare CFME. The peak current is larger for drop casting than electrodeposition. Peak positions also shift with different coatings; the oxidation peak moves slightly to lower potentials with electrodeposition, but shifts to higher potentials with drop casting. Figure 1C shows example current vs. time traces for injecting a bolus of dopamine at these electrodes. Ideally, the shape should be square, but adsorption of dopamine causes the shape to be more rounded.[41] The drop casting method has a much slower current rise time and larger noise

compared to bare CFMEs and the other two coated GO/CFMEs. This slow time response is likely due to a thick coating that slows down the dopamine diffusion into and out of the surface and is not ideal for biological measurements because it will distort the time response. However, enhanced adsorption did not influence the time response in FSCV time scale.

Average data for GO coating methods are displayed on the bottom of Figure 1. Figure 1D displays average increases in background charging current and there is a significant effect of coating method on background current (One-way ANOVA, $p<0.0001$, n= 4-6 per group, error bars are SEM). Current for drop casting was significantly greater than bare electrodes (Bonferroni post-test, $p<0.0001$), while the current for electrodeposition and dip coating were not significantly different than bare. Figure 1E shows average increases in anodic current for dopamine and there is an overall effect of coating method on dopamine current (One-way ANOVA, $p<0.0001$, n= 4-6 per group). Drop casting has a significantly larger current than bare electrodes and larger increases than dip coating and electrodeposition (Bonferroni post-test, $p<0.0001$). Electrodeposition also significantly enhanced the current compared to bare CFMEs ($p<0.001$). Fig. 1F compares the average rise times, from 10% of the maximum to 90% of the maximum, for the current vs. time curves. There is an overall main effect of coating and drop casting significantly increased the rise time compared to the other two methods and bare CFMEs (One-way ANOVA multiple comparison, main effect $p<0.0001$, Bonferroni post-test, $p<0.0001$), which indicates a thick GO coating causes slower response times. In addition, ΔE_p of the electrodes was also compared in Figure 2, drop casting shows a significant increase compared to bare CFMEs, but dip coating or electrodeposition shows no significant change (one-way ANOVA multiple comparison, main effect $p<0.0001$). The ΔE_p increase of drop casting also proved that GO aggregated on the surface, slowing electron transfer.

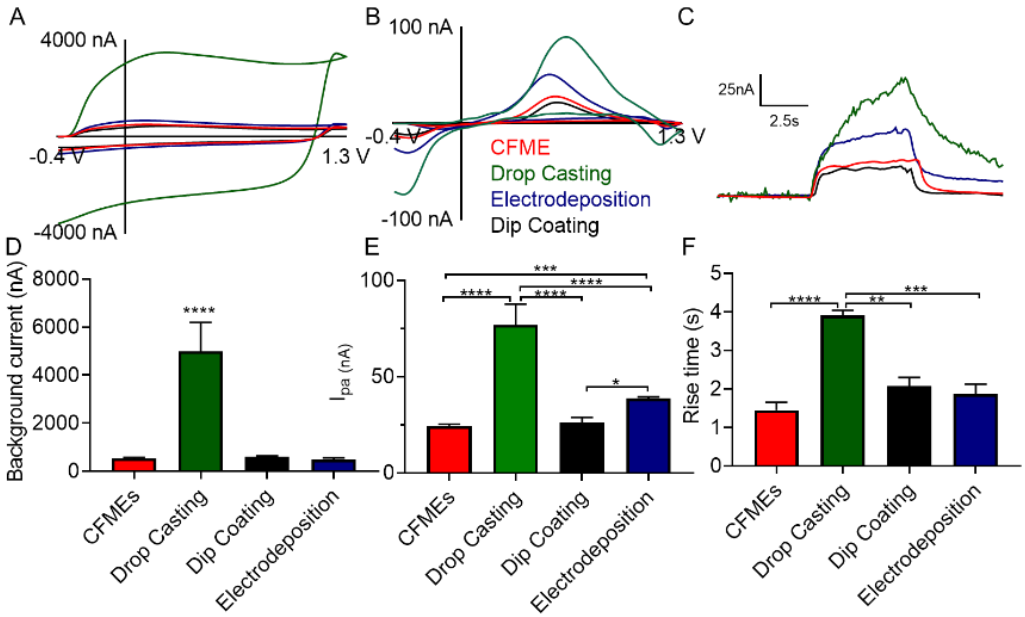

Figure 1. Comparison of GO coating methods. (A) Background charging current by different coating methods (bare: red, drop casting: green, electrodeposition: blue, dip coating: black). (B) Examples of background-subtracted CVs for 1 μM dopamine after different coating methods. (C) Example current vs. time trace of the electrode response to a square bolus injection of 1 μM dopamine. (D) Average background charging current (n=4-6, one-way ANOVA main effect $p<0.0001$, Bonferroni post-test.) (E) Average anodic peak current of 1 μM dopamine (n=4-6, error bars represent SEM, one-way ANOVA with Bonferroni's multiple comparisons test $p<0.0001$), (F) Average rise time (time from 10% of to 90% of the maximum current). (n=4-6, one-way ANOVA with Bonferroni's multiple comparisons test.) *$p<0.05$, **$p<0.01$, ***$p<0.001$, ****$p<0.0001$. Error bars are SEM.

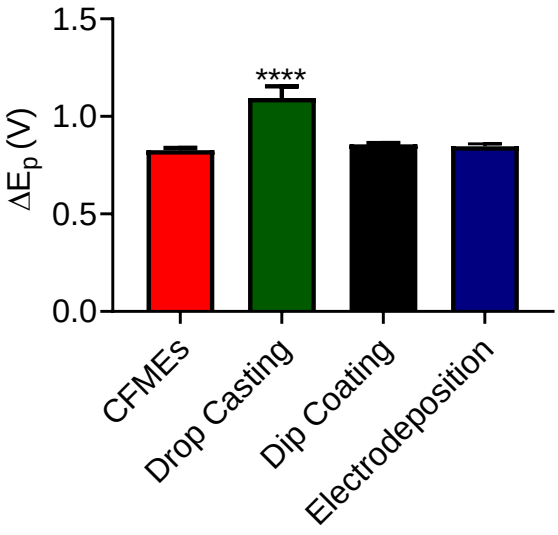

Figure 2. Average ΔEp by different coating method. (n=4–6, error bars represent SEM, one-way ANOVA with Bonferroni post-test compared to the control (red bars) ****$p<0.0001$)

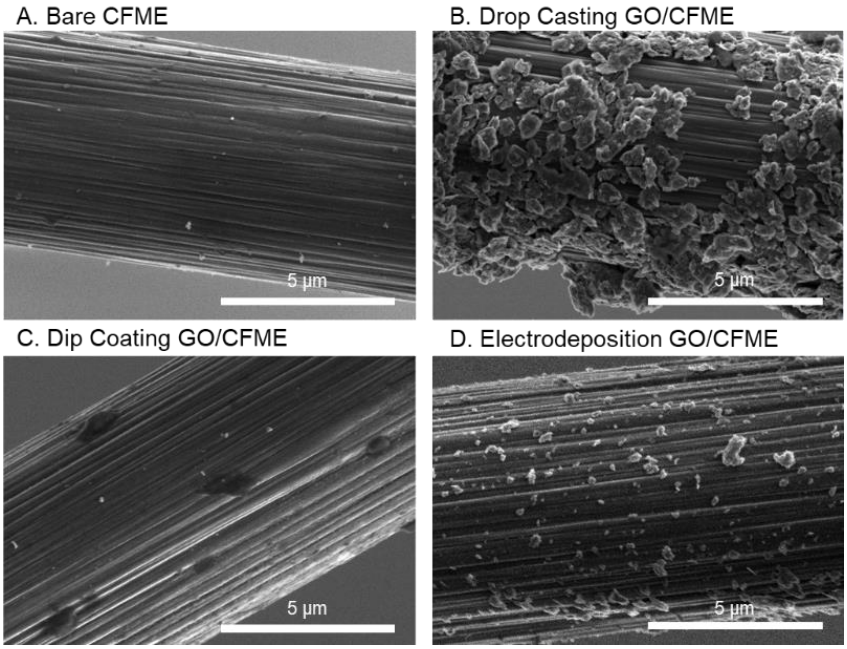

Figure 3. SEM images of (A) bare CFME, (B) drop casting GO/CFME, (C) dip coating GO/CFME, (D) electrodeposition GO/CFME.

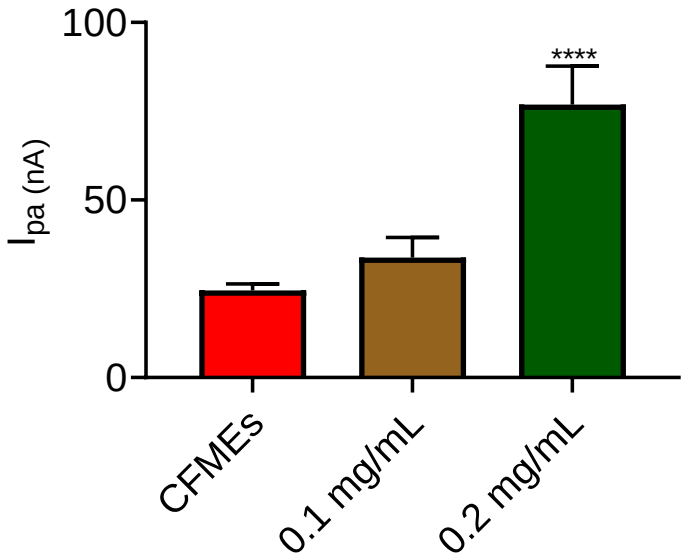

Figure 4. Average anodic peak current by drop casting in different concentration. (2 drops, 20 µL per drop) (n=4–6, error bars represent SEM, one-way ANOVA with Bonferroni post-test compared to the control (red bars) ****p<0.0001)

Fig. 3 compares the electrode surfaces with the different coating methods. The bare CFME surface (Figure 3A) is relatively smooth, with some striations. With drop casting, there is an

obvious thick coating of GO on the surface of the electrode (Fig. 3B). For dip coating (Fig. 3C), there is almost no coating with GO. With electrodeposition (Fig. 3D), GO is deposited in a sparse coating on the surface. The thickness of GO coating is in nanometer range by electrodeposition but more on the micron scale by drop casting.

The electrochemical data and SEM images together tell a story about the extent of GO coating and how that affects electrochemical signals. Drop casting GO increased the dopamine oxidation current by 3-fold but the background charging current increased nearly 10-fold, which means the surface area of the electrode increased more than the Faradaic signal.[42] The SEM results in Figure 3B show large GO aggregates on the surface. Therefore, GO coating by drop casting produces a thick layer, and not all of it is on the surface accessible for electrochemistry. Other concentrations of GO were tested for drop casting (Fig. 4), but lower concentrations did not show significant current enhancement, while higher concentrations provided such a thick layer that the amplifier was overloaded, meaning the background current was over 10,000 nA. The thick coating on the surface creates a multilayer structure that slows dopamine diffusion to the electrode surface, and this causes the rise time to slow significantly (Figure 1B and 1F). The significantly larger average ΔE_p also proved that the thick coating by drop casting decreases the kinetics of the reaction (Figure 2). Additionally, GO aggregation on the carbon fiber surface led to a large variability in the currents between electrodes, and an unstable charging background because noise is proportional to background charging current.[43] For these reasons, drop casting was not considered an ideal method of coating GO on the surface.

The dip coating method failed to coat GO on the electrode surface, likely because the GO preferred to agglomerate in solution and did not adhere to the carbon fiber surface without any driving force.[44] There was little GO that adhered to the electrode and little change in electrochemical properties with dip coating. Thus, dip coating is not a good method for depositing GO on CFMEs. However, dip coating is also a control group for electrodeposition, and a better signal for electrodeposition than dip coating demonstrates that applying a potential

is advantageous for coating GO on the electrode.

Electrodeposition was the most successful method for depositing a thin layer of GO on the electrode surface. Several other carbon nanomaterials, such as carbon nanotubes and carbon nanohorns,[13,28] have been successfully electrodeposited on CFMEs using CV, so we used CV here. Compared to dip coating and drop casting, electrodeposition showed the best overall results of increasing sensitivity without slowing the time response. Electrodeposition enhances GO coating as negatively charged GO and sodium dodecyl sulfate particles are attracted to the carbon fiber surface when the positive potential is applied.[38,45] The SEMs in Figure 3D show that electrodeposition provides a thin coating on the surface, and this thin coating did not significantly increase the background current, which is a measure of surface area. Thus, the 2-fold current enhancement after electrodeposition is due not to an increase in overall surface area but to adding sites that promote dopamine adsorption. The small increase in background current is advantageous because the noise remains low. Moreover, the rise time for the i-t curve (Figure 1D) remained fast because there were no large agglomerations of GO that would trap and slow dopamine diffusion. Therefore, electrodeposition method is the most promising method for GO deposition, compared to dip coating and drop casting. Next, we optimized CV waveforms for electrodeposition.

5.3.2 Optimization of GO Electrodeposition Method

The electrodeposition method was further optimized by changing different parameters of the cyclic voltammetry for electrodeposition, such as scan rate, number of cycles, and the potential range of the triangular waveform. Here, we used a triangular waveform from -0.2 V to 1.0 V to optimize the scan rate and the numbers of CV cycles. First, the scan rate of CV was varied from 50 mV/s to 150 mV/s. Fig. 5A shows the average anodic peak current significantly increased with 10 cycles of 50 mV/s and 100 mV/s, however, the signal started to decrease at a higher scan rate of 150 mV/s (one-way ANOVA, main effect $p<0.0001$, n=4-6, Bonferroni post-tests,

error bars are SEM). For the optimal scan rate of 100 mV/s, 5 cycles was compared to 10 cycles, and the improvement in currents were similar.

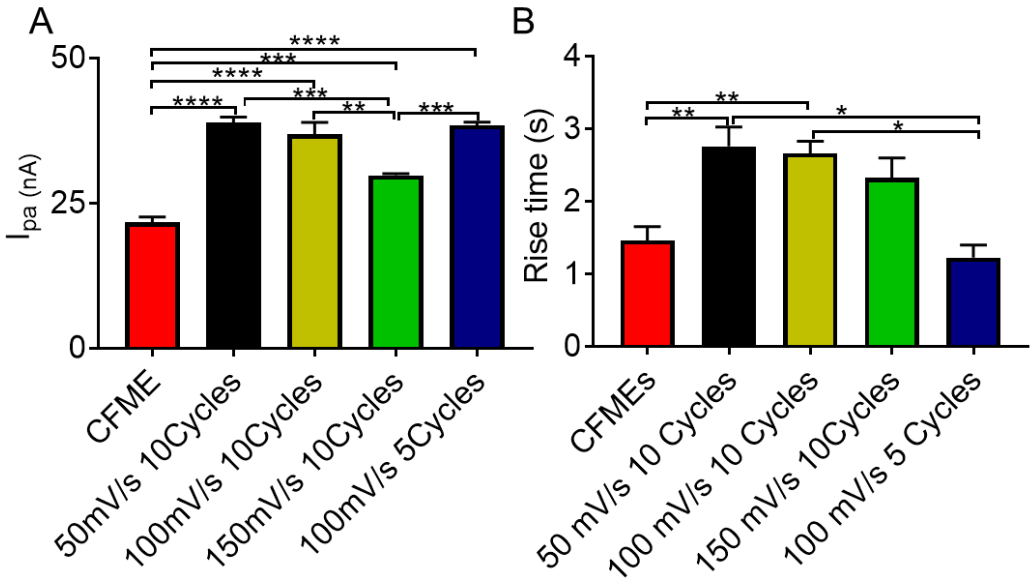

Figure 5. Optimization of scan rate and number of cycles for electrodeposition. Cyclic voltammetry scanned from -0.2 V to 1.0 V. (A) Average anodic peak current comparisons of electrodeposition using different scan rate and number of cycles. (B) Average rise time by different parameters. (n=4-6, one-way ANOVA with Bonferroni post-test. Main effect $p<0.0001$), *$p<0.05$, **$p<0.01$, ***$p<0.001$, ****$p<0.0001$. Error bars are SEM.

Figure 5B shows the average rise time of the GO/CFMEs coated by different CV parameters and there is a significant effect of electrodeposition parameters (one-way ANOVA, main effect $p=0.0005$, error bars are SEM). Scanning at 50 mV/s and 100 mV/s for 10 cycles produced rise times significantly slower than bare CFMEs. The rise time for 100 mV/s for 5 cycles is not significantly different than bare CFMEs. The slower rise time indicates that more GO is aggregating on the surface. The increased rise time at 50 mV/s and 100 mV/s for 10 cycles is likely due to the longer electrodeposition time because the slower scan rate and more cycles allow more GO particle aggregation on the surface, which slows down the rise time response. Therefore, 100 mV/s for 5 cycles was the optimal scan rate and number of cycles, and the potential range optimization was performed using these parameters.

Next, we optimized the potential range for the electrodeposition, testing the effects of

extending the anodic and cathodic limits. The potential range was extended from -1.2 V to 1.5 V to compare whether a further reduction of GO or a further oxidation of GO results in better performance of dopamine measurement.[46,47] Two new waveforms were compared to bare CFMEs and the standard waveform used previously (-0.2 to 1.0 V): the oxidation waveform from -0.2 V to 1.5 V (100 mV/s, 5 cycles), and the extended waveform -1.2 V to 1.5 V (100 mV/s, 5 cycles). In addition, a no GO control was performed where the extended waveform (-1.2 V to 1.5 V) was applied to the electrode in a solution without GO in order to prove that it is not only waveform activation of the CFME that is giving the effect.[48] Figure 6 shows the average anodic peak current for dopamine and there is a significant main effect of waveform on dopamine current (One-way ANOVA, main effect $p<0.0001$, $n=6$). All three electrodeposition waveforms enhanced the dopamine peak current significantly compared to bare CFMEs (Dunnett's post-test, $p<0.0001$) but the waveform only (-1.2 V to 1.5 V, no GO) control did not have significantly greater current than CFMEs. The extended waveform (-1.2 V to 1.5 V) showed the largest average current increase and the average current is also higher than the standard waveform (-0.2 V to 1.0 V) and the oxidation waveform. While increased adsorption could slow the temporal response, the extended waveform did not increase the rise time of the electrode (average 1.5 s), because the timescale of FSCV is only 0.1 s, slower than adsorption.[41]

The extended waveform from -1.2 V to 1.5 V showed the best anodic peak current increase because scanning to 1.5 V can further oxidize GO to increase the oxygen functional groups, which enhances dopamine adsorption. However, the highly positive potential may also create epoxy groups on the GO basal plane and reduce the conductivity.[31] The reason the cathodic limit was lowered to -1.2 V is that the hydroxyl group and the epoxy group on GO can be reduced at this negative potential. The carboxyl group, which is mainly present at the edge plane, cannot be reduced because it requires -2.0 V for reduction.[40] Therefore, the -1.2 V to 1.5 V waveform provides more oxygen functional groups on the edge plane and prevents a further oxidation on the basal plane, but -0.2 V to 1.5 V waveform decrease the conductivity of the GO

basal plane by reducing epoxy groups. A reduction waveform from -1.2 V to 0.2 V was also applied for the optimization, but the electrodeposition failed because of large aggregation of reduced graphene oxide (rGO) on the electrode surface after coating, which overloaded the instrument amplifier. The increased aggregation suggests that the reduction of GO on the basal plane results in a structure more similar to graphene. Thus, rGO is more likely to aggregate layer by layer by π-π stacking compared to GO. With the aggregates, the amount of material on the electrode significantly increased and thus, the background charging current increased,[49] overloading the instrument amplifier. However, most of that aggregated material is not on the surface that is exposed to the solution and is not useful for electrochemistry. The control experiment proved that the current increase is not due to the carbon fiber surface activation by a high positive potential,[50] and the current increase comes from the GO coated on the surface. Therefore, the optimal method for modifying CFMEs with GO is electrodeposition with cyclic voltammetry from -1.2 V to 1.5 V at 100 mV/s for 5 cycles.

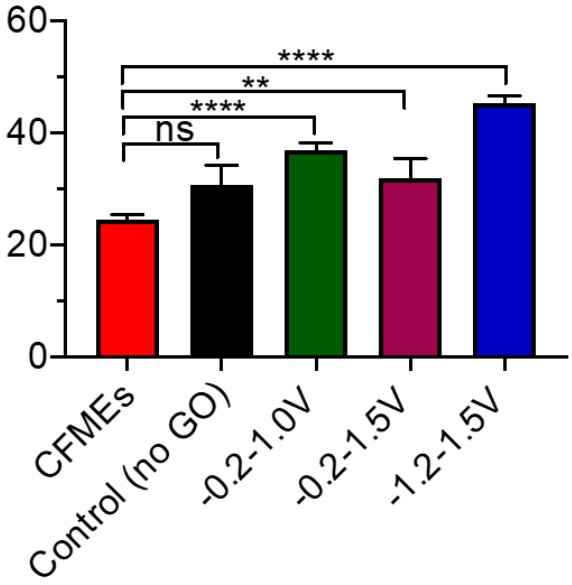

Figure 6. Average anodic peak current comparison for the waveform optimization and the control experiment. The control was done by applying the extended waveform (-1.2 V to 1.5 V) to the bare CFME in the solution without GO (n=6-8, error bars represent SEM, one-way ANOVA with Dunnett's comparison to CFMEs, **p<0.01, ****p<0.0001, ns=no significance). Error bars are SEM.

5.3.3 Analytical Performance of the GO/CFMEs

Figure 7A shows the relationship between the scan rate and anodic peak current. The scan rate was varied from 50 V/s to 1000 V/s, and the log scan rate and log anodic peak current is linear with a slope of 1.15 (R^2= 0.9989) which is near to 1. Therefore, the scan rate is proportional to the anodic peak current on the optimized GO/CFMEs, and the dopamine redox reaction is adsorption-controlled at the GO/CFME.[41] Figure 7B shows the concentration dependence of the dopamine anodic peak current at GO/CFME. The electrode was tested in different concentration dopamine solutions from 25 nM to 100 µM. The optimized GO/CFME shows a linear relationship from 25 nM to 1 µM (R^2=0.9949). At higher concentrations, however, the anodic peak current is nonlinear with concentration because the adsorption sites on the electrode are saturated and the kinetics are more diffusion-controlled.[42] This trend to become non-linear at higher concentrations is similar to bare CFMEs and other modified CFMEs such as CNT-coated CFMEs and carbon nanohorn-coated CFMEs.[28,41] Although the linear range in this work is slightly smaller than some other coated CFMEs,[9,28] most *in vivo* dopamine measurements are less than 1 µM,[1,51,52] so the linear range is suitable for brain slice or *in vivo* dopamine measurements. The sensitivity of optimized GO/CFME is 43 nA/µM, and high sensitivity will facilitate measurements of smaller concentrations of dopamine release. In Fig. 7C, the CV of 25 nM dopamine is shown, and the peaks for dopamine are clearly visible. The LOD for the optimized GO/CFME is 11 nM, calculated using a S/N ratio of 3 from the current vs time curve.

Figure 7D shows the stability test of the GO/CFME electrode. The coating on the electrode needs to be stable for hours in order to make biological measurements. Therefore, the FSCV waveform was applied for 4 hours to the electrode in the flow cell, and 1 µM dopamine solution was injected every hour to measure the anodic peak current. The anodic peak current did not decrease significantly in a 4 h period, (one-way ANOVA multiple comparison, main effect, p=0.4328, n=4) and the normalized peak current was over 90% of the

initial signal after 4 h. Thus, the GO/CFME electrodes are stable and the GO does not fall off during the time course of a typical experiment, even when the waveform is applied continuously.

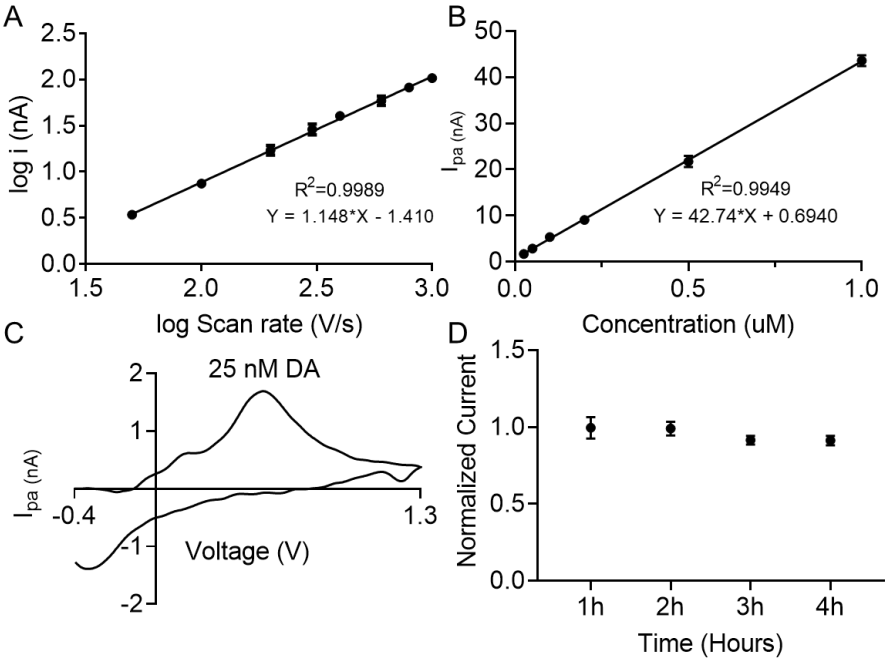

Figure 7. Analytical performance of the optimized GO/CFME. (A) Scan rate experiment. (n=4) The slop of the log *i* and log v is 1.15, which is close to 1, indicating adsorption-control. (B) Concentration dependence. Plot of the anodic peak current of dopamine vs. dopamine concentration. The plot shows the linear range from 25 nM to 1 µM (n=3). (C) Example CV of 25 nM dopamine measurement in PBS pH=7.4. (D) Stability test. Anodic peak current was measured every hour for 4h (n=4) as the FSCV waveform was constantly applied. Error bars are SEM.

While this is the first study of directly coat GO on CFMEs, previous studies also found that coating GO on glassy carbon electrode surfaces enhance the electrochemical performance and increase the sensitivity.[40,53] Moreover, while we are the first to use electrodeposition with graphene oxide, it has been applied in coating other nanomaterials on glassy carbon as well as CFMEs.[4,28] For graphene oxide, because enhancement of oxygen functional groups increases adsorption for dopamine, future experiments could focus on surface treatments to functionalize more oxygen functional groups on the electrode surface. For example, oxygen plasma or laser treatment could provide more active sites on the edge plane to further enhance the sensitivity.[19,20] However, if GO is too functionalized with oxygen, it will lose its conductivity, so

adding more oxygen groups is a balance between promoting adsorption and maintaining conductivity.

5.3.4 GO/CFME in Brain Slice Experiment

To further prove the optimized GO/CFME can be applied in biological experiments, electrically stimulated dopamine release was measured in mice brain slices. Here, we used biphasic stimulation pulses to electrically evoke dopamine in the caudate-putamen region of C57B mice and used optimized GO/CFME to measure the stimulated dopamine release. Figure 6 shows that GO/CFME provides a good time response for measuring dopamine release in the brain tissue, and the transient dopamine lasts for about 1.7 s. The traces for stimulations 1 and 2 do not come quite back down to baseline, which is normal compared to previous publications, and the slight reduction in “hang-up” with the third stimulation may due to pH shift in the brain environment.[54,55] Using a precalibration factor, the amount released is about 25 nM. The small concentration might due to biofouling in the brain tissue, but the current signal has similar scale compared to other published carbon-based electrode for stimulated dopamine measurement.[4,54] Further experiment could be done to investigate the biofouling on the coated electrode, examining signals before and after tissue implantation. Figure 6 also shows the CV for dopamine release. The time course of dopamine release was similar as to previous work with bare CFME, but the amount of dopamine we measured was smaller.[55] Thus, the GO/CFME is useful for measuring small amounts of dopamine in biological tissue.

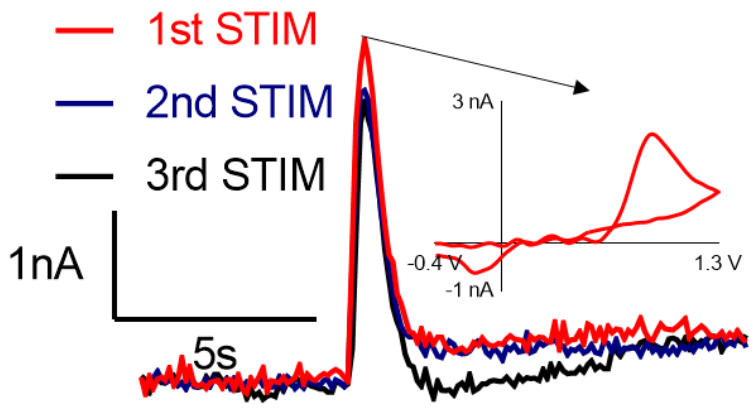

Figure 6. Brain slice experiment. Stimulated dopamine release was electrically evoked using biphasic stimulation pulses (300 µA, 5 pulses at 60 Hz) The i-t curve of the electrical stimulated dopamine release in caudate-putamen region. Subtracted CV of the 1st stimulated dopamine release is attached near the arrow.

5.4 Conclusions

We compared three different coating method to deposit graphene oxide on bare carbon-fiber microelectrodes, and electrodeposition provides the best coating result with a 2-fold anodic current increase without sacrificing rise time, and 11 nM for the LOD. Although drop casting has a higher signal increase compared to electrodeposition method, drop casting slows down the rise time and provides poor reproducibility. Further optimization of the electrodeposition method shows that a broader potential range of the CV waveform (-1.2 V to 1.5 V) provides a higher anodic peak current of dopamine, and the GO coating is very stable on the electrode surface. In addition, the optimized GO/CFME was used to successfully measure electrically-stimulated dopamine release in mouse brain slice. Overall, this is the first study to directly coat the commercialized graphene oxide powder on the carbon-fiber microelectrode, and shows that electrodeposition is useful as a method for GO deposition. GO is a potential carbon-based material to enhance the sensitivity for cationic neurotransmitters and improve in vivo measurements.

5.5 References

(1) Venton, B. J.; Wightman, R. M. Psychoanalytical Electrochemistry: Dopamine and Behavior. *Anal. Chem.* **2003**, *75* (19), 414 A-421 A. https://doi.org/10.1021/ac031421c.

(2) Robinson, D. L.; Hermans, A.; Seipel, A. T.; Wightman, R. M. Monitoring Rapid Chemical Communication in the Brain. *Chem. Rev.* **2008**, *108*, 2554–2584. https://doi.org/10.1021/cr068081q.

(3) Ganesana, M.; Lee, S. T.; Wang, Y.; Venton, B. J. Analytical Techniques in Neuroscience: Recent Advances in Imaging, Separation, and Electrochemical Methods. *Anal. Chem.* **2017**, *89* (1), 314–341. https://doi.org/10.1021/acs.analchem.6b04278.

(4) Puthongkham, P.; Venton, B. J. Recent Advances in Fast-Scan Cyclic Voltammetry. *Analyst* **2020**. https://doi.org/10.1039/C9AN01925A.

(5) Yang, C.; Denno, M. E.; Pyakurel, P.; Venton, B. J. Recent Trends in Carbon Nanomaterial-Based Electrochemical Sensors for Biomolecules: A Review. *Anal. Chim. Acta* **2015**, *887*, 17–37. https://doi.org/10.1016/j.aca.2015.05.049.

(6) Bucher, E. S.; Wightman, R. M. Electrochemical Analysis of Neurotransmitters. *Annu. Rev. Anal. Chem.* **2015**, *8* (1), 239–261. https://doi.org/10.1146/annurev-anchem-071114-040426.

(7) Wilson, L. R.; Panda, S.; Schmidt, A. C.; Sombers, L. A. Selective and Mechanically Robust Sensors for Electrochemical Measurements of Real-Time Hydrogen Peroxide Dynamics in Vivo. *Anal. Chem.* **2018**, *90* (1), 888–895. https://doi.org/10.1021/acs.analchem.7b03770.

(8) Venton, B. J.; Cao, Q. Fundamentals of Fast-Scan Cyclic Voltammetry for Dopamine Detection. *Analyst* **2020**. https://doi.org/10.1039/C9AN01586H.

(9) Huffman, M. L.; Venton, B. J. Carbon-Fiber Microelectrodes for in Vivo Applications. *Analyst* **2009**, *134* (1), 18–24. https://doi.org/10.1039/b807563h.

(10) Cao, Q.; Puthongkham, P.; Venton, B. J. Review: New Insights into Optimizing Chemical and 3D Surface Structures of Carbon Electrodes for Neurotransmitter Detection. *Anal. Methods* **2019**, *11* (3), 247–261. https://doi.org/10.1039/c8ay02472c.

(11) Xiang, L.; Yu, P.; Hao, J.; Zhang, M.; Zhu, L.; Dai, L.; Mao, L. Vertically Aligned Carbon Nanotube-Sheathed Carbon Fibers as Pristine Microelectrodes for Selective Monitoring of Ascorbate in Vivo. *Anal. Chem.* **2014**, *86* (8), 3909–3914. https://doi.org/10.1021/ac404232h.

(12) Swamy, B. E. K.; Venton, B. J. Subsecond Detection of Physiological Adenosine Concentrations Using Fast-Scan Cyclic Voltammetry. *Anal. Chem.* **2007**, *79* (2), 744–750. https://doi.org/10.1021/ac061820i.

(13) Yang, C.; Jacobs, C. B.; Nguyen, M. D.; Ganesana, M.; Zestos, A. G.; Ivanov, I. N.; Puretzky, A. A.; Rouleau, C. M.; Geohegan, D. B.; Venton, B. J. Carbon Nanotubes Grown on Metal Microelectrodes for the Detection of Dopamine. *Anal. Chem.* **2016**, *88* (1), 645–652. https://doi.org/10.1021/acs.analchem.5b01257.

(14) Xiao, N.; Venton, B. J. Rapid, Sensitive Detection of Neurotransmitters at Microelectrodes Modified with Self-Assembled SWCNT Forests. *Anal. Chem.* **2012**, *84*

(18), 7816–7822. https://doi.org/10.1021/ac301445w.

(15) Schmidt, A. C.; Wang, X.; Zhu, Y.; Sombers, L. A. Carbon Nanotube Yarn Electrodes for Enhanced Detection of Neurotransmitter Dynamics in Live Brain Tissue. *ACS Nano* **2013**, *7* (9), 7864–7873. https://doi.org/10.1021/nn402857u.

(16) Harreither, W.; Trouillon, R.; Poulin, P.; Neri, W.; Ewing, A. G.; Safina, G. Carbon Nanotube Fiber Microelectrodes Show a Higher Resistance to Dopamine Fouling. *Anal. Chem.* **2013**, *85* (15), 7447–7453. https://doi.org/10.1021/ac401399s.

(17) Ross, A. E.; Venton, B. J. Nafion-CNT Coated Carbon-Fiber Microelectrodes for Enhanced Detection of Adenosine. *Analyst* **2012**, *137* (13), 3045–3051. https://doi.org/10.1039/c2an35297d.

(18) Jacobs, C. B.; Ivanov, I. N.; Nguyen, M. D.; Zestos, A. G.; Venton, B. J. High Temporal Resolution Measurements of Dopamine with Carbon Nanotube Yarn Microelectrodes. *Anal. Chem.* **2014**, *86* (12), 5721–5727. https://doi.org/10.1021/ac404050t.

(19) Yang, C.; Wang, Y.; Jacobs, C. B.; Ivanov, I. N.; Venton, B. J. O2 Plasma Etching and Antistatic Gun Surface Modifications for CNT Yarn Microelectrode Improve Sensitivity and Antifouling Properties. *Anal. Chem.* **2017**, *89* (10), 5605–5611. https://doi.org/10.1021/acs.analchem.7b00785.

(20) Yang, C.; Trikantzopoulos, E.; Nguyen, M. D.; Jacobs, C. B.; Wang, Y.; Mahjouri-Samani, M.; Ivanov, I. N.; Venton, B. J. Laser Treated Carbon Nanotube Yarn Microelectrodes for Rapid and Sensitive Detection of Dopamine in Vivo. *ACS Sensors* **2016**, *1* (5), 508–515. https://doi.org/10.1021/acssensors.6b00021.

(21) Taylor, I. M.; Robbins, E. M.; Catt, K. A.; Cody, P. A.; Happe, C. L.; Cui, X. T. Enhanced Dopamine Detection Sensitivity by PEDOT/Graphene Oxide Coating on in Vivo Carbon Fiber Electrodes. *Biosens. Bioelectron.* **2015**, *89*, 400–410. https://doi.org/10.1016/j.bios.2016.05.084.

(22) McCreery, R. L. Advanced Carbon Electrode Materials for Molecular Electrochemistry. *Chem. Rev.* **2008**, *108* (7), 2646–2687. https://doi.org/10.1021/cr068076m.

(23) Zhu, M.; Zeng, C.; Ye, J. Graphene-Modified Carbon Fiber Microelectrode for the Detection of Dopamine in Mice Hippocampus Tissue. *Electroanalysis* **2011**, *23* (4), 907–914. https://doi.org/10.1002/elan.201000712.

(24) Zestos, A. G.; Yang, C.; Jacobs, C. B.; Hensley, D.; Venton, B. J. Carbon Nanospikes Grown on Metal Wires as Microelectrode Sensors for Dopamine. *Analyst* **2015**, *140* (21), 7283–7292. https://doi.org/10.1039/c5an01467k.

(25) Cao, Q.; Hensley, D. K.; Lavrik, N. V; Venton, B. J. Carbon Nanospikes Have Better Electrochemical Properties than Carbon Nanotubes Due to Greater Surface Roughness and Defect Sites. *Carbon N. Y.* **2019**, *155*, 250–257. https://doi.org/https://doi.org/10.1016/j.carbon.2019.08.064.

(26) Li, Z.; Cui, X.; Zheng, J.; Wang, Q.; Lin, Y. Effects of Microstructure of Carbon Nanofibers for Amperometric Detection of Hydrogen Peroxide. *Anal. Chim. Acta* **2007**, *597* (2), 238–244. https://doi.org/10.1016/j.aca.2007.06.046.

(27) Koehne, J. E.; Marsh, M.; Boakye, A.; Douglas, B.; Kim, I. Y.; Chang, S.-Y.; Jang, D.-P.; Bennet, K. E.; Kimble, C.; Andrews, R.; Meyyappan, M.; Lee, K. H. Carbon Nanofiber Electrode Array for Electrochemical Detection of Dopamine Using Fast Scan Cyclic

Voltammetry. *Analyst* **2011**, *136* (9), 1802–1805. https://doi.org/10.1039/c1an15025a.

(28) Puthongkham, P.; Yang, C.; Venton, B. J. Carbon Nanohorn-Modified Carbon Fiber Microelectrodes for Dopamine Detection. *Electroanalysis* **2018**, *30* (6), 1073–1081. https://doi.org/10.1002/elan.201700667.

(29) Puthongkham, P.; Venton, B. J. Nanodiamond Coating Improves the Sensitivity and Antifouling Properties of Carbon Fiber Microelectrodes. *ACS Sensors* **2019**, *4*, 2403–2411. https://doi.org/10.1021/acssensors.9b00994.

(30) Mkhoyan, K. A.; Contryman, A. W.; Silcox, J.; Stewart, D. A.; Eda, G.; Mattevi, C.; Miller, S. Atomic and Electronic Structure of Graphene-Oxide. *Nano Lett.* **2009**, *9* (3), 17–21.

(31) Chen, D.; Feng, H.; Li, J. Graphene Oxide : Preparation , Functionalization , and Electrochemical Applications. *Chem. Rev.* **2012**, *112* (11), 6027–6053. https://doi.org/10.1021/cr300115g.

(32) Kim, F.; Cote, L. J.; Huang, J. Graphene Oxide: Surface Activity and Two-Dimensional Assembly. *Adv. Mater.* **2010**, *22* (17), 1954–1958. https://doi.org/10.1002/adma.200903932.

(33) Eda, B. G.; Chhowalla, M. Chemically Derived Graphene Oxide : Towards Large-Area Thin-Film Electronics and Optoelectronics. *Adv. Mater.* **2010**, *887* (5), 2392–2415. https://doi.org/10.1002/adma.200903689.

(34) Li, X.; Zhang, G.; Bai, X.; Sun, X.; Wang, X.; Wang, E.; Dai, H. Highly Conducting Graphene Sheets and Langmuir – Blodgett Films. **2008**, *3* (September), 1–5. https://doi.org/10.1038/nnano.2008.210.

(35) Compton, O. C.; Nguyen, S. T. Graphene Oxide , Highly Reduced Graphene Oxide , and Graphene : Versatile Building Blocks for Carbon-Based Materials **. *Small* **2010**, *6* (6), 711–723. https://doi.org/10.1002/smll.200901934.

(36) Banks, C. E.; Compton, R. G. New Electrodes for Old: From Carbon Nanotubes to Edge Plane Pyrolytic Graphite. *Analyst* **2006**, *131* (1), 15–21. https://doi.org/10.1039/B512688F.

(37) Bissessur, R.; Scully, S. F. Intercalation of Solid Polymer Electrolytes into Graphite Oxide. *Solid State Ionics* **2007**, *178*, 877–882. https://doi.org/10.1016/j.ssi.2007.02.030.

(38) Paredes, J. I.; Martı, A.; Tasco, J. M. D. Graphene Oxide Dispersions in Organic Solvents. *Langmuir* **2008**, No. 18, 10560–10564.

(39) Gao, F.; Cai, X.; Wang, X.; Gao, C.; Liu, S.; Gao, F.; Wang, Q. Sensors and Actuators B : Chemical Highly Sensitive and Selective Detection of Dopamine in the Presence of Ascorbic Acid at Graphene Oxide Modified Electrode. *Sensors Actuators B. Chem.* **2013**, *186*, 380–387.

(40) Chen, L.; Tang, Y.; Wang, K.; Liu, C.; Luo, S. Direct Electrodeposition of Reduced Graphene Oxide on Glassy Carbon Electrode and Its Electrochemical Application. *Electrochem. commun.* **2011**, *13*, 133–137. https://doi.org/10.1016/j.elecom.2010.11.033.

(41) Bath, B. D.; Michael, D. J.; Trafton, B. J.; Joseph, J. D.; Runnels, P. L.; Wightman, R. M. Subsecond Adsorption and Desorption of Dopamine at Carbon-Fiber Microelectrodes. *Anal. Chem.* **2000**, *72* (24), 5994–6002. https://doi.org/10.1021/ac000849y.

(42) Bard, A. J.; Faulkner, L. R. *Electrochemical Methods: Fundamentals and Applications*, 2nd ed.; John Wiley and Sons: New York, 2001.

(43) Morgan, D. M.; Weber, S. G. Noise and Signal-to-Noise Ratio in Electrochemical Detectors. *Anal. Chem.* **1984**, *56* (13), 2560–2567. https://doi.org/10.1021/ac00277a065.

(44) G. Gómez-Santos. Thermal van Der Waals Interaction between Graphene Layers. *Phys. Rev. B* **2009**, *80* (24), 1–8. https://doi.org/10.1103/PhysRevB.80.245424.

(45) Pu, N.; Wang, C.; Liu, Y.; Sung, Y.; Wang, D.; Ger, M. Journal of the Taiwan Institute of Chemical Engineers Dispersion of Graphene in Aqueous Solutions with Different Types of Surfactants and the Production of Graphene Films by Spray or Drop Coating. *J. Taiwan Inst. Chem. Eng.* **2012**, *43* (1), 140–146. https://doi.org/10.1016/j.jtice.2011.06.012.

(46) Devadas, B.; Rajkumar, M.; Chen, S.; Saraswathi, R. Electrochemically Reduced Graphene Oxide / Neodymium Hexacyanoferrate Modified Electrodes for the Electrochemical Detection of Paracetomol. *Int. J. Eletrochemical Sci.* **2012**, *7*, 3339–3349.

(47) Unnikrishnan, B.; Palanisamy, S.; Chen, S. A Simple Electrochemical Approach to Fabricate a Glucose Biosensor Based on Graphene – Glucose Oxidase Biocomposite. *Biosens. Bioelectron.* **2013**, *39*, 70–75. https://doi.org/10.1016/j.bios.2012.06.045.

(48) Roberts, J. G.; Moody, B. P.; McCarty, G. S.; Sombers, L. A. Specific Oxygen-Containing Functional Groups on the Carbon Surface Underlie an Enhanced Sensitivity to Dopamine at Electrochemically Pretreated Carbon Fiber Microelectrodes. *Langmuir* **2010**, *26* (11), 9116–9122. https://doi.org/10.1021/la9048924.

(49) Jacobs, C. B.; Vickrey, T. L.; Venton, B. J. Functional Groups Modulate the Sensitivity and Electron Transfer Kinetics of Neurochemicals at Carbon Nanotube Modified Microelectrodes. *Analyst* **2011**, *136* (17), 3557–3565. https://doi.org/10.1039/c0an00854k.

(50) Heien, M. L. A. V; Phillips, P. E. M.; Stuber, G. D.; Seipel, A. T.; Wightman, R. M. Overoxidation of Carbon-Fiber Microelectrodes Enhances Dopamine Adsorption and Increases Sensitivity. *Analyst* **2003**, *128*, 1413–1419. https://doi.org/10.1039/b307024g.

(51) Robinson, D. L.; Venton, B. J.; Heien, M. L. A. V; Wightman, R. M. Detecting Subsecond Dopamine Release with Fast-Scan Cyclic Voltammetry in Vivo. *Clin. Chem.* **2003**, *49* (10), 1763–1773. https://doi.org/10.1373/49.10.1763.

(52) Rice, M. E.; Patel, J. C.; Cragg, S. J. REVIEW DOPAMINE RELEASE IN THE BASAL GANGLIA. *Neuroscience* **2011**, *198*, 112–137. https://doi.org/10.1016/j.neuroscience.2011.08.066.

(53) Yuan, B.; Xu, C.; Deng, D.; Xing, Y.; Liu, L.; Pang, H.; Zhang, D. Graphene Oxide / Nickel Oxide Modified Glassy Carbon Electrode for Supercapacitor and Nonenzymatic Glucose Sensor. *Electrochim. Acta* **2013**, *88*, 708–712.

(54) Yang, C.; Cao, Q.; Puthongkham, P.; Lee, S. T.; Ganesana, M.; Lavrik, N. V; Venton, B. J. 3D-Printed Carbon Electrodes for Neurotransmitter Detection. *Angew. Chemie Int. Ed.* **2018**, *57* (43), 14255–14259. https://doi.org/10.1002/anie.201809992.

(55) Ross, A. E.; Venton, B. J. Adenosine Transiently Modulates Stimulated Dopamine Release in the Caudate-Putamen via A1 Receptors. *J. Neurochem.* **2015**, *132* (1), 51–

60. https://doi.org/10.1111/jnc.12946.

Chapter 6

Conclusions and Future Directions

6.1 Contribution to the field

In this dissertation, I investigated the mechanisms of rapid adenosine neuromodulation in mouse brain slices. In addition, I also optimized carbon-fiber microelectrode performance by coating electrodes with nanomaterials. This chapter will summarize the main impacts of my studies and discuss the future directions.

6.1.1 The mechanisms of rapid adenosine release and modulation in the brain

My dissertation characterized two modes of rapid adenosine in mouse brain slices using FSCV: (1) spontaneous adenosine release, and (2) mechanically-stimulated adenosine release. Although rapid adenosine formation and release mechanisms have been investigated for several years, we still do not fully understand the rapid formation and modulation of adenosine in the brain. **Chapter 2** compared rapid adenosine release in three types of mice: wild-type mice, A_1KO mice, and A_{2A}KO mice. The average number of spontaneous adenosine events was significantly higher in A_1KO mice, but the concentration of spontaneous adenosine did not change in A_1KO mice. These results indicate that the frequency of spontaneous adenosine is presynaptically modulated by A_1 receptors. A_{2A} receptors did not modulate the frequency of spontaneous adenosine but affected the concentration of spontaneous adenosine. Results for spontaneous adenosine in brain slices showed similar trends to the *in vivo* results. Mechanically-stimulated adenosine showed a significantly higher concentration in A_1KO mouse brain slices, but the concentration was not significant different in A_{2A}KO mice. Therefore, A_1 receptors also modulate mechanically-stimulated adenosine. This is the first study to investigate how adenosine receptors directly modulate rapid adenosine release. Since A_1 receptors play a main role in rapid adenosine modulation, rapid adenosine might relate to neuroprotection in the brain. These results also indicate that rapid adenosine might interact with or affect other neurotransmitter release in the brain. Understanding the role of adenosine receptors in rapid

adenosine modulation will provide more information for pharmacological designs on relative diseases.

Chapter 3 focused on rapid adenosine formation. Previous studies showed that rapid adenosine formation was mainly from extracellular ATP degeneration.[1–3] Therefore, ATP channels are candidate release sites for extracellular rapid adenosine formation. Pannexin channels are transmembrane proteins that regulate ATP release.[4] ATP is rapidly released from Pannexin 1 channels; Pannexin 1 channels are also mechanosensitive to ATP release.[5] Therefore, Pannexin 1 might be one of the mechanisms of rapid adenosine formation. **Chapter 3** measured spontaneous adenosine and mechanically-stimulated adenosine separately in Pannexin1 knockout mice. The results indicated that Pannexin 1 channels were not the mechanisms of spontaneous adenosine release, but Pannexin 1 channels partially affected mechanically-stimulated adenosine release. In addition, a high dose of carbenoxolone did not further influence rapid adenosine formation indicating other pannexin channels and connexins did not mediate rapid adenosine formation. This is the first time to investigate the role of Pannexin 1 channels on rapid adenosine formation. Although pannexins and connexins are not the mechanisms of spontaneous adenosine formation, this research still contributes important information for future studies on spontaneous adenosine formation. Future studies could focus on the role of exocytosis and adenosine transporters on rapid adenosine formation.

In summary, this thesis provides more understanding on the formation and modulation of rapid adenosine in the brain. The role of adenosine receptors on rapid adenosine modulation indicates that rapid adenosine is important for local neuroprotection. Since A_1 and A_{2A} receptors are abundant in the brain and modulate other neurotransmitter release, future studies could investigate the rapid adenosine neuromodulation on dopamine, serotonin, and glutamate release to further understand the neuroprotection roles of rapid adenosine. For rapid adenosine formation, gap junction proteins and pannexins are not the main mechanism of release.

Although ATP can be released via pannexin channels rapidly in some other tissues, this mechanism does not contribute to spontaneous adenosine release. Combined with findings from our previous studies, exocytosis of ATP and adenosine could be the main mechanisms of spontaneous formation.[1,6–8] The mechanosensitive pannexin 1 channel also partially modulates mechanically-stimulated adenosine release; this provides a clue that some other mechanosensitive ion channels in the membrane may also influence the formation of mechanically-stimulated adenosine. The Ca^{2+} mechanosensitive ion channels could be investigated in the future for mechanically-stimulated adenosine formation.

6.1.2 Understanding the range of rapid adenosine release in the brain

A carbon-fiber microelectrode combined with FSCV is the main technique for rapid adenosine characterization in our lab. However, single electrode detection limits the spatial resolution of measurements. **Chapter 4** improved the spatial resolution for rapid adenosine measurement by using dual channel FSCV. This is the first time that rapid adenosine was simultaneously monitored at two different sites in the brain. By varying the distance between the two electrodes, the range of rapid adenosine signaling was characterized. Mechanically-stimulated adenosine was simultaneously measured within 200 μm, but spontaneous adenosine was localized and randomly released within 50 μm. These results also indicate that mechanically-stimulated adenosine and spontaneous adenosine might perform different roles in neuromodulations in the brain. The fast response to the stimulation illustrates that mechanically-stimulated adenosine could efficiently cause neuroprotection by inhibiting other neurotransmitters released when the damage or injury happens.[9–11] Spontaneous adenosine might be related to cell activity, and thus localized neuromodulation would occur in regions of high activity.

Future studies could apply multiple electrodes in the brain to simultaneously monitor different neurotransmitter release. Multiple channel FSCV could provide more information on rapid adenosine modulation compared to single electrode measurements. In addition, rapid adenosine varied in different brain regions,[12–14] the range of rapid adenosine release might be different. For example, Figure 6.1 shows mechanically-stimulated adenosine release in the caudate in dual channel FSCV. Stimulated adenosine was detectable at a 200 µm distance in the caudate; this range is larger than the stimulated adenosine in the CA1 region. Therefore, future studies could also focus on different brain regions to characterize the range of rapid adenosine. Overall, **Chapter 4** provided more spatial information on rapid adenosine release, which has never been characterized before. These results provide a better understanding of the spatial and temporal profiles of adenosine available to act at receptors, which is crucial for future studies that design neuroprotective treatments based on rapid adenosine signaling.

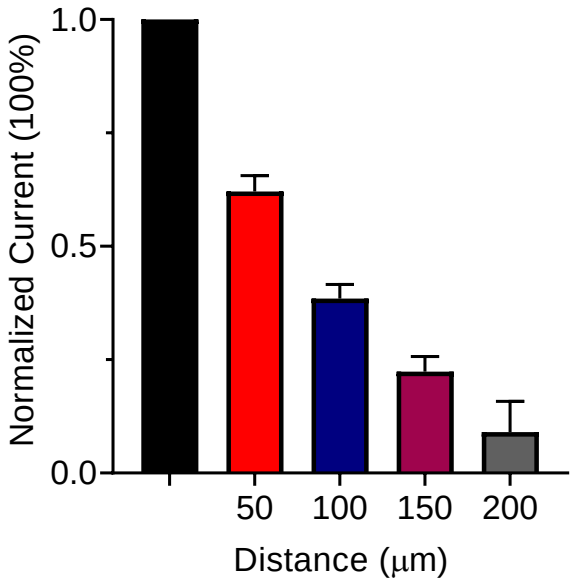

Figure 6.1 Mechanically-stimulated adenosine release in the caudate in dual channel FSCV. Current is normalized to the current measured on the stimulation electrode (which is 1). n=16 slices from 8 mice. Error bars are SEM.

6.1.3 Graphene oxide coating improves the performance of dopamine detection.

CFMEs have been applied to detect dopamine in FSCV for decades due to its good electrochemical performance and stability. However, the sensitivity of CFMEs for dopamine detection is limited by the surface roughness and the oxygen functional groups. Improving the sensitivity of the electrode will provide more information on the low concentration changes of dopamine in the brain.[15,16] Coating nanomaterials on the electrode surface enhanced the electrode performance, but the coating methods are various in different applications.[17–19] **Chapter 5** presented graphene oxide (GO) coated CFMEs for dopamine detection. The coating methods including drop casting, dip coating, and electrodeposition were also compared and optimized in the chapter. The results showed that the electrodeposition method has a better coating on the surface, and GO coated CFME enhanced the sensitivity of dopamine detection. In addition, the modified electrode was also applied in brain slices to detect stimulated dopamine release.

The advantage of this work is that GO was directly coated on the microelectrode surface via simple methods. Previous studies reduced graphene oxide first and coated it on the electrode, or coated graphene oxide with conductive polymer together on the surface.[20,21] This work showed how GO itself contributed to the electrode performance, and it also compared different coating methods that were normally ignored in other work. The comparison showed that drop casting caused aggregation on the surface of the coated nanoparticles that tend to stack. In addition, previous work on nanomaterial-modified CFMEs was only tested in the flow cell; but this work further applied the GO/CFMEs in brain slices for biological approaches. Moreover, the abundant oxygen functional groups of GO will provide a substrate to immobilize enzymes or DNA sequences for biosensors or aptamer sensors fabrication in the future.[22] Finally, the coating results indicate that GO is also a good carbon-based material for dopamine

sensing, and pure GO microelectrodes such as growing on metal wires will provide more dopamine adsorption than CFMEs.

6.2 Future Directions

6.2.1 Neurotransmitter detection via multiplex analytical tools

Carbon-fiber microelectrodes combined with FSCV have been applied for rapid changes in neurotransmission and neuromodulation for decades; however, this technique only measures electroactive analytes, and its spatial resolution is also limited by the number of working electrodes.[15,16] Genetically-encoded sensors have been developed for neurotransmitter and neuromodulator measurements recently.[23–25] Genetically engineered G-protein coupled receptors or bacterial periplasmic binding proteins, the two main types of sensor design, change the fluorescence when they are bound with the analytes.[26] The fluorescence technique provides good spatial resolution, and the engineered proteins offer selectivity and sensitivity. Genetically-encoded sensors are also not limited to electroactive analytes; they are also applied for nonelectroactive neurotransmitters detection such as glutamate, GABA, and Ach.[27–29] In addition, genetically-encoded sensors are also applied to monitor neuron activities *in vivo* by measuring calcium change.[30] However, fluorescence sensors are difficult to simultaneously monitor multiple analytes, they are normally limited by two colors (red and green).[31] Therefore, combining FSCV with genetically-encoded sensors will be a benefit to detect complex neuromodulation in high spatial and temporal resolution.

Our lab has performed multiplexed GRAB sensor and FSCV measurements in brain slices to demonstrate the ability to combine two techniques. Figure 6.2 shows the simultaneous serotonin detection via two techniques. The top figure shows how GRAB sensors are expressed in the brain; a CFME was applied nearby the expressing cell for electrochemical detection.

Electrically-stimulated serotonin was monitored simultaneously via multiplex tools, and the signal vs time trends are shown at the bottom of Figure 6.2. The results indicate that both techniques have a fast time response after the stimulation, but GRAB sensors showed slow reuptake due to the k_{off} of GPCR. These results indicate that multiplexing tools improve the temporal and spatial profiles of neurotransmitter detection.

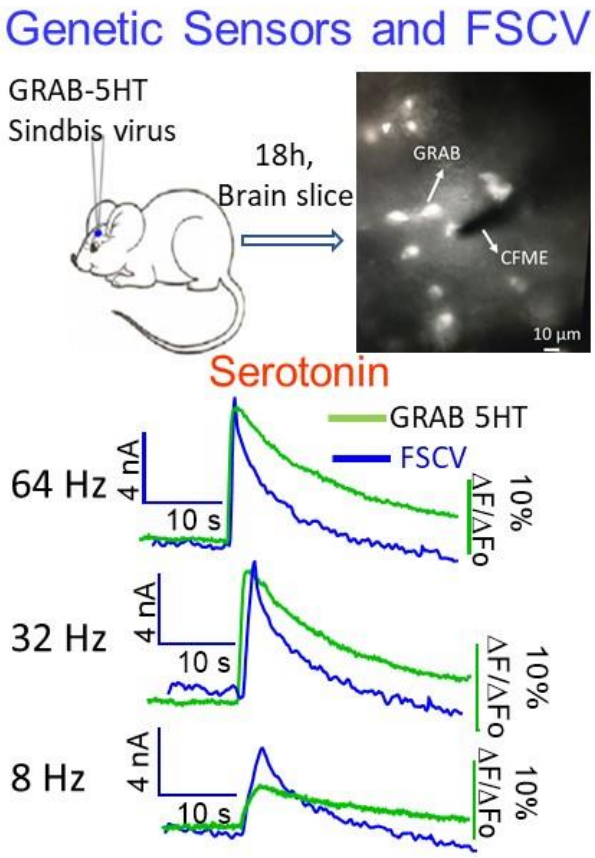

Figure 6.2 FSCV and GRAB sensors recording stimulated serotonin release simultaneously. Traces for 20 pulse stimulations at 3 different stim frequencies (64, 32, 8 Hz). Both sensors increase rapidly with the stimulation, but the off kinetics is a bit faster for FSCV.

Future directions will be focused on multiple analyte detection via FSCV and GRAB sensors. Chapter 2-4 showed that rapid adenosine release could act as a neuromodulator in the brain, but it is difficult to monitor the complex neuromodulation of rapid adenosine by only using FSCV. Therefore, I proposed to investigate rapid adenosine neuromodulation via multiplexing techniques.

6.2.1.1 Investigation of Rapid adenosine neuromodulation

Chapter 4 indicates that mechanically-stimulated adenosine might have a neuroprotective role in the brain during stress or damage. To prove the prediction, I propose to simultaneously detect mechanically-stimulated adenosine and other neurotransmitters like dopamine, serotonin, and glutamate in the brain slice to investigate if the adenosine release inhibits neurotransmitter release in the brain. Figure 6.3 shows the schematic of the proposed experiment for rapid adenosine modulation on dopamine in the caudate region. Mechanically-stimulated adenosine will still be monitored by FSCV, meanwhile, $GRAB_{DA}$ sensors will be applied to detect dopamine release. Electrically-stimulated dopamine will be measured by fluorescence, and the intensity of dopamine release will be compared with and without adenosine influence. In addition, the distance between the electrode (adenosine release site) and the expressing cell (dopamine release site) can be varied to investigate the spatial effects. The hypothesis is that mechanically-stimulated adenosine will suppress the stimulated dopamine release. After the proof of concept, it will be possible to investigate how mechanically-stimulated adenosine modulates other neurotransmitter release. For example, glutamate release will be measured via GRAB sensors, and we predict that adenosine modulates glutamate release, and suppresses glutamate excitotoxicity, particularly during the stroke.[32,33] Therefore, FSCV combined genetically-encoded sensors will be available to monitor the complex role of mechanically-stimulated adenosine modulation.

For spontaneous adenosine neuromodulation, the challenge will be how to control the electrical stimulations with random adenosine events. A manually-controlled stimulation tool will be needed to make it adaptable. Also, spontaneous adenosine was collected for hours in FSCV, but for the fluorescence technique, the simultaneous detection time needs to be shortened to 1.5 minutes to prevent photobleaching. The hypothesis is that spontaneous adenosine only

modulates dopamine or glutamate nearby the expressing cell (within 50 µm). The modulation will be transient, only few seconds as the adenosine signal is presented.

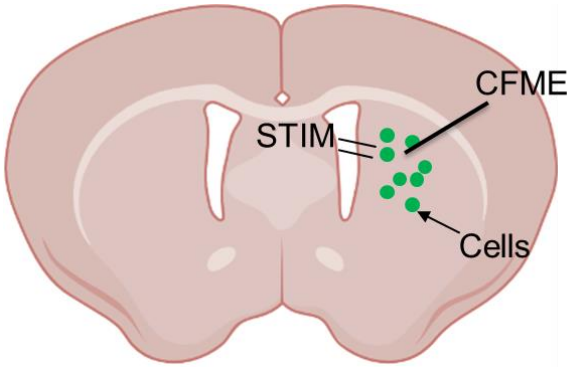

Figure 6.3 Schematic of the proposed experiment. Monitoring adenosine (FSCV) and its downstream modulation of dopamine or glutamate (genetically-encoded sensors). The green circles are the expressing cells.

6.2.1.2 Rapid adenosine and neuronal activity

Mechanically-stimulated adenosine is activity-dependent, chelating calcium with 1 mM EDTA significantly decreased the concentration of stimulated adenosine. Genetically-encoded sensors are already available for calcium detection (GCaMP6f) with fast time response *in vivo.*[34,35] Mechanically-stimulated adenosine will be collected by FSCV. Thus, simultaneously monitoring mechanically-stimulated adenosine and neuronal activity will present the mechanisms of rapid adenosine modulation, and the knowledge will link to the diseases that are related to neuronal activity. The hypothesis will be mechanically-stimulated adenosine will dampen the neuronal activity immediately, and will affect hundreds of micrometers distance. The neuroprotection effect will decrease as the distance between the cell and the stimulation site increases.

Chapter 4 also revealed that spontaneous adenosine release was random and highly localized in the brain. There is evidence that spontaneous adenosine could diffuse or modulate neurotransmission at the 50 µm range. Previous studies showed that spontaneous adenosine was activity-dependent, and its formation was from ATP degeneration. Therefore, spontaneous adenosine release might be related to local neuronal activity. The hypothesis is that

spontaneous adenosine release will dampen the local cell neuronal activity, but will not affect other cells which are 50 µm away. This will be the first study on rapid adenosine release modulation of neuronal activity.

Overall, multiplexing analytical tools will allow simultaneous measurements on both electroactive and nonelectroactive analytes with high temporal and spatial profiles. Understanding the complex neuromodulation of rapid adenosine in real-time will help future investigations on the mechanisms of neurodegeneration diseases and provide new insight for drug development on neuronal disorder diseases.

6.2.2 Optimizing different types of microelectrodes in brain slice detection.

CFMEs and other carbon-based microelectrodes have been developed for dopamine detection for twenty years, but most of the modified or new carbon microelectrodes are not applied in biological measurement.[36] **Chapter 5** optimized the microelectrode performance by coating graphene oxide on the CFME surface. One of the practical problems of applying new microelectrodes in brain measurements is that there are no direct comparisons between the new electrodes and CFMEs performance in the brain tissue. Therefore, I propose a direct microelectrode performance in the brain slice model to analyze if the new microelectrodes are better than CFMEs. Figure 6.4 shows the experimental design, a CFME and the new type of microelectrode will be inserted in the caudate-putamen region to simultaneously detect electrically-stimulated dopamine via multiple channel FSCV. Since both electrodes are measuring the same stimulated dopamine release, we can directly compare the electrode performance simultaneously. Carbon nanospikes microelectrodes, carbon nanotube yarn microelectrodes, nanodiamond modified carbon-fiber microelectrodes, and CFMEs will be compared in this experiment.[18,37–40] The hypothesis is that new carbon microelectrodes have better performance than CFMEs, which are similar to what they were claimed in flow cell studies. If the performance of new types of microelectrodes does not perform well in the brain

slice, their fabrication will need to be optimized for biological applications. In addition, mechanically-stimulated adenosine release could also be compared to filter a better electrode for rapid adenosine detection in brain slices in the future.

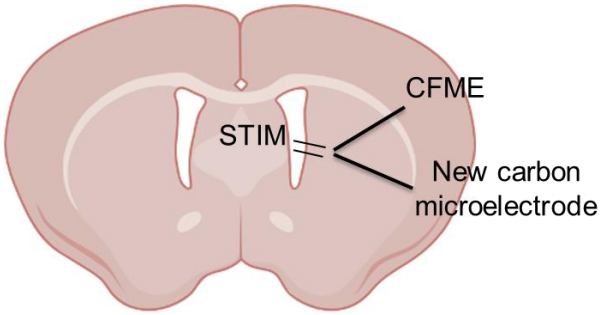

Figure 6.4 Schematic of the proposed experiment. Two different types of microelectrodes are applied in the caudate to simultaneously detect stimulated dopamine release.

6.3 Final Conclusions

In conclusion, this thesis expanded the FSCV research in three main directions. First, the mechanisms of rapid adenosine neuromodulation and rapid adenosine formation were characterized using global knockout mice. Second, the range of rapid adenosine release in brain slices was characterized for the first time by using dual channel FSCV. Finally, this thesis also optimized the microelectrode performance by coating graphene oxide on CFMEs and applied it in brain slice measurements. Investigations of new types of micro/nano electrodes in biological systems are also important for future upgrading in brain measurements. In the future, combining FSCV and genetically-encoded sensors will improve the temporal and spatial profiles. By simultaneously monitoring electroactive and nonelectroactive neurotransmitters, more complex neuromodulation of rapid adenosine in the brain will be clear. Multiplexing tools will reveal more real-time neurotransmitter interactions.

6.4 References

(1) Nguyen, M. D.; Venton, B. J. Fast-Scan Cyclic Voltammetry for the Characterization of

Rapid Adenosine Release. *Comput. Struct. Biotechnol. J.* **2015**, *13*, 47–54. https://doi.org/10.1016/j.csbj.2014.12.006.

(2) Wang, Y.; Venton, B. J. Comparison of Spontaneous and Mechanically-Stimulated Adenosine Release in Mice. *Neurochem. Int.* **2019**, *124* (December 2018), 46–50. https://doi.org/10.1016/j.neuint.2018.12.007.

(3) Ross, A. E.; Nguyen, M. D.; Privman, E.; Venton, B. J. Mechanical Stimulation Evokes Rapid Increases in Extracellular Adenosine Concentration in the Prefrontal Cortex. *J. Neurochem.* **2014**, *130* (1), 50–60. https://doi.org/10.1111/jnc.12711.

(4) Schock, S. C.; LeBlanc, D.; Hakim, A. M.; Thompson, C. S. ATP Release by Way of Connexin 36 Hemichannels Mediates Ischemic Tolerance in Vitro. *Biochem. Biophys. Res. Commun.* **2008**, *368* (1), 138–144. https://doi.org/10.1016/j.bbrc.2008.01.054.

(5) Bao, L.; Locovei, S.; Dahl, G. Pannexin Membrane Channels Are Mechanosensitive Conduits for ATP. *FEBS Lett.* **2004**, *572* (1–3), 65–68. https://doi.org/10.1016/j.febslet.2004.07.009.

(6) Ross, A. E.; Nguyen, M. D.; Privman, E.; Venton, B. J. Mechanical Stimulation Evokes Rapid Increases in Extracellular Adenosine Concentration in the Prefrontal Cortex. *J. Neurochem.* **2014**, *130* (1), 50–60. https://doi.org/10.1111/jnc.12711.

(7) Nguyen, M. D.; Ross, A. E.; Ryals, M.; Lee, S. T.; Venton, B. J. Clearance of Rapid Adenosine Release Is Regulated by Nucleoside Transporters and Metabolism. *Pharmacol. Res. Perspect.* **2015**, *3* (6), 1–12. https://doi.org/10.1002/prp2.189.

(8) Lee, S. T.; Venton, B. J. Regional Variations of Spontaneous, Transient Adenosine Release in Brain Slices. *ACS Chem. Neurosci.* **2018**, *9* (3), 505–513. https://doi.org/10.1021/acschemneuro.7b00280.

(9) Cunha, R. A. Neuroprotection by Adenosine in the Brain: From A1 Receptor Activation to A2A Receptor Blockade. *Purinergic Signalling*. 2005, pp 111–134. https://doi.org/10.1007/s11302-005-0649-1.

(10) Boison, D. Adenosine as a Neuromodulator in Neurological Diseases. *Curr. Opin. Pharmacol.* **2008**, *8* (1), 2–7. https://doi.org/https://doi.org/10.1016/j.coph.2007.09.002.

(11) Chen, J. F.; Huang, Z.; Ma, J.; Zhu, J. M.; Moratalla, R.; Standaert, D.; Moskowitz, M. A.; Fink, J. S.; Schwarzschild, M. A. A(2A) Adenosine Receptor Deficiency Attenuates Brain Injury Induced by Transient Focal Ischemia in Mice. *J. Neurosci.* **1999**, *19* (21), 9192–9200. https://doi.org/10.1523/JNEUROSCI.19-21-09192.1999.

(12) Lee, S. T.; Venton, B. J. Regional Variations of Spontaneous, Transient Adenosine Release in Brain Slices. *ACS Chem. Neurosci.* **2018**, *9* (3), 505–513. https://doi.org/10.1021/acschemneuro.7b00280.

(13) Wang, Y.; Copeland, J.; Shin, M.; Chang, Y.; Venton, B. J. CD73 or CD39 Deletion Reveals Different Mechanisms of Formation for Spontaneous and Mechanically Stimulated Adenosine and Sex Specific Compensations in ATP Degradation. *ACS Chem. Neurosci.* **2020**, *11* (6), 919–928. https://doi.org/10.1021/acschemneuro.9b00620.

(14) Chang, Y.; Wang, Y.; Venton, B. J. A1and A2AReceptors Modulate Spontaneous Adenosine but Not Mechanically Stimulated Adenosine in the Caudate. *ACS Chem. Neurosci.* **2020**, *11* (20), 3377–3385. https://doi.org/10.1021/acschemneuro.0c00510.

(15) Venton, B. J.; Cao, Q. Fundamentals of Fast-Scan Cyclic Voltammetry for Dopamine Detection. *Analyst* **2020**. https://doi.org/10.1039/C9AN01586H.

(16) Puthongkham, P.; Venton, B. J. Recent Advances in Fast-Scan Cyclic Voltammetry. *Analyst* **2020**, *145* (4), 1087–1102. https://doi.org/10.1039/C9AN01925A.

(17) Puthongkham, P.; Yang, C.; Venton, B. J. Carbon Nanohorn-Modified Carbon Fiber Microelectrodes for Dopamine Detection. *Electroanalysis* **2018**, *30* (6), 1073–1081. https://doi.org/10.1002/elan.201700667.

(18) Puthongkham, P.; Venton, B. J. Nanodiamond Coating Improves the Sensitivity and Antifouling Properties of Carbon Fiber Microelectrodes. *ACS Sensors* **2019**, *4*, 2403–2411. https://doi.org/10.1021/acssensors.9b00994.

(19) Yang, C.; Denno, M. E.; Pyakurel, P.; Venton, B. J. Recent Trends in Carbon Nanomaterial-Based Electrochemical Sensors for Biomolecules: A Review. *Anal. Chim. Acta* **2015**, *887*, 17–37. https://doi.org/10.1016/j.aca.2015.05.049.

(20) Si, W.; Lei, W.; Zhang, Y.; Xia, M.; Wang, F.; Hao, Q. Electrodeposition of Graphene Oxide Doped Poly (3 , 4-Ethylenedioxythiophene) Film and Its Electrochemical Sensing of Catechol and Hydroquinone. *Electrochim. Acta* **2012**, *85*, 295–301.

(21) Taylor, I. M.; Robbins, E. M.; Catt, K. A.; Cody, P. A.; Happe, C. L.; Tracy, X. Enhanced Dopamine Detection Sensitivity by PEDOT / Graphene Oxide Coating on in Vivo Carbon Fi Ber Electrodes. *Biosens. Bioelectron.* **2017**, *89*, 400–410. https://doi.org/10.1016/j.bios.2016.05.084.

(22) Chen, D.; Feng, H.; Li, J. Graphene Oxide : Preparation , Functionalization , and Electrochemical Applications. *Chem. Rev.* **2012**, *112* (11), 6027–6053. https://doi.org/10.1021/cr300115g.

(23) Tian, L.; Hires, S. A.; Mao, T.; Huber, D.; Chiappe, M. E.; Chalasani, S. H.; Petreanu, L.; Akerboom, J.; McKinney, S. A.; Schreiter, E. R.; Bargmann, C. I.; Jayaraman, V.; Svoboda, K.; Looger, L. L. Imaging Neural Activity in Worms, Flies and Mice with Improved GCaMP Calcium Indicators. *Nat. Methods* **2009**, *6* (12), 875–881. https://doi.org/10.1038/nmeth.1398.

(24) Wan, J.; Peng, W.; Li, X.; Qian, T.; Song, K.; Zeng, J.; Deng, F.; Hao, S.; Feng, J.; Zhang, P.; Zhang, Y.; Zou, J.; Pan, S.; Shin, M.; Venton, B. J.; Zhu, J. J.; Jing, M.; Xu, M.; Li, Y. A Genetically Encoded Sensor for Measuring Serotonin Dynamics. *Nat. Neurosci.* **2021**, *24* (5), 746–752. https://doi.org/10.1038/s41593-021-00823-7.

(25) Patriarchi, T.; Mohebi, A.; Sun, J.; Marley, A.; Liang, R.; Dong, C.; Puhger, K.; Mizuno, G. O.; Davis, C. M.; Wiltgen, B.; von Zastrow, M.; Berke, J. D.; Tian, L. An Expanded Palette of Dopamine Sensors for Multiplex Imaging in Vivo. *Nat. Methods* **2020**, *17* (11), 1147–1155. https://doi.org/10.1038/s41592-020-0936-3.

(26) Lin, L.; Gupta, S.; Zheng, W. S.; Si, K.; Zhu, J. J. Genetically Encoded Sensors Enable Micro- and Nano-Scopic Decoding of Transmission in Healthy and Diseased Brains. *Mol. Psychiatry* **2021**, *26* (2), 443–455. https://doi.org/10.1038/s41380-020-00960-8.

(27) Jing, M.; Zhang, P.; Wang, G.; Feng, J.; Mesik, L.; Zeng, J.; Jiang, H.; Wang, S.; Looby, J. C.; Guagliardo, N. A.; Langma, L. W.; Lu, J.; Zuo, Y.; Talmage, D. A.; Role, L. W.; Barrett, P. Q.; Zhang, L. I.; Luo, M.; Song, Y.; Zhu, J. J.; Li, Y. A Genetically Encoded Fluorescent Acetylcholine Indicator for in Vitro and in Vivo Studies. *Nat. Biotechnol.* **2018**,

36 (8). https://doi.org/10.1038/nbt.4184.

(28) Marvin, J. S.; Shimoda, Y.; Magloire, V.; Leite, M.; Kawashima, T.; Jensen, T. P.; Kolb, I.; Knott, E. L.; Novak, O.; Podgorski, K.; Leidenheimer, N. J.; Rusakov, D. A.; Ahrens, M. B.; Kullmann, D. M.; Looger, L. L. A Genetically Encoded Fluorescent Sensor for in Vivo Imaging of GABA. *Nat. Methods* **2019**, *16* (8), 763–770. https://doi.org/10.1038/s41592-019-0471-2.

(29) Dürst, C. D.; Wiegert, J. S.; Helassa, N.; Kerruth, S.; Coates, C.; Schulze, C.; Geeves, M. A.; Török, K.; Oertner, T. G. High-Speed Imaging of Glutamate Release with Genetically Encoded Sensors. *Nat. Protoc.* **2019**, *14* (5), 1401–1424. https://doi.org/10.1038/s41596-019-0143-9.

(30) Qian, Y.; Piatkevich, K. D.; Mc Larney, B.; Abdelfattah, A. S.; Mehta, S.; Murdock, M. H.; Gottschalk, S.; Molina, R. S.; Zhang, W.; Chen, Y.; Wu, J.; Drobizhev, M.; Hughes, T. E.; Zhang, J.; Schreiter, E. R.; Shoham, S.; Razansky, D.; Boyden, E. S.; Campbell, R. E. A Genetically Encoded Near-Infrared Fluorescent Calcium Ion Indicator. *Nat. Methods* **2019**, *16* (2), 171–174. https://doi.org/10.1038/s41592-018-0294-6.

(31) Sun, F.; Zhou, J.; Dai, B.; Qian, T.; Zeng, J.; Li, X.; Zhuo, Y.; Zhang, Y.; Wang, Y.; Qian, C.; Tan, K.; Feng, J.; Dong, H.; Lin, D.; Cui, G.; Li, Y. Next-Generation GRAB Sensors for Monitoring Dopaminergic Activity in Vivo. *Nat. Methods* **2020**, *17* (11), 1156–1166. https://doi.org/10.1038/s41592-020-00981-9.

(32) Popoli, P.; Frank, C.; Tebano, M. T.; Potenza, R. L.; Pintor, A.; Domenici, M. R.; Nazzicone, V.; Pèzzola, A.; Reggio, R. Modulation of Glutamate Release and Excitotoxicity by Adenosine A2A Receptors. *Neurology* **2003**, *61* (11 suppl 6), S69 LP-S71. https://doi.org/10.1212/01.WNL.0000095216.89483.A2.

(33) Ciruela, F.; Casadó, V.; Rodrigues, R. J.; Luján, R.; Burgueño, J.; Canals, M.; Borycz, J.; Rebola, N.; Goldberg, S. R.; Mallol, J.; Cortés, A.; Canela, E. I.; López-Giménez, J. F.; Milligan, G.; Lluis, C.; Cunha, R. A.; Ferré, S.; Franco, R. Presynaptic Control of Striatal Glutamatergic Neurotransmission by Adenosine A1–A2A Receptor Heteromers. *J. Neurosci.* **2006**, *26* (7), 2080–2087. https://doi.org/10.1523/JNEUROSCI.3574-05.2006.

(34) Akerboom, J.; Chen, T.-W.; Wardill, T. J.; Tian, L.; Marvin, J. S.; Mutlu, S.; Calderón, N. C.; Esposti, F.; Borghuis, B. G.; Sun, X. R.; Gordus, A.; Orger, M. B.; Portugues, R.; Engert, F.; Macklin, J. J.; Filosa, A.; Aggarwal, A.; Kerr, R. A.; Takagi, R.; Kracun, S.; Shigetomi, E.; Khakh, B. S.; Baier, H.; Lagnado, L.; Wang, S. S.-H.; Bargmann, C. I.; Kimmel, B. E.; Jayaraman, V.; Svoboda, K.; Kim, D. S.; Schreiter, E. R.; Looger, L. L. Optimization of a GCaMP Calcium Indicator for Neural Activity Imaging. *J. Neurosci.* **2012**, *32* (40), 13819–13840. https://doi.org/10.1523/JNEUROSCI.2601-12.2012.

(35) Badura, A.; Sun, X. R.; Giovannucci, A.; Lynch, L. A.; Wang, S. S. H. Fast Calcium Sensor Proteins for Monitoring Neural Activity. *Neurophotonics* **2014**, *1* (2), 1–12. https://doi.org/10.1117/1.NPh.1.2.025008.

(36) Cao, Q.; Puthongkham, P.; Venton, B. J. Review: New Insights into Optimizing Chemical and 3D Surface Structures of Carbon Electrodes for Neurotransmitter Detection. *Anal. Method* **2019**, *11*, 247–261. https://doi.org/10.1039/c8ay02472c.

(37) Cao, Q.; Shao, Z.; Hensley, D.; Venton, B. J. Carbon Nanospike Coated Nanoelectrodes for Measurements of Neurotransmitters. *Faraday Discuss.* **2021**. https://doi.org/10.1039/d1fd00053e.

(38) Cao, Q.; Hensley, D. K.; Lavrik, N. V; Venton, B. J. Carbon Nanospikes Have Better Electrochemical Properties than Carbon Nanotubes Due to Greater Surface Roughness and Defect Sites. *Carbon N. Y.* **2019**, *155*, 250–257. https://doi.org/https://doi.org/10.1016/j.carbon.2019.08.064.

(39) Shao, Z.; Puthongkham, P.; Hu, K. K.; Jia, R.; Mirkin, M. V.; Venton, B. J. Thin Layer Cell Behavior of CNT Yarn and Cavity Carbon Nanopipette Electrodes: Effect on Catecholamine Detection. *Electrochim. Acta* **2020**, *361*, 137032. https://doi.org/10.1016/j.electacta.2020.137032.

(40) Yang, C.; Wang, Y.; Jacobs, C. B.; Ivanov, I. N.; Venton, B. J. O2 Plasma Etching and Antistatic Gun Surface Modifications for CNT Yarn Microelectrode Improve Sensitivity and Antifouling Properties. *Anal. Chem.* **2017**, *89* (10), 5605–5611. https://doi.org/10.1021/acs.analchem.7b00785.

Appendix

List of publications of this dissertation

1. **Chang, Y.**, Wang, Y., & Venton, B. J. (2020). A1 and A2A Receptors Modulate Spontaneous Adenosine but Not Mechanically Stimulated Adenosine in the Caudate. ACS chemical neuroscience, 11(20), 3377-3385.

2. **Chang, Y.**, & Venton, B. J. (2022). Dual-Channel Electrochemical Measurements Reveal Rapid Adenosine is Localized in Brain Slices. ACS Chemical Neuroscience.

3. **Chang, Y.**, & Venton, B. J. (2020). Optimization of graphene oxide-modified carbon-fiber microelectrode for dopamine detection. Analytical Methods, 12(22), 2893-2902.

4. Lee, S.*, **Chang, Y.***, & Venton, B. J. (2022). Pannexin1 channels regulate mechanically-stimulated but not spontaneous adenosine release. (submitted) (* equal contribution)

5. Shao, Z., **Chang, Y.**, & Venton. B. J. (2022). Carbon microelectrodes with customized shapes for neurotransmitter detection. (Under manuscript)